AN INVESTIGATION INTO THE FORMATION OF SILANE-BASED SELF-ASSEMBLED MONOLAYERS AND THE DENSITY OF DEFECTS IN THESE SAMS

by

Hanifa Jalali
B.Sc., Simon Fraser University, 2005

THESIS SUBMITTED IN PARTIAL FULFILLMENT OF
THE REQUIREMENTS FOR THE DEGREE OF

MASTER OF SCIENCE

In the
Department of Chemistry

© Hanifa Jalali 2008

SIMON FRASER UNIVERSITY

Fall 2008

All rights reserved. This work may not be
reproduced in whole or in part, by photocopy
or other means, without permission of the author.

APPROVAL

Name: **Hanifa Jalali**

Degree: **Master of Science**

Title of Thesis: **An investigation into the formation of silane-based self-assembled monolayers and the density of defects in these SAMs**

Examining Committee:

Chair: **Dr. Peter Wilson**
Associate Professor

_____

Dr. Byron D. Gates
Senior Supervisor
Assistant Professor

_____

Dr. Andrew J. Bennet
Supervisor
Professor

_____

Dr. Steven Holdcroft
Supervisor
Professor

_____

Dr. Hua-Zhong (Hogan) Yu
Internal Examiner
Associate Professor

Date Defended/Approved: **September 8, 2008**

ABSTRACT

Silane-based self-assembled monolayers (SAMs) are commonly used as protective coatings against chemical etchants and adhesion of biomolecules. The conventional methods of producing SAMs are very time consuming and energy intensive processes. This thesis presents an efficient technique to produce silane-based SAMs approximately 300 times faster while consuming over 750 times less energy than the conventional method. Silane-based SAMs produce monolayers containing various types of defects. New techniques are developed to identify defects in SAMs and to correct for them. Chemical amplification of defects is developed for easily detecting defects in SAMs by traditional microscopy and spectroscopy techniques. Extraction and refilling methods are used to increase the packing density of the molecules in these monolayers and reduce the number of defects present in SAMs. By increasing the efficiency of silane deposition and improving the packing density of molecules, high quality SAMs can be produced within a short period of time.

Keywords: Self-assembled monolayers, Silane, Defects, Microwave-assisted deposition, Electroless metal deposition

To my family with all my love

ACKNOWLEDGEMENTS

My love for Chemistry started many years ago, when I first began working in Dr. Jason Clyburne's laboratory at SFU. As an inexperienced undergraduate student, with the help of Diane Dickie and Madhvi Ramnial, I learned how to explore simple (and at times complicated) facts of the field. Later on, I worked on a collaborative project between Jason and Dr. Hogan Yu. My interest in Materials Science grew while attacking the new challenges of this project. My thanks go to Jason, Hogan, and their group members for introducing me to the joy of Chemistry.

An undergraduate research program was not enough to satisfy my need explore science. Dr. Byron Gates, opened his lab to me and welcomed me as a graduate student. He allowed me to explore, learn, and enhance my knowledge of chemistry by providing a comfortable, friendly, and educational environment. My supervisory committee members, Drs. Andrew Bennet and Steven Holdcroft, along with Byron, led me towards reaching my goals. Hogan and his group generously allowed me to use their equipment. Many members of the Chemistry Department and 4D LABS including Dr. Andrew Lewis, Liang Hong, and Dr. Simon Trudel helped me through my graduate career. My sincere thanks to all for sharing their knowledge and time with me.

While preparing my thesis, many people provided me with constructive feedback: Nathanael Sieb, Emilie Vision, Nazanin Shafiee Mobrhan, Drs. Nabyl

Merbouh, Madhvi Ramnial, and John Canal proof read my work. Thank you all for your support.

Besides learning chemistry, I had the opportunity to work as a teaching assistant for various courses in our Chemistry Department. I would like to thank Dr. Lee Hanlan for allowing me to develop a passion for teaching and for her mentorship over the years.

The most important part of my experience at SFU was not learning chemistry, but learning how to live. My time at SFU allowed me to find who I am and what I want from life. I owe this knowledge to my friends and family. At SFU, I made many great friends whom will be a part of my life and my heart for years to come. Nazanin Mobrhan Shafiee, Nathanael Sieb, Bryan Wood, Amir Bahman Samsam Bakhtiari, Michael Wang, Cesar Escobar, Amanda Gronotte, and Emilie Viosin have helped me not only with science but with the dilemmas of life. Thank you all for the friendship and laughter we shared over the years.

Last but certainly not least, I would like to thank my family: my parents, Hadi and Soudabeh, for being my mentor and support in life; my little brother, Payam, for bringing a smile to my face when things were not going well; and my fiancé, Trevor, for his understanding and support through the good and the bad over the past five years.

TABLE OF CONTENTS

Approval ii
Abstract iii
Dedication iv
Acknowledgements v
Table of Contents vii
List of Figures ix
List of Tables xiv
Glossary xv
Chapter 1: Introduction to Self-Assembled Monolayers 1
1.1 Self-Assembled Monolayers (SAMs) 1
1.2 Silane-Based SAMs 3
1.3 Microwave Enhanced Reactions 6
1.4 Introduction to Defects in SAMs 8
1.5 Electroless Metal Deposition (EMD) 11
1.6 Methods of Characterizing SAMs 13
1.6.1 Contact Angle Measurements 14
1.6.2 Spectroscopic Ellipsometry 16
1.6.3 Fourier Transform Infrared (FTIR) Spectroscopy 17
1.6.4 Scanning Electron Microscopy (SEM) 18
1.6.5 Energy Dispersive X-ray Spectroscopy (EDS) 20
1.6.6 X-ray Photoelectron Spectroscopy (XPS) 22
1.6.7 Atomic Force Microscopy (AFM) 23
1.7 Overview of Thesis 25
Chapter 2: Microwave-Assisted Deposition of SAMs 27
2.1 Introduction to Microwave-Assisted Deposition of SAMs 27
2.2 Experimental 29
2.2.1 Materials 29
2.2.2 Cleaning the Substrate 30
2.2.3 Deposition of Microwave-Based SAMs 30
2.2.4 Extraction and Refilling of Defects in Silane-Based SAMs 31
2.2.5 Contact Angle Measurements 31
2.3 Results and Discussion of Microwave-Assisted Deposition of SAMs 32
2.3.1 The Choice of Solvent for Microwave-Assisted Deposition of SAMs 34

2.3.2 Effect of Concentration of FAS on the Quality of SAMs 40
2.3.3 Improving the Packing Density of the Physically Adsorbed Monolayers Prior to Irradiation 44
2.4 Conclusions on Microwave-Assisted Deposition of SAMs 49

Chapter 3: Defects in Silane-Based SAMs 51

3.1 Introduction to Dominant Types of Defects and Correction Techniques 51
3.1.1 Silane-Based Self-Assembled Monolayers 53
3.1.2 Conventional Synthesis of Silane-Based SAMs 54
3.1.3 Microwave-Prepared Deposition of SAMs 54
3.1.4 Characterization of Defects in SAMs 57
3.2 Experimental 61
3.2.1 Materials 61
3.2.2 Cleaning the Substrate 62
3.2.3 Deposition of Conventional SAMs 62
3.2.4 Extraction and Refilling of Defects in Silane-Based SAMs 63
3.2.5 Contact Angle Measurements 63
3.2.6 Spectroscopic Ellipsometry Analysis 63
3.2.7 Chemical Amplification and FTIR Measurements 64
3.2.8 Electroless Silver Deposition and AFM, SEM, and XPS Analysis 64
3.3 Results and Discussion on the Analysis of Defects 65
3.3.1 Contact Angle Measurements on Silane-Based SAMs 66
3.3.2 Spectroscopic Ellipsometry Measurements 72
3.3.3 Chemical Amplification of Defects and FTIR Measurements 75
3.3.4 Detection of Defects by AFM and SEM Imaging and XPS Analysis 79
3.4 Conclusions on Identification and Correction of Defects 98

Chapter 4: Overall Conclusions and Future Directions 101

4.1 Conclusions 101
4.2 Future Work 102
4.2.1 Investigating the Effect of Water Content on the Formation of SAMs 102
4.2.2 Study of the Influence of Nitric Acid on the Electroless Metal Deposition Process 104
4.2.3 Nuclear Magnetic Resonance (NMR) of Silane-Based SAMs 104
4.2.4 Attenuated Total Reflectance (ATR) IR Spectroscopy of Molecules in SAMs 106
4.2.5 Kelvin Probe Force Microscopy (KFM) of Defects in SAMs 107
4.2.6 Correction of Defects by Refilling Pinholes with Different Molecules 108

Appendix 2: Additional DATA 111

Appendix 3: References 119

LIST OF FIGURES

Figure 1-1 A schematic of self-assembled monolayers represents the three components of self-assembling molecules. Head groups interact with the surface, as spacer chains reinforce the structure of monolayers. Terminal functional groups are often used to modify the properties of a surface. 2

Figure 1-2 There are two steps in the deposition of self-assembled monolayers. (A) The silane molecules in the solution are dispersed and randomly oriented. (B) In the first step of self-assembly, the substrate-silane interactions and the van der Waals interactions between the silane molecules localize the molecules on the surface into densely packed monolayers. (C) Once the substrate is heated, the silane molecules condense onto the surface to form SAMs. 5

Figure 1-3 There are various sources of defects in silane-based SAMs: (A) pinhole defects consist of bare regions of the silicon oxide coated single crystalline silicon substrate; (B) physically adsorbed impurities on the surface effect the wettability of the substrate; (C) missing hydroxyl groups from the surface prevents the attachment of silane molecules onto the surface; (D) irregularities in the crystalline silicon substrate is reflected in the density of the molecules in SAMs on the substrate; and (E) metal impurities present on the substrate prevent silane molecules from forming covalent bonds to the surface. 10

Figure 1-4 A schematic representation of the incident light (I_i), the reflected light (I_r) and the transmitted light (I_t) shows the change in their polarization in an ellipsometry measurement. 17

Figure 1-5 In a scanning electron microscope, the interaction of the incident electrons with the sample generates secondary electrons, backscattered electrons, and X-rays. These signals are detected to generate topographical and compositional information about a sample. 20

Figure 1-6 A schematic representation of the emission process in the energy dispersive X-ray spectroscopy (EDS) shows a primary electron beam ejecting a core electron and generating an electron hole. This electron hole is filled in with an electron from an outer shell and energy released during the relaxation process is detected. 21

Figure 1-7 Atomic force microscopy (AFM) generates a topographical map of a surface by detecting the changes in the cantilever and different regions of a surface. 24

Figure 2-1 The effect of solvents and irradiation time on microwave-enhanced deposition of SAMs is monitored using water contact angle measurements. Silane molecules are deposited onto silicon oxide substrates from a 3.5 mM solution of FAS in 2-propanol, xylene, or toluene in a microwave oven at 300 Watts. The contact angles indicate that toluene is optimal solvent for the deposition of SAMs in a microwave oven. Note: the lines are used as guides for the eye to observe the trends. 37

Figure 2-2 The effect of FAS concentration on the packing density of molecules in SAMs is monitored using contact angle measurements. Silicon oxide substrates are immersed in solutions with varying concentration of FAS in toluene and irradiated for 75 seconds at 300 Watts. An increase in the FAS concentration results in an increase in the wettability of the resultant SAMs. 43

Figure 2-3 The effect of immersion time on the quality of microwave-prepared SAMs, after 75 seconds of heating at 300 Watts in a microwave oven, is evaluated by contact angle measurements. Increasing the immersion time results in the formation of densely pack silane-based SAMs. The 3.5 mM, 14 mM, and 28 mM solutions of FAS are prepared from silanes with a higher water content than those used for the preparation of the 7 mM solutions. 46

Figure 3-1 This schematic represents two types of defects in SAMs. (i) The pinhole defects and (ii) physically adsorbed molecules present on the surface after different correction steps. (A) The as-deposited silane-based SAMs are shown as well as (B) the extracted SAMs, where self-assembled monolayers are repeatedly washed with solvents to remove physically adsorbed molecules from the surface. (C) The refilling method is used to decrease the density of the pinhole defects in monolayers. 52

Figure 3-2 This schematic representation shows each silane deposition (S) and extraction (E) step. The number defects in silane-based SAMs decreases with repeated extraction and refilling steps. These images are of exaggerated samples to demonstrate the effect of extraction and refilling of defects. 67

Figure 3-3 Water contact angle measurements after each silane deposition (S) and extraction (E) step indicate an overall improvement in the wettability of SAMs. The silane molecules are deposited using the conventional approach during each deposition step. Note: the line is used as a guide for the eye to observe the trend..... 68

Figure 3-4 Water contact angles are collected after each silane deposition and extraction step for SAMs formed using both the microwave-prepared and conventional SAMs. Note: these lines are used as guides for the eye to observe the trends. 70

Figure 3-5 In this schematic representation, SAMs with (A) a low packing density of molecules are compared to (B) those with high packing density. The film thickness (h) increases and the adhesion angle (Θ) decreases as the molecules pack more densely in these monolayers. 73

Figure 3-6 The thickness of E1, E2, and E3 SAMs are measured for at least three points on each substrate using a spectroscopic ellipsometer. The thickness of the monolayers increases as the number defects decreases in silane-based SAMs. 74

Figure 3-7 Schematic representations of (A) FAS-based SAMs, (B) FPS-amplified SAMs, and (C) the extracted SAMs show FPS molecules attaching to the exposed silanol groups on the substrate or the physically adsorbed molecules on the surface. They may also physically adsorb to SAMs. Extraction removes the majority of the physically adsorbed molecules from the surface. 76

Figure 3-8 FTIR spectra of (A) untreated FAS-based SAMs is compared to those after (B) chemical amplification of defects in SAMs with IR-active FPS molecules. This chemical amplification enables us to monitor the presence of defects before and (C) after extraction of the FPS-treated FAS-based SAMs. The intensity of the IR peaks decreases after the extraction of physically adsorbed molecules from the surface. 78

Figure 3-9 SEM images of electroless silver deposition on S1 to E3 substrates (in a silver nitrate (1 mM) and buffered hydrofluoric acid (1% v/v) solution for 5 minutes) indicate that the density of silver particles (white spots) decreases on refilled and extracted substrates. 81

Figure 3-10 AFM images of SAMs are collected after electroless silver deposition by immersion of S1 to E3 substrates in to a silver nitrate (1 mM) and buffered hydrofluoric acid (1% v/v) solution for 5 minutes. Extraction and refilling of the defects increase the size and density of regions protected by SAMs. 83

Figure 3-11 Scanning electron microscopy image of electroless silver deposition (5 mM $AgNO_3$, 1% (v/v) HF, 16 h deposition) on a (A) silicon oxide substrate and (B) the corresponding EDS spectrum (2 μm^2 area and 100 seconds acquisition time) indicate that silver particles form on the surface of silicon oxide in the absence of silane-based SAMs. 86

Figure 3-12 X-ray photoelectron spectra of silver (3d) peak after performing EMD (1 mM $AgNO_3$ and 1% (v/v) HF) on S1, E1, S2, E2, S3, E3 and bare SiO_2 (Std) substrates suggest that correcting for defects reduces the amount of silver deposited on the substrates protected by SAMs. 88

Figure 3-13 The quantity of the silver on different surfaces is monitored by calculating the area under the XPS peaks for EMD treated (1 mM $AgNO_3$, 1% (v/v) HF, 5 minutes of deposition) SiO_2 and corrected SAMs. Note: the lines are used as guides for the eye to observe the trends. 89

Figure 3-14 The average size of the particles formed by EMD on S1 to E3 SAMs indicates that the corrected SAMs prevent the formation of large particles on the sites of the defects. The error bars are calculated as twice the standard deviation values. Note: the line is used as a guide for the eye to observe the trend. 91

Figure 3-15 Reaction of FAS molecules with silver ions in the presence of hydrofluoric acid results in the formation of a white powder. This powder is imaged using (A) transmission electron microscopy and analyzed by (B) energy dispersive X-ray spectroscopy. This data suggests that silver particles may form in the presence of silane molecules, but in the absence of a silicon oxide substrate. 92

Figure 3-16 Increasing the silver salt concentration and the deposition time lead to an increase in the size of the silver particles formed on the E3 SAMs. The silver salt concentration is calculated in millimolar. The concentration of the buffered hydrofluoric is kept constant (1% v/v) for all the data points shown in this graph. Note: the lines are used as guides for the eye to observe the trends. 95

Figure 3-17 The size of particles formed by immersing the E3 SAMs into a 1 mM solution of silver nitrate reduces upon decreasing the concentration of the buffered hydrofluoric acid and the reaction time. Note: the lines are used as guides for the eye to observe the trends. 97

Figure 4-1 An ATR crystal is often covered with SAMs to improve the signal-to-noise ratio of an IR signal to easily detect the molecules present in the monolayers. 106

Figure 4-2 Fluorophenyl silane-based SAMs are refilled with phenyl silanes to increase the intermolecular forces within the self-assembled monolayers. Note: The methyl groups of FPS molecules have been removed to enhance the clarity of the image. 109

Figure A.1 The AFM image of silicon substrate before the electroless deposition of silver (A) shows much smoother topography than

(B) after the immersion of the substrate into 1 mM silver nitrate and 1% (v/v) buffered HF for 5 minutes. 111

Figure A.2 AFM images of EMD on E3 substrates indicate that the number of silver particles decreases upon reducing the concentration of silver salt in the solution. The concentration of the buffered HF (1% v/v) and the deposition time (5 min) for these samples are kept constant. 113

Figure A.3 AFM images of EMD on E3 substrates indicate that the number of silver particles decreases upon reducing the concentration of silver salt in the solution. The concentration of the buffered HF (1% v/v) and the deposition time (1 min) for these samples are kept constant. 114

Figure A.4 AFM images of EMD on E3 substrates indicate that the number of silver particles decreases upon reducing the concentration of silver salt in the solution. The concentration of the buffered HF (1% v/v) and the deposition time (30 sec) for these samples are kept constant. 115

Figure A.5 AFM images of E3 substrates immersed in a 1% (v/v) HF solution for varying period of time indicate that the surface roughness due to HF decreases as the deposition time is decreased. 116

Figure A.6 AFM images of EMD on E3 substrates indicate that the number of silver particles decreases upon decreasing the concentration of buffered HF in the solution. The concentration of the silver nitrate (1 mM) and the deposition time (5 min) for these samples are kept constant. 116

Figure A.7 AFM images of EMD on E3 substrates indicate that the number of silver particles decreases upon decreasing the concentration of buffered HF in the solution. The concentration of the silver nitrate (1 mM) and the deposition time (1 min) for these samples are kept constant. 117

Figure A.8 AFM images of EMD on E3 substrates indicate that the number of silver particles decreases upon decreasing the concentration of buffered HF in the solution. The concentration of the silver nitrate (1 mM) and the deposition time (30 sec) for these samples are kept constant. 117

Figure A.9 The XPS survey scans are shown for the substrates (S1, E1, S2, E2, S3, E3, and standard SiO2) after the silver treatment..... 118

LIST OF TABLES

Table 1-1 Reduction potential values for metals commonly used in EMD.[51] 12

Table 2-1 Boiling point, dielectric constant (ε'), dielectric loss (ε''), and loss tangent (tan δ) values for six common solvents measured at 2.45 GHz.[44] 35

Table 3-1 IR vibrations of FPS molecules.[19, 24, 109] 77

GLOSSARY

AFM	Atomic Force Microscopy
ATR	Attenuated Total Reflectance
CMP	Chemical Mechanical Polishing
FAS	Chloro-(3,3,4,4,5,5,6,6,7,7,8,8,9,9,10,10,10-heptadecafluoro-decyl)-dimethyl-silane
FPS	Chloro-dimethyl-(2-pentafluorophenyl-ethyl)-silane
c-AFM	Conductive Atomic Force Microscopy
DPN	Dip Pen Nanolithography
EMD	Electroless Metal Deposition
EDS	Energy Dispersive X-ray Spectroscopy
FTIR	Fourier Transform Infrared
KFM	Kelvin Probe Force Microscopy
μCP	Microcontact Printing
MEMS	Microelectromechanical Systems
NMR	Nuclear Magnetic Resonance
SEM	Scanning Electron Microscopy
SAMs	Self-Assembled Monolayers
TEM	Transmission Electron Microscopy
UHV	Ultra High Vacuum
XPS	X-ray Photoelectron Spectroscopy

CHAPTER 1: INTRODUCTION TO SELF-ASSEMBLED MONOLAYERS

1.1 Self-Assembled Monolayers (SAMs)

Self-assembled monolayers (SAMs) are ordered arrangements of molecules that have assembled into single layers on a surface.[1] They were first discovered by Zisman in 1946 when he formed a monomolecular film of surfactants on a clean metal surface.[1] Over the past two decades, SAMs have often been used to model systems for fundamental studies such as controlling protein adhesion on substrates[2] and modifying the wettability and other interfacial properties of surfaces.[3, 4] These monolayers are also used to selectively pattern substrates in microcontact printing,[5] to reduce friction and stiction of surfaces in microelectromechanical systems (MEMS),[6, 7] and to modify the properties of metals, metal oxides and semiconductor surfaces[8] that are used in various fields of science.

Self-assembled monolayers are usually formed by placing a clean metal or semiconductor substrate in a solution of molecules.[9] Adhesion of molecules to the substrate lowers the free energy of the surface.[4] The change in the free energy is dependant on the surfactant used and can be modified as required.[10] The adhesion of functional molecules to the surface and the formation of SAMs are spontaneous processes due to the favourable interaction of the surfactant molecules with themselves and the surface.

The self-assembling molecules can be divided into three key components (Figure 1-1): i) the head group, ii) the linker or spacer chain, and iii) the terminal functional group. The head group interacts with the surface to provide the most exothermic step in the self-assembly process (tens of kcal/mol). The spacer or linker chains (e.g., alkyl chains) are brought close to each other through van der Waals interactions. The interaction between the linker chains is exothermic (<10 kcal/mol) and is considered to be the first step in the process of self-assembly.[9] The final component of these molecules is their terminal functional groups. These functional groups are disordered at room temperature and by bringing them into close proximity of one another is an endothermic process (~0.7kcal per *gauche* bond).[11] Formation of SAMs is an easy and accessible process used for the expression of different functional groups on the surface and tailoring the interfacial properties of a substrate.

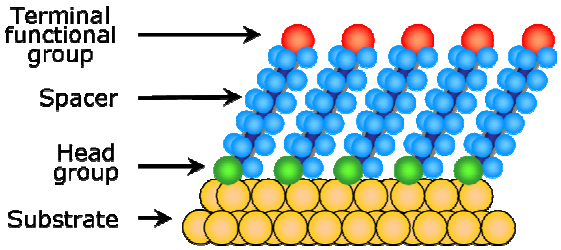

Figure 1-1 A schematic of self-assembled monolayers represents the three components of self-assembling molecules. Head groups interact with the surface, as spacer chains reinforce the structure of monolayers. Terminal functional groups are often used to modify the properties of a surface.

Formation of SAMs does not require specialized equipment such as a Langmuir-Blodgett trough or an ultra high vacuum (UHV) system.[12] Their ease of

synthesis and accessibility allow for convenient modification of the physical and chemical properties (e.g., wettability) of surfaces.[9, 12-14] Self-assembled monolayers are often used as etch resists to pattern surfaces in micro- and nanofabrication[15] or to generate low friction surfaces in engineering microelectromechanical systems.[2] They are also used in immobilizing proteins and other biomolecules in biological sciences.[16]

Three of the most commonly studied SAMs are formed from: i) the interaction of thiols with gold substrates,[12, 17] ii) the reaction of alkene derivatives reacting with silicon substrates, [18] iii) the attachment of silane molecules onto hydroxyl-terminated substrates.[9, 19, 20] A vast amount of research has been done on gold-thiol systems.[12, 17, 21, 22] The studies discussed here are conducted on the silicon oxide substrates that are modified with silane-based SAMs. In this thesis, investigations into techniques used to monitor the formation and assess the quality of the silane-based SAMs are discussed.

1.2 Silane-Based SAMs

Silane molecules form robust SAMs on a variety of surfaces such as aluminium oxide,[23] quartz,[24] mica,[25, 26] glass,[27] and more commonly silicon dioxide,[9, 24, 28] as well as many other substrates. Silane-based SAMs on silicon oxide surfaces are used for a variety of applications, such biological sensors and interfaces,[29] organic electronics,[30] and printing self-aligned source-drain contacts in microelectronics.[31] These monolayers form spontaneously due to the exothermic nature of the self-assembly process. Formation of polysiloxanes (Si-O-Si) between the silanol (Si-OH) groups of the silane molecules and the

substrate (SiO_2) is the main driving force in the formation of these monolayers. The formation of SAMs is, however, highly dependent on the amount of the surface bound water and the temperature of the condensation reaction.[32, 33] Another challenge in the reproducibility of the formation of these monolayers is overcoming the formation of molecular islands on the surface as opposed to the desired uniform film.[11, 34] In addition, di- and trichlorosilane derivatives can co-polymerize either on the surface or in the solution. The formation of these oligomers may lead to the generation of poorly packed self-assembled monolayers.[35] Monochlorosilane derivatives are used to prevent the formation of oligomers on the silicon oxide surface. In order to generate high quality silane-based SAMs, it is important to first understand the self-assembly process in detail.

There is evidence of a two step process for the formation of silane-based SAMs (Figure 1-2).[36] The first step is the assembly of silane molecules on a substrate. This assembly is achieved when the clean substrate (i.e., free of airborne or contaminants) is immersed into a solution of silane molecules dissolved in an organic solvent. Silane molecules physically adsorb onto the silicon oxide surface and rearrange to form densely packed monolayers. This packing is due to both the van der Waals interactions between the linker chains and substrate-silane interactions (Figure 1-2 B). The second step in the formation of the silane-based SAMs involves condensation reactions. During the condensation step, the substrate is heated and siloxane (Si-O-Si) bonds are formed between silane molecules and the silicon oxide surface. The

condensation of the silane molecules onto the surface generates covalently bound SAMs on the silicon oxide substrate (Figure 1-2 C). Both solution and vapour-phase deposition of silane-based SAMs follow these two steps.

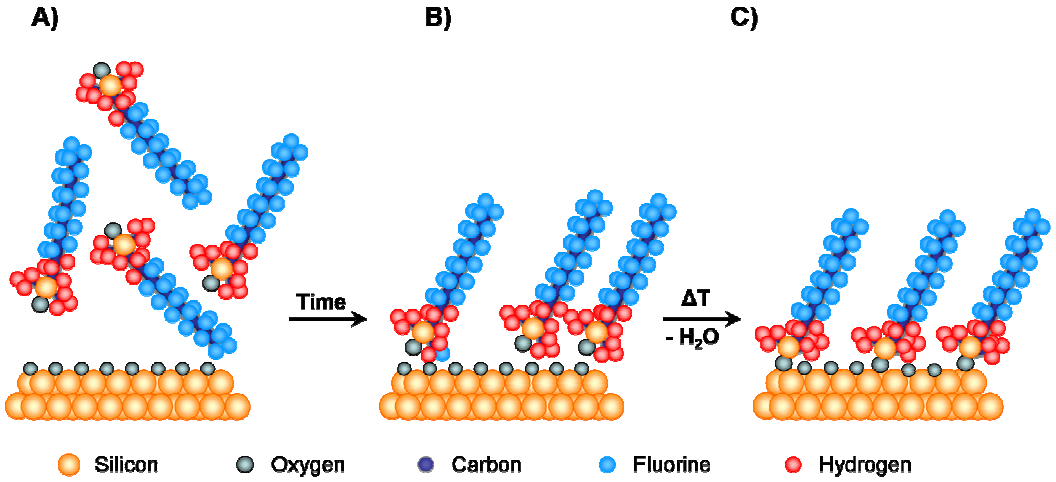

Figure 1-2 There are two steps in the deposition of self-assembled monolayers. (A) The silane molecules in the solution are dispersed and randomly oriented. (B) In the first step of self-assembly, the substrate-silane interactions and the van der Waals interactions between the silane molecules localize the molecules on the surface into densely packed monolayers. (C) Once the substrate is heated, the silane molecules condense onto the surface to form SAMs.

There are a few different approaches to the formation of self-assembled monolayers, all of which follow the two steps mentioned above. In all solution-phase silane deposition techniques, the first step is physical adsorption of silane molecules on the SiO_2 covered single crystalline silicon substrate, which is achieved by immersing the freshly cleaned (e.g., O_2 plasma cleaned or piranha washed) substrate into the silane solution at room temperature. A number of techniques can carry out the second step, in which these molecules are bound to the substrate by a condensation reaction. This thesis describes two different methods of condensation: the conventional thermal approach and a new

microwave approach. In the conventional thermal approach, the physically adsorbed SAMs are chemically linked to the substrate through a condensation step at high temperature (usually above 100 ºC) in an oven for a few hours. This thermal condensation is time consuming. It is, therefore, important to identify a method in which silane-based SAMs are generated faster than that required in the conventional thermal technique.

Here, the use of microwave irradiation to speed up the deposition of SAMs is reported. The interaction of the microwaves with the polar molecules in the solution provides the heat required for the formation of the siloxane bonds. This technique requires less than 50% of the time taken by the conventional thermal approach. The shorter reaction time reduces the necessary energy for the deposition of these monolayers by roughly 750 times. Due to the short reaction time and localization of microwave-produced energy, these reactions require higher concentrations of the silane molecules in the solution.

1.3 Microwave Enhanced Reactions

Microwave ovens were first used to accelerate a chemical reaction in 1986, specially for the hydrolysis of benzamide to benzoic acid under acidic conditions.[37] Over the past two decades microwaves have been employed to increase the rate of reactions in many areas of chemistry including organic synthesis,[38] analytical chemistry,[39] solid-state chemistry,[40] polymer chemistry,[39, 41] medicinal chemistry,[42] and nanoparticles synthesis.[43] In this thesis, microwave irradiation is used to speed up the condensation of silane-based SAMs onto silicon oxide coated single crystalline polished silicon substrates.

Microwaves interact with polar molecules and generate heat in the solution. Microwaves are electromagnetic waves consisting of an electric component and a magnetic component. The microwave frequency ranges from 300 MHz to 300 GHz. When polar molecules are placed in the path of microwave irradiation, they rotate to align their dipole moments with the electric field. However, the electric field component oscillates at ~10^9 cycles per second and the average kinetic relaxation of a molecule requires ~10^5 cycles per second seconds. Thus, polar molecules are constantly rotating in the applied microwave electric field in order to align their dipole moments with the electric field. This molecular rotation generates heat due to friction in the solution during microwave irradiation.[38, 44] Heat can be generated due to the presence of polar solvents, solutes, or catalysts in a microwave reaction.

Solvents can play different roles in a microwave-assisted synthesis. For example, polar solvents (e.g., ethanol) may be used to generate heat, whereas non-polar solvents (e.g., hexane) are often used as heat sinks to maintain the reaction at a constant temperature. Some solvents (such as chloroform or pyridine) can decompose at high temperature in the microwave oven and form harmful gases.[44] It is, therefore, important to identify possible side products before attempting a microwave reaction.

The first microwave reactions were carried out in domestic household microwave ovens, with little to no control of the temperature and pressure in the reaction. Current monomode and multimode microwave reactors allow precise control of the temperature and pressure inside the reaction vessel. Monomode

reactors provide accurate temperature control of a specific site within the microwave chamber. Multimode reactors also allow scientists to run multiple reactions with simultaneous control over the temperature and pressure of each reaction. Such microwave reactors are, however, expensive with their cost ranging from tens of thousands of dollars for a simple monomode reactor, to more than a hundred thousand dollars for a top of the line multimode reactor. For this reason, a domestic household microwave oven was used to carry out the initial experiments, detailed in this thesis.

Household microwave ovens irradiate different parts of the microwave chamber with different intensities. This non-uniform heating results in varying reaction rates in the different regions of the microwave chamber. Thus, the use of a household microwave for chemical reactions makes it difficult to identify and calculate the exact power introduced to the reaction vessel. Moreover, there is little control on the temperature of the reaction vessels. Regardless of the lack of precise control on the temperature of the reaction, SAMs are formed in domestic household microwave ovens. These household microwave ovens are accessible, affordable, and convenient for these preliminary studies to investigate the feasibility of the microwave-enhanced formation of silane-based SAMs. It is anticipated that using a microwave reactor, one will be able to deposit SAMs with even higher reproducibility.

1.4 Introduction to Defects in SAMs

Self-assembled monolayers are considered to be highly ordered, close-packed arrangements of molecules on the surface.[11] The applicability of SAMs

in materials and biological sciences is highly depended on the minimization of defects present in these monolayers. Defects in SAMs may result in macro, micro or nanoscale deficiencies on surfaces that are modified with these monolayers. For example, defects may act as a source of erratic signals in microelectronics[3] or could result in corrosion of the substrate in the presence of etchants.[22, 45] Defects may also diminish the applicability of SAMs in nano- and microfabrication processes,[5] lower the sensitivity of biosensors, and reduce the biospecificity in microarrays. It is, therefore, important to identify the location, and quantify the density of defects in SAMs.

Self-assembled monolayers contain various types of defects resulting from extrinsic or intrinsic sources.[12] Extrinsic sources of defects include cleanliness of the substrate, purity of the solvent and solute, as well as the method of preparation of the substrate. The intrinsic defects are due to the dynamic nature of self-assembly and are more difficult to eliminate in comparison with the extrinsic defects. Weak absorbate-surface interactions are an intrinsic source of defects in SAMs. Sufficiently strong intermolecular interactions are required to overcome entropy driven disorder to align the molecules into densely packed monolayers on a surface.[46] Another intrinsic source of defects in these monolayers is the sterically imposed strain on the molecules in SAMs, which ultimately lowers the stability of the self-assembled monolayers.[12] These extrinsic and intrinsic defects diminish the ability of SAMs to efficiently modify the physical and chemical properties of a substrate.

There are many intrinsic and extrinsic sources of defects causing irregularities in the silane-based SAMs (Figure 1-3). Pinholes are nanometer (or larger) sized holes in SAMs and are often formed when molecules do not cover the entire the surface (Figure 1-3 A).[3] Silane molecules or solvent impurities may physically adhere to the surface due to van der Waals interactions and result in the formation of extrinsic defects in these monolayers (Figure 1-3 B). There are

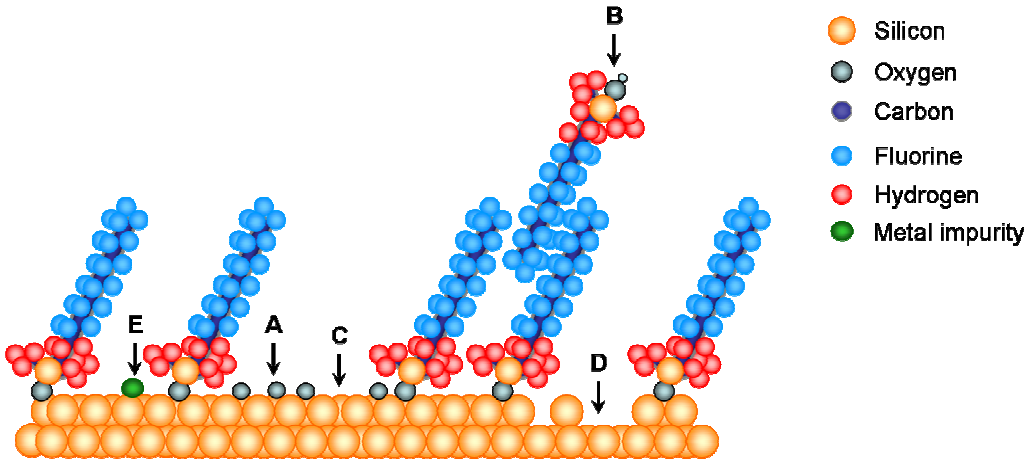

Figure 1-3 There are various sources of defects in silane-based SAMs: (A) pinhole defects consist of bare regions of the silicon oxide coated single crystalline silicon substrate; (B) physically adsorbed impurities on the surface effect the wettability of the substrate; (C) missing hydroxyl groups from the surface prevents the attachment of silane molecules onto the surface; (D) irregularities in the crystalline silicon substrate is reflected in the density of the molecules in SAMs on the substrate; and (E) metal impurities present on the substrate prevent silane molecules from forming covalent bonds to the surface.

many other sources of defects such as the occasional absence of hydroxyl groups on the silicon oxide surface (Figure 1-3 C), the molecular irregularities on the silicon oxide substrate (Figure 1-3 D), and metallic impurities remaining from the chemical-mechanical polishing (CMP) processes used to manufacture these

substrates (Figure 1-3 E). It is important to identify these defects in SAMs and to monitor their density during the correction process.

Various techniques, such as contact angle measurements, are used to detect the presence of SAMs on the surface. Most defects in silane-based SAMs are, however, too small to be detected using microscopy and spectroscopy techniques.[12] Various techniques are developed to tag or otherwise mark defects such that they are detectable using the instruments available in a typical Chemistry Department. These defects are commonly amplified using an electroless metal deposition (EMD) technique, where the metal particles grow on the exposed defects in SAMs.[47] The density of the defects is monitored by coupling the chemical amplification techniques (such as EMD) to various spectroscopy and microscopy methods. A detailed discussion of the amplification and the characterization techniques used in this thesis are provided in this chapter.

1.5 Electroless Metal Deposition (EMD)

Electroless metal deposition is the spontaneous reduction of metal ions to metal seeds and their growth into metallic particles or films in the absence of an external electrical source. Electroless deposition of metals such as Ag, Au, Pd, and Pt results in the formation of nanoparticle films and is compatible with patterning techniques such as microcontact printing (μCP), dip pen nanolithography (DPN), and photolithography.[47] Electroless metal deposition is an easy and accessible approach to the selective deposition of metal nanoparticles onto a surface. Many physical properties of metal nanoparticle

(e.g., Ag, Au, Pd, and Pt) films can be precisely controlled by monitoring the size of the nanoparticles, as well as the thickness and roughness of the metal film. These physical properties can be used to monitor the progress of an electroless deposition process.[48] This precise control over the properties of the deposited metal films allows these films to be used as high-surface area catalysts and probes for surface-enhanced Raman spectroscopy.[49, 50] Many metals (e.g., Ag, Au, Pd, and Pt) can be electrolessly deposited on a silicon substrate.[47,48] Silver is easily reduced due to its low reduction potential compared to the other three metals (Table 1-1). It is, therefore, a better system to study molecular-scale defects in silane-based SAMs.

Table 1-1 Reduction potential values for metals commonly used in EMD.[51]

Reactions	E° (V)
$Ag^{+} + e^{-} \rightarrow Ag$	0.80
$Pd^{2+} + 2e^{-} \rightarrow Pd$	0.95
$Pt^{2+} + 2e^{-} \rightarrow Pt$	1.18
$Au^{3+} + 3e^{-} \rightarrow Au$	1.50

Electroless metal deposition is fast, low cost and autocatalytic.[52, 53] In an autocatalytic process, the reduced metal serves as a catalyst for further reduction of ions. Autocatalytic processes tend to form thick films and can easily be detected using atomic force microscopy (AFM), scanning electron microscopy (SEM), and X-ray photoelectron spectroscopy (XPS). The reducing agent in electroless metal deposition can be a solute or a substrate that acts as a source

of electrons. For instance, the silicon substrate can act as the reducing agent during the electroless deposition of metals on the site of defects in SAMs. Electroless metal deposition is a quick and accessible technique used to amplify defects in silane-based SAMs.

In this research, silver nanoparticles are electrolessly deposited on silicon substrates covered with silane-based SAMs. Silver nanoparticles only grow in the presence of exposed silicon and thus they highlight the location of defects in the deposited monolayers. These silver particles are located and analyzed using atomic force microscopy, scanning electron microscopy, and X-ray photoelectron spectroscopy.

1.6 Methods of Characterizing SAMs

Self-assembled monolayers are often used to protect surfaces from oxidation or otherwise modify surface properties.[54] The successful modification of a surface is predominantly dependent on the packing density and the number of defects present in these monolayers. The quality and packing density of SAMs are often evaluated using contact angle measurements,[55-58] ellipsometry,[59-61] Fourier transformed infrared (FTIR) spectroscopy,[36, 62-64] scanning electron microscopy (SEM),[65-69] energy dispersive X-ray spectroscopy (EDS),[65, 70, 71] X-ray photoelectron spectroscopy (XPS),[72-74] and various types of scanning probe microscopy techniques such as atomic force microscopy (AFM) and Kelvin probe force microscopy (KFM).[34, 72, 75-77] The majority of these techniques provide information that is averaged over a large (a few square micrometers to a few square millimeters) area of the surface.

To achieve molecular-scale information and to identify the location and density of defects, these techniques are coupled with chemical amplification of defects in SAMs. This chemical amplification highlights the location of the defects, so that they are detectable from the surrounding surface by techniques such as FTIR spectroscopy, atomic force microscopy, scanning electron microscopy, and X-ray photoelectron spectroscopy. In the following sections, a summary of each of these techniques is discussed along with its advantages and disadvantages in investigating defects in SAMs.

1.6.1 Contact Angle Measurements

Water contact angle of a surface is a measure of its surface free energy.[78] Deposition of SAMs onto a silicon oxide surface decreases its surface free energy and, therefore, changes the wettability of a surface.[79] The free energy of the surfaces modified with SAMs is monitored by placing a small (e.g., 2 μL) droplet of water on top of the surface and measuring its contact angle The value is defined by Young's equation:

$$\gamma_L \cdot \cos\theta = \gamma_{SV} - \gamma_S \qquad \textbf{Equation 1-1}$$

Young's modulus (γ) is a measure of the tension between the molecules of the liquid (γ_L), or solid and vapour (γ_{SV}) or solid and liquid (γ_{SL}).[80] As the solid-liquid interaction increases the contact angle (θ) reduces. Therefore, one would expect a hydrophilic surface to have a low water contact angle value.

Advancing and receding contact angles are often measured to gain an understanding of the surface heterogeneity. Advancing contact angle is evaluated by continual addition of water droplets to the surface. The added water continuously moves physically adsorbed particles or molecules away from the center of the droplets. Continuous removal of the droplets from the surface enables us to measure the receding contact angles. Water droplets interact with parts of the surface with different wettability during the advancing and receding contact angle measurements. The advancing and receding contact angles often differ in value. Advancing contact angles are usually higher than the receding contact angles. The difference is referred to as the wetting hysteresis. This hysteresis is attributed to the interaction of the water droplets with the various parts of the surface with different roughness, surface heterogeneity, and adsorbed solution impurities.[81] The presence of physically adsorbed molecules or particles on the surface may be the cause of the variation in the surface roughness and heterogeneity.

Silane-based SAMs on silicon oxide substrates are often used to reduce the surface free energy of the hydrophilic silicon oxide substrate. It is known that the addition of $–CF_3$ functional groups to a surface significantly reduces its surface free energy.[82] Scientist have used fluorinated molecules to generate hydrophobic surfaces for many biological and industrial applications.[83] Self-assembled monolayers of fluoroalkyl silane derivatives are generated on silicon oxide coated single crystalline silicon substrates to study the quality and packing density of silane-based SAMs by measuring the wettability of the modified

surface. The presence of fluorinated SAMs on a surface is easily detected using contact angle measurements. These measurements, however, provide an average over a large area (few square millimeters) of the surface and do not provide molecular level information such as the location of defects in SAMs.

1.6.2 Spectroscopic Ellipsometry

Spectroscopic ellipsometry is a method of accurately measuring various properties such as thickness, refractive index, and extinction coefficient of thin metal, polymer or semiconductor films.[59-61] The vertical resolution of this technique is < 0.1 Å. This technique enables researchers to identify the average thickness of individual layers in a multilayered sample.

Spectroscopic ellipsometry measures the properties of a substrate by illuminating the surface with linear polarized light (Figure 1-4). Linear polarization is achieved when the phase and amplitude of the light in the x and y directions are equal along the direction of propagation. According to Snell's Law, this light may reflect from or transmit through the substrate at the surface-air interface.[84] The interaction of the light with the surface changes the phase and amplitude of the reflected light and results in the polarization of the reflected light being modified from linear to elliptical. The changes in the amplitude of the incident light and that of the reflected light are measured and the amplitude ratio (tan Ψ) is calculated. The difference in the phase of the incident light and the reflected light is denoted as the phase-shift (Δ). The amplitude ratio and the phase shift values are used along with various models to calculate different parameters such as layer thickness or refractive index of various films.[84]

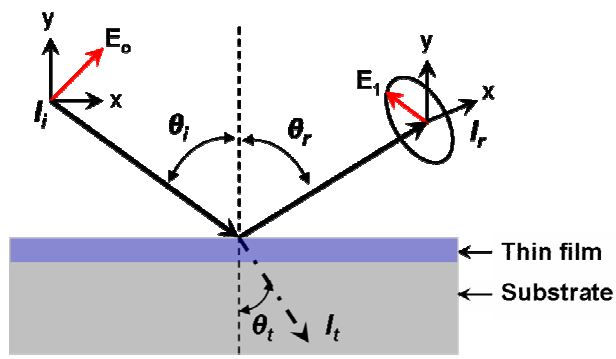

Figure 1-4 A schematic representation of the incident light (I_i), the reflected light (I_r) and the transmitted light (I_t) shows the change in their polarization in an ellipsometry measurement.

Spectroscopic ellipsometry is a quick and non-destructive technique to study the properties of SAMs. This technique provides an average film thickness over a large area of the surface (usually1 mm^2, depending on the instrument). The spatial resolution of this technique is insufficient for collecting molecular-scale information of a substrate. Spectroscopic ellipsometry cannot provide information concerning the location of defects on a surface.

1.6.3 Fourier Transform Infrared (FTIR) Spectroscopy

Fourier transform infrared (FTIR) spectroscopy is used in materials science to quickly identify the chemical composition of materials.[36, 62-64] This technique identifies molecules by measuring their infrared absorption (or emission) spectrum. In a FTIR spectrometer, molecules are illuminated with two IR beams (one with fixed length and other with variable length).[85] The energy of the IR irradiation is absorbed by molecules and is transformed into molecular vibrations. This absorption is quantized and specific to different covalent bonds

within various chemical functional groups. The combination of the two IR beams produces a series of constructive and destructive interference patterns and results in variation in the intensities of the IR irradiation forming an interferogram. Fourier transformation converts this interferogram to an IR spectrum, which can be used to identify the functional groups present on the surface.[86]

There are many advantages in using FTIR spectroscopy. For instance, it allows simultaneous analysis of multiple frequencies. Its high signal-to-noise ratio, high resolution (<0.001 cm^{-1}), and low detection limit (micro- or nanograms of sample) makes it a quick and qualitative measurement to identify the presence of organic compounds in self-assembled monolayers.[87, 88] Thus, FTIR spectroscopy is a useful tool in studying SAMs.

It is important to note that the detection limit of FTIR is dependent on environmental factors such as the temperature and the level of water and CO_2 present in the air. In addition, this spectroscopy technique provides an average value over regions of at least 10-15 μm of the surface and, does not allow for identification of the location or accurate assessment of the size of defects. Fourier transform infrared spectroscopy is a quick and convenient tool to qualitatively study self-assembled monolayers, but it is not useful for identifying the location of defects in SAMs.

1.6.4 Scanning Electron Microscopy (SEM)

Scanning electron microscopy (SEM) is a technique that is used to generate three-dimensional images of nano and microscale particles or biological

molecules on surfaces.[89, 90] In a scanning electron microscope, a focused beam of electrons penetrates and interacts with the molecules on the surface of the substrate. These interactions result in the generation of secondary electrons, back scattered electrons, and X-rays (Figure 1-5). These signals are detected and analyzed in order to collect information about the topography, crystallinity, and composition of a surface.[91]

The primary electrons penetrates the surface and generate secondary electrons, back scattered electrons and X-ray. Secondary electrons are generated when an incident electron results in the ionization of an atom on the substrate. The electron ejected from the atom is known as the secondary electron and provides topographical information about a substrate. The interaction of the primary electrons with the sample's electrons results in the emission of low energy secondary electrons. The orientation of the features on the surface influences the number of secondary electrons reaching the detector. The variation in the intensity of the secondary electron beam is used to generate a map of surface topography. The backscattered electrons are generated when the incident electrons interact with the surface and are scattered at 180 degrees to that of the incident beam. These high-energy electrons penetrate deep into the surface. The energy of the backscattered electrons is directly related to the atomic weight of the elements in the sample. The signals collected from the backscattered electrons provide information about the composition of the surface. Scanning electron microscopy is often coupled with energy dispersive X-ray spectroscopy (EDS) to analyze the X-rays emitted from the surface, due to

electron relaxation in the atoms. The collected X-rays provide compositional information about the surface. This technique will be discussed in detail in the next section.

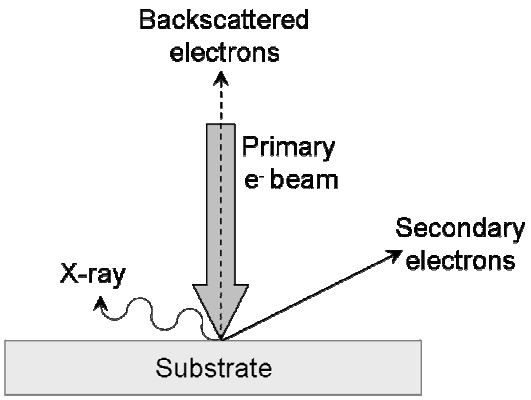

Figure 1-5 In a scanning electron microscope, the interaction of the incident electrons with the sample generates secondary electrons, backscattered electrons, and X-rays. These signals are detected to generate topographical and compositional information about a sample.

Scanning electron microscopy is a quick and useful technique to generate valuable information about the topography of a surface, as the spatial resolution of SEM can be as low as ~5 nm. This spatial resolution is insufficient to identify molecular-scale defects in SAMs.[92] Scanning electron microscopy can, however, provide important information such as density and distribution of defects in SAMs, when they are sufficiently amplified.

1.6.5 Energy Dispersive X-ray Spectroscopy (EDS)

Energy dispersive X-ray spectroscopy (EDS) is used to identify the atomic composition of a surface.[65, 70, 71] A specific amount of energy is required to remove core electrons from different atoms. Energy dispersive X-ray spectroscopy uses this phenomenon to simultaneously identify the presence of a

wide range of atoms (beryllium to americium) on the surface.[91] In this technique, the surface is bombarded with electrons to remove an electron from the inner shell of the atom, forming an electron hole. This hole may be filled in with an electron from the outer shell, resulting in the release of energy in the form of an X-ray (Figure 1-6). The X-rays are detected and their energies are correlated to transition energies for outer shell electrons of specific elements. This technique enables simultaneous identification of various elements on a surface.

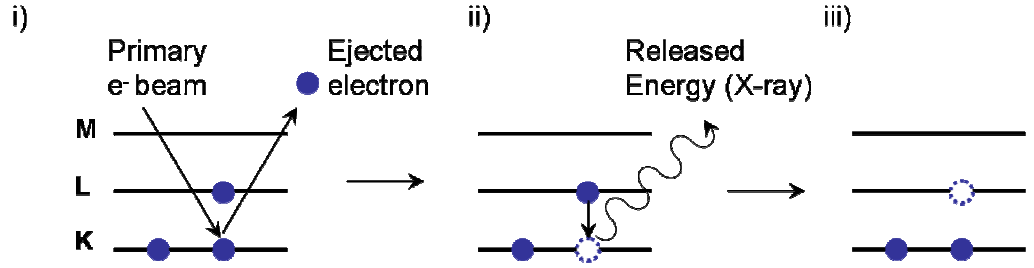

Figure 1-6 A schematic representation of the emission process in the energy dispersive X-ray spectroscopy (EDS) shows a primary electron beam ejecting a core electron and generating an electron hole. This electron hole is filled in with an electron from an outer shell and energy released during the relaxation process is detected.

Energy dispersive X-ray spectroscopy is not a surface specific technique. The primary electrons penetrate and sample a large depth (1 μm or more depending on the accelerating voltage) into the substrate. This technique is also insufficient in identifying the molecular-scale defects in monolayers. In addition, the sensitivity of this technique varies for different elements. The spatial resolution of EDS ranges from 0.03 μm to several micrometers.[91] Energy dispersive X-ray spectroscopy does not provide any information about the location of defects in SAMs due to the low spatial resolution and large

penetration depth of the primary electrons. It is important to develop a technique to amplify the defects in silane-based SAMs so they are easily distinguishable from the background and air-borne contaminants.

1.6.6 X-ray Photoelectron Spectroscopy (XPS)

X-ray photoelectron spectroscopy (XPS) provides information about the composition and oxidation states of atoms present on the surface.[72-74] In this technique, the surface is bombarded by X-ray photons of specific energy (hv). The binding energy (E_B) of a core electron is dependant on the atomic orbital the electron occupies and the chemical environment of the atom. The binding energy of an electron may be overcome by the energy (hv) of an incident X-ray photon. This phenomenon is known as the photoelectric effect and may cause the ejection of an electron with the kinetic energy (E_K). This kinetic energy is measured by an electron spectrometer with a work function Φ_d and is used to identify the atoms present on the surface. Conservation of energy suggests:

$$E_B = hv - E_k - \Phi_d \qquad \textbf{Equation 1-2}$$

The energy of the ejected electron is dependent on the orbital and the chemical state of the atom and can be detected by a spectrometer.

X-rays penetrate to a depth of tens of angstroms into the surface and provide information on the thickness of the film, absorbate morphology (clusters/islands of molecules or a uniform and conformal layer), as well as the mode of adsorption of molecules to the surface (covalently bound or physically

adsorbed). X-ray photoelectron spectroscopy penetrates 5 to 100 angstroms into the surface and has a detection limit of 0.1 atom percent with a spatial resolution of 30 μm.[81] The low penetration depth of the XPS enables us to identify the composition of the surface and not the bulk substrate. This technique cannot be employed to map the location and distribution of defects, but may be used when coupled with chemical amplification to highlight and compare the density of defects in different silane-based SAMs.

1.6.7 Atomic Force Microscopy (AFM)

Atomic force microscopy (AFM) can be used to produce a topographical map of a surface.[29, 48, 72, 75] It uses a sharp (typically <10 nm diameter) probing tip made of silicon or silicon nitride to scan the surface. The AFM cantilever is oscillated at a frequency in the range from 70 kHz to 350 kHz. This frequency is often near the fundamental oscillation frequency of the cantilever and is employed to increase the detection sensitivity to small topographical changes on the surface. For example, for tapping mode imaging, the cantilever is often oscillated at -5% of its frequency of fundamental resonance. In the proximity of a surface, the resonant frequency of the cantilever changes due to forces encountered between the surface and the tip. These forces, including capillary, electrostatic, van der Waals and frictional forces, range between 10^{-13} and 10^{-6} N.[81, 93] The tip to surface interactions result in a shift in the frequency of oscillation and can be detected by monitoring the changes in the laser beam reflected off the back of the cantilever (Figure 1-7). These frequency changes

are used to produce a three dimensional topographical map of the surface and to provide subatomic vertical resolution.

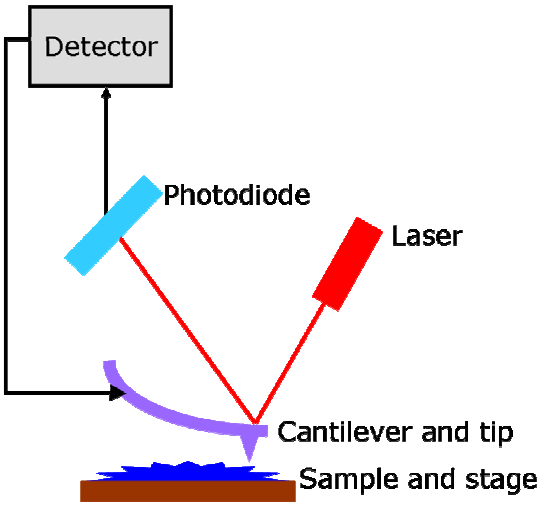

Figure 1-7 Atomic force microscopy (AFM) generates a topographical map of a surface by detecting the changes in the cantilever and different regions of a surface.

There are two common modes of atomic force microscopy imaging: tapping mode and contact mode. In tapping mode, the tip oscillates above the surface and the slight changes in the oscillation frequencies are detected. This mode of AFM imaging is much less harmful to the surface than contact mode imaging, where the tip is in physical contact with the surface. Contact mode imaging could damage or alter the surface by displacing the physically adsorbed particles on the substrate. Tapping mode AFM is used in this thesis to characterize semiconductor surfaces. The height of silane-based SAMs ranges from ten to thirty angstroms. Tapping mode AFM imaging is often used to detect the presence of these SAMs. The lateral spatial resolution of an AFM is, however, limited by the diameter of the AFM tip (typically >10 nm) and is insufficient to obtain molecular information in the x-y direction (unless sharp tips

with small diameters are used). This technique is a useful tool for identifying defects in SAMs only after the defects are highlighted using chemical amplification prior to imaging.

1.7 Overview of Thesis

In this thesis, the conventional technique used to form silane-based SAMs is discussed and a new technique to deposit these monolayers using microwave irradiation is introduced. The advantages and disadvantages of using these deposition techniques are highlighted and the quality of the overall SAMs is compared by investigating the density of defects present in these monolayers. Chapter 2 provides detailed information on the deposition of silane-based SAMs using both the conventional thermal technique and the microwave-prepared deposition methods.

Self-assembled monolayers deposited by both conventional and microwave methods contain molecular-scale (or larger) defects. The presence of defects in these monolayers lowers the quality and applicability of these SAMs in uniformly protecting or altering properties of surfaces. Identification of these defects is the first step in improving the applicability of SAMs in protecting surfaces and modifying their physical and chemical properties.

Identification of the location and density of defects requires tools that provide molecular-scale information about SAMs and the substrate. The presence of silane-based SAMs on a substrate is monitored using water contact angle, FTIR, and ellipsometry measurements. These techniques are limited in

their assessment of SAMs, as they do not provide any information on the location and density of defects in SAMs.

Most surface techniques available to chemists average the results over a large (few micro- or millimeter) area and are not applicable in molecular-scale studies. Few microscopy methods are available to provide maps of the surface with nanometer scale resolution. To identify the location of the defects, chemical amplification is required prior to using these microscopy techniques. Two methods of amplification are used to highlight the location of defects. Electroless metal deposition technique is used to form silver nanoparticles on the exposed defects. These nanoparticles are much larger than the molecular defects themselves, and are much easier to identify using atomic force microscopy and scanning electron spectroscopy. The amount of silver formed on different silane-based SAMs is quantified using X-ray photoelectron spectroscopy.

The types of defects in SAMs are further investigated by chemical amplification of the defects using IR-active molecules. This amplification allows the use of FTIR spectroscopy to identify the presence of defects in the silane-based SAMs. Once, the location and density of the defects are identified, various techniques are used to decrease the number of defects in these monolayers. This transformation is monitored using the microscopy and spectroscopic techniques mentioned above. Detailed information on amplification, identification, and correction of defects is discussed at length in Chapter 3. This thesis will be concluded by proposing future studies to identify defects and to characterize microwave-prepared SAMs.

CHAPTER 2: MICROWAVE-ASSISTED DEPOSITION OF SAMS

2.1 Introduction to Microwave-Assisted Deposition of SAMs

Deposition of silane-based self-assembled monolayers is a time and energy intensive process. Yet, these monolayers are often used in materials science to pattern or otherwise modify semiconductor surfaces. It is important to develop a sustainable, time efficient process to form silane-based SAMs without compromising their quality.

Over the past two decades, microwave irradiation has been employed to increase the rate of chemical reactions in different fields of chemistry and biochemistry. Over the past few years, material chemists have begun to take advantage of microwave-enhanced reactions since these reactions provide rapid volumetric heating, high reaction rates and selective high yield products.[94] Microwave-assisted chemistry is also considered a green approach to chemical synthesis due to its speed and efficiency.[95] A variety of nanostructures with different compositions have been synthesized[43, 94, 96] and their surfaces have been decorated[97] using microwave-assisted chemistry. Microwave irradiation has also been used to speed up the solution-phase deposition of gold films on glass substrates.[98] A method to deposit silane-based SAMs on silicon oxide coated single crystalline silicon substrate using microwave irradiation is reported in this thesis. Unfortunately, microwave irradiation is not spread uniformly in the

chamber of microwave ovens and moreover there is no precise control over the reaction temperature. This lack of control and non-uniform heating is the reason for the presence of the rotating stage in standard household microwave ovens. For these studies, the location of the “hot spots” in the microwave chamber is identified. Hot spots refer to the areas where the microwave irradiation is at its highest intensity. Reaction vessels are placed in these hot spots to increase the efficiency with which the microwaves accelerate the reactions.

In planning any microwave reaction, one should be cautious of the type of solvent used. For instance, chlorinated solvents such as dichloromethane and chloroform generate harmful hydrogen chloride gas. Nitrogenous solvents such as dimethylformamide, acetonitrile and pyridine form CO, CO_2 and N_xO_y gases that are also dangerous to the users.[44] Another concern is solvents with a low flash point that may cause a fire in the microwave oven. Commercial microwave reactors are built to contain any fire, but kitchen microwave ovens are not constructed for such applications. Domestic household microwave ovens can be modified to lower the risk of fire. For instance, one may constantly purge the microwave chamber or the reaction vessel with an inert gas such as nitrogen. The absence of oxygen lowers the chance of fire or explosion during the microwave heating and makes microwave-assisted chemistry a safe approach to heating chemical reactions.

Microwave reactors are often used in both academic and industrial laboratories. They provide precise control of the temperature of the reaction vessel by controlling the intensity of microwaves entering the microwave

chamber. Household microwave ovens are an easily accessible replacement for a microwave reactor. A microwave reactor was not available for this research and, therefore, a domestic household microwave oven was used for all of the reactions reported in this thesis. Both the microwave reactors and the household microwave ovens operate at a frequency of 2.45 GHz, which does not overlap with the frequency used for radar and cellular phones.[42, 44] In this chapter, investigations into using microwave irradiation to speed up the deposition of silane-based SAMs on silicon oxide covered single crystalline silicon substrates are discussed.

2.2 Experimental

2.2.1 Materials

Single-side polished (100) silicon wafers (SiliconSense, Inc.) were used as the substrate of choice for the deposition of silane-based self-assembled monolayers. These substrates were cleaned using a 7:2 mixture of sulfuric acid (Anachemia Canada Inc.) and 50% (v/v) hydrogen peroxide (VWR) to remove any organic molecules from the surface. A solution of FAS (90%, Alfa Aesar) in various solvents such as toluene (Reagent Grad, Caledon Laboratories Ltd.), 2-propapnol (Reagent Grad, Caledon Laboratories Ltd.), or xylene (Reagent Grad, Caledon Laboratories Ltd.) was prepared. The cleaned substrates were immersed in this solution. A digital AST Optima contact angle system with a horizontal light beam was employed to study the wettability of SAMs. Cleaning the Substrate

2.2.2 Cleaning the Substrate

Silicon substrates were immersed into a piranha solution, a 7:2 by volume mixture of sulfuric acid and hydrogen peroxide respectively, for 15 minutes. (**Caution:** *This mixture reacts violently with organic material and should be handled with care.)* Piranha solution was used to remove organic molecules from the surface. The substrates were subsequently rinsed with ~ 500 mL of 18.2 MΩ water and dried under a stream of nitrogen gas.

2.2.3 Deposition of Microwave-Based SAMs

Microwave-based SAMs were prepared on clean silicon oxide substrates. They were immersed into a solution of FAS (20 mL) in various solvents (toluene, xylene or 2-propanol), in an evaporating dish covered with a watch glass. This step provided the required time for the generation of the physically adsorbed monolayers on the SiO_2 surface. These SAMs were covalently linked to the substrate through the condensation step in the appropriate oven.

Piranha cleaned and dried silicon oxide substrates were incubated into a 20 mL solution of FAS in various solvents (toluene, xylene, and 2-propanol) with concentrations ranging from 1 μM to 1 mM. The incubation time varied from zero to 120 minutes for different samples. This incubation provided the required time for silane molecules to assemble and physically adsorb to the surface of the substrate. To condense the silane molecules to the substrate, the immersed substrate in the solution was heated in the microwave at 300 Watts for zero to 150 seconds (varying with different experiments). The substrate, now covered

with SAMs, was removed from the solution, rinsed with approximately 200 mL of toluene, and dried with nitrogen gas.

2.2.4 Extraction and Refilling of Defects in Silane-Based SAMs

The substrates covered with SAMs were placed in a Soxhlet extractor and rinsed with roughly 150 mL toluene at ~111 ℃ for 3 hours to remove the physically adsorbed molecules. The solvent evaporated and condensed in the water-based condenser. The clean, condensed solvent poured over the substrate and repeatedly rinsed the physically adsorbed molecules from the surface. This evaporation and condensation of solvent was repeated multiple times during the extraction period. This extraction removed any physically adsorbed molecules or particles from the surface and resulted in exposure of pinholes in SAMs.

The exposed pinholes were refilled by immersing the substrate into the FAS solution in toluene. To refill the conventional SAMs, the substrates were immersed into a 1 mM solution of FAS in toluene for 3 hours at room temperature prior to condensation in the 100 ℃ convection oven for 3 hours. For the microwave-prepared SAMs, the substrates were immersed into 7 mM solution of toluene for 5 minutes prior to microwave irradiation at 300 Watts for 75 seconds.

2.2.5 Contact Angle Measurements

The packing density of SAMs was studied before and after extractions, using a digital AST Optima contact angle system with a horizontal light beam. The quality of SAMs was studied by measuring the advancing and receding

contact angles. High purity (18.2 MΩ) water droplets (2.0 ± 0.3 μL) were dispensed onto or removed from the surface at room temperature to measure the advancing and receding contact angles. Digital images of the droplet were captured and used to measure the water contact angles. The error bars were calculated as twice the standard deviation of the advancing and receding contact angles.

2.3 Results and Discussion of Microwave-Assisted Deposition of SAMs

Silane-based SAMs are often used as a protective coating on semiconductor surfaces against adhesion of unwanted molecules or corrosive chemicals.[54] It is important to decrease the time (six hours) required for the formation of these monolayers and develop an efficient method to deposit silane-based SAMs without compromising their quality. Microwave-enhanced reactions have been used in various fields of chemistry for increasing reaction rates, product specificity, and energy efficiency.[38, 42, 99, 100] Microwave heating is used to accelerate the condensation step in the deposition of silane-based SAMs on an oxide covered silicon substrate. Microwave heating is specific to polar molecules and allows for a rapid increase in the temperature of a solution. This heating is independent of the thermal conductivity of the solvent and does not alter the structure of the molecules.[44] Microwave heating allows one to quickly increase the temperature of solvents to high temperatures.

During a microwave-assisted reaction, the polar molecules in the solution heat up rapidly and can result in increasing the solvent temperature to values

above its boiling point. This effect, referred to as “super-heating”, occurs when all molecules of solvents are heated at the same rate. In any vessel, boiling and evaporation occurs only at the liquid-air interface. During the microwave irradiation, all the polar molecules in the solution simultaneously heat up, independent of their placement in the solution.[44] In the absence of stirring, the gas bubbles are less likely to form and the solvent tends to super-heat. The super-heating of the solution mixture to temperatures above its boiling point can be prevented by constantly stirring the solution mixture. The temperature of the solution decreases to its boiling point when the solvent molecules start to boil and generate gas bubbles in the presence of impurities, defects, or stirring. Super-heating can be used to increase the reaction rate. Empirical observations suggest that increasing the reaction temperature by 10 ºC doubles the rate of the reaction.[42, 101] The rapid heating of the solution mixture to high temperatures in the microwave oven speeds up the deposition of SAMs. Microwave irradiation can, therefore, provide a time and energy efficient approach to formation of silane-based SAMs.

Various factors influence the quality SAMs deposited on oxidized silicon in a microwave oven. These factors include choice of solvent, irradiation time, microwave power, and solute concentration. In this study, the influence of these factors on the packing density of silane-based SAMs deposited in a domestic household microwave oven operating at 2.45 GHz frequency with a pulsed power of 300 Watts is investigated. The quality of these SAMs is monitored using water contact angle measurements. The goal of this research is to achieve

hydrophobic SAMs using microwave irradiation in a shorter period of time than that usually required for conventionally heated reactions.

2.3.1 The Choice of Solvent for Microwave-Assisted Deposition of SAMs

Solvents play an important role in a microwave-enhanced synthesis. The ability of a solvent to convert electromagnetic energy to thermal energy is dependent on its dielectric constant (ε') and dielectric loss (ε''). Dielectric constant is the measure of the ability of a solvent to store electric charge and it ranges in value from 1 to 80. The solvents with high dielectric constant store electric charge more effectively than solvents with low dielectric constant. Solvents with low dielectric constant often heat up rapidly in a microwave-assisted reaction. Dielectric loss represents the amount of input electromagnetic energy that is converted into heat and ranges from 0.03 to 50 for different solvents. Solvents with high dielectric loss convert electromagnetic energy into heat more rapidly. Solvents with a small dielectric constant and a large dielectric loss heat rapidly in the presence of microwaves. The effect of these two factors is summarized into a physical term called the loss tangent (tan δ). The loss tangent of a solvent is defined as the efficiency of a solvent in converting electromagnetic energy to heat.[44] The loss tangent (tan δ) is defined as follows:

$$\tan \delta = \varepsilon''/\varepsilon' \qquad \textbf{Equation 2-1}$$

Table 2-1 summarizes the boiling point temperature, dielectric constant, dielectric loss, and loss tangent values for six commonly used solvents.

Table 2-1 Boiling point, dielectric constant (ε'), dielectric loss (ε''), and loss tangent (tan δ) values for six common solvents measured at 2.45 GHz.[44]

Solvent	Boiling Point (º C)	Dielectric Constant (ε')	Dielectric Loss (ε'')	Loss Tangent (tan δ)
Xylene	144	2.6	0.047	0.018
Hexane	69	1.9	0.038	0.020
Toluene	111	2.4	0.096	0.040
Water	100	80.4	9.889	0.123
2-Propanol	82	18.3	14.622	0.799
Ethanol	78	24.3	22.866	0.941

Solvents with high tan δ value and low boiling point temperature (such as 2-propanol) heat up quickly and evaporate rapidly in a microwave oven. Solvents with low tan δ require a longer time to heat up and are categorized as low absorbance level solvents.[44] Xylene and toluene are examples of low absorbance level solvents and may be used to remove the excess heat from the solution during microwave synthesis or deposition of SAMs. Solvents with a high boiling point and low vapour pressure are preferred for the formation of silane-based SAMs in a microwave oven.

Solvents usually heat up to temperatures above their boiling point in a microwave oven, which is the main cause of the increase in the rate of the microwave-enhanced reactions.[42] To study the effect of solvents in the formation of SAMs deposited in a microwave oven, chloro-3,3,4,4,5,5,6,6,7,7,8,8,9,9,10,10,10-heptadecafluoro-decyl)-dimethyl-silane (otherwise referred to here as FAS) is dissolved in various organic solvents.

Silicon oxide covered single crystalline silicon substrates are first cleaned with piranha solution. They are subsequently rinsed with 18.2 MΩ water, dried with nitrogen gas, and immersed in the FAS solution. The substrates are heated in this solution in a household microwave oven at 300 Watts for times ranging from 25 to 150 seconds. The quality of the resultant SAMs are evaluated based on their water contact angle measurements. Figure 2-1 displays the effect of various solvents on the wettability of the microwave-prepared SAMs. The contact angle values are an average of multiple data points collected on different regions of at least five substrates. The error bars are calculated as twice the standard deviation values to ensure 95% accuracy. In this study, chlorinated or nitrogenous solvents are not used due to the various hazardous decomposition reactions.

The solvents used in this study are 2-propanol, xylene, and toluene. These three solvents are not known to decompose into harmful gases, but repeated exposure to their vapours is harmful and, therefore, the microwave oven should be used in a fumehood. These solvents have a range of loss tangent (tan δ) values, boiling point temperatures, and vapor pressures. These variations in physical characteristics of the solvents enable us to identify the optimal solvent for the deposition of silane-based SAMs in a microwave oven.

In a microwave-assisted reaction, polar solvents may be used to generate heat in solution.[44] These solvents tend to have high loss tangent values and heat up rapidly in the presence of microwaves. Among the tested solvents, 2-propanol has the highest tan δ (0.799) and is categorized as a high absorbance

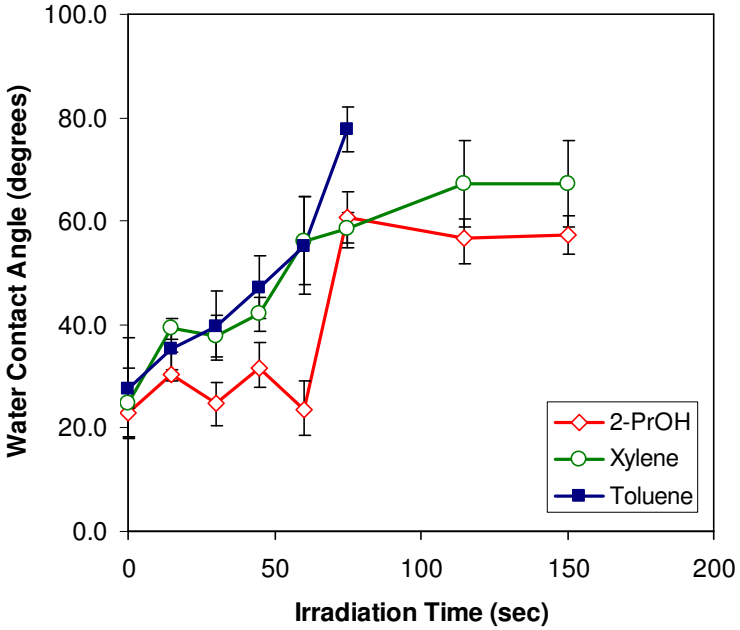

Figure 2-1 The effect of solvents and irradiation time on microwave-enhanced deposition of SAMs is monitored using water contact angle measurements. Silane molecules are deposited onto silicon oxide substrates from a 3.5 mM solution of FAS in 2-propanol, xylene, or toluene in a microwave oven at 300 Watts. The contact angles indicate that toluene is optimal solvent for the deposition of SAMs in a microwave oven. Note: the lines are used as guides for the eye to observe the trends.

solvent. It also has a high vapour pressure and heats and evaporates rapidly in a microwave oven. A cleaned, dried substrate is immersed and heated in a 3.5 mM solution of FAS in 2-propanol in a microwave oven at 300 Watts. After 75 seconds of microwave irradiation, the solvent in the solution completely evaporates and results in either the chemical adhesion (e.g., covalent attachment) or physical adsorption of silane molecules onto the surface. Figure 2-1 shows a rapid increase in the water contact angle values due to the deposition of the silane molecules upon evaporation of the solvent. Rapid evaporation of 2-propanol leads to unorganized adhesion of the silane molecules in proximity to the substrate. Many silane molecules may not be covalently

linked to the substrate and can be physically adsorbed onto the surface. This solvent is, therefore, not suitable for microwave deposition of silane-based SAMs.

Xylene is a convenient solvent for microwave synthesis. It has a low tan δ value (0.018), high boiling point, and low vapor pressure. These physical properties suggest that xylene can heat up to high temperatures during microwave heating. A cleaned silicon oxide substrate is immersed into a 3.5 mM solution of FAS in xylene and heated in a microwave oven at 300 Watts. Xylene does not evaporate during the microwave irradiation and SAMs formed out of the xylene solution have higher contact angle values than those formed in a 2-propanol solution. The substrates are irradiated for a range of times from 5 to 150 seconds. Increasing the irradiation time to 120 seconds results in the formation of SAMs with increasing water contact angle values. The contact angle values remain constant for the substrates when they are heated beyond 120 seconds. This plateau in the water contact angle values could be due to the solution mixture reaching a constant temperature (i.e., the boiling point of the solvent) or sterically imposed strain on the molecules in SAMs. High temperatures increase the kinetic energy of the molecules in the solution. The increased kinetic energy can lead to the removal of some silane molecules from the physically adsorbed monolayers and cause the observed plateau in the contact angles. Xylene, with its low loss tangent and high boiling point, is an adequate solvent for the deposition of silane-based SAMs.

Toluene is another intriguing choice for these microwave-prepared reactions. In the conventional method, silane-based SAMs are often deposited from toluene.[102] Similar to xylene, toluene has a low tan δ value (0.040). The boiling point temperature of toluene (111 ℃) is lower than that of xylene, but is much higher than the boiling point of 2-propanol. These SAMs are deposited from a 3.5 mM solution of FAS in toluene using a domestic household microwave oven. The surfaces coated with SAMs become more hydrophobic as the irradiation time increases. Toluene is a low absorbance level solvent with tan δ of 0.040. When the toluene solution is irradiated for longer than 75 seconds, the dissolved gas in solution begins to release. The released gas pushes the substrate to the surface of the solution and prevents further formation of self-assembled monolayers. The water contact angle of the substrates covered with SAMs is measured after each irradiation. The wettability and, therefore, the packing density of the molecules in SAMs increase upon increasing the irradiation time. The water contact angle values of SAMs deposited by heating the substrate for 75 seconds in toluene are much higher than the best wettability achieved in the other two solvents (Figure 2-1). Toluene is, therefore, selected as the most optimal solvent from those tested here for microwave-prepared deposition of SAMs.

Microwave-prepared deposition of SAMs from other solvents such as ethanol has also been examined. Ethanol causes a violent effervescence, due to its high vapour pressure and low boiling point and results in the ejection of the substrate from the solution. Ethanol is, therefore, not studied in detail and the

contact angle values of these surfaces are not included in Figure 2-1. Hexane has the lowest boiling point among the solvents presented in Table 2-1. Hexanes would evaporate rapidly during microwave irradiations and the influence of this solvent on silane deposition is not examined. Silane molecules are not soluble in water and cross-link rapidly in the presence of water in the solution. Water is, therefore, not suitable for the deposition of silane-based SAMs. Microwave reactions are favoured for their fast reaction rate, but the choice of solvent in these reactions is limited. It is important to identify and study the physical properties of the solvents prior to their use in a microwave reaction. The microwave-assisted deposition of SAMs in toluene solution leads to the formation of more densely packed self-assembled monolayers than those generated in the other solvents evaluated here. Toluene is, therefore, used for further investigation into the deposition of SAMs in the microwave oven.

2.3.2 Effect of Concentration of FAS on the Quality of SAMs

Another important factor in the formation of SAMs is the concentration of the silane precursor in the solution. To identify the effect of silane concentration on the quality of the resultant microwave-prepared SAMs, silicon oxide coated single crystalline silicon substrates, which are previously cleaned with piranha solution and dried with nitrogen gas, are irradiated in different concentrations of silane. The goal of this investigation is to increase the wettability of the microwave-prepared SAMs by varying the concentration of FAS.

In the previous studies, SAMs that were deposited from a solution of FAS in toluene had the most hydrophobic surfaces compared to those deposited from

xylene or 2-propanol. In the following studies, toluene is used to investigate the effect of FAS concentration on the quality of microwave-prepared SAMs. Silane-based SAMs are formed on the piranha-cleaned silicon oxide coated silicon substrates. These substrates are immersed into a FAS solution in toluene and heated in the microwave at 300 Watts for 75 seconds. The concentration of the FAS ranges from 0 to 28 mM for different samples, but all other parameters are kept constant for all reactions. The quality of the resultant SAMs are monitored by water contact angle measurements. The contact angle values presented in Figure 2-2 are the average of the data collected from multiple regions on at least five substrates. The error bars are calculated as twice the standard deviation values to provide 95% accuracy.[103] The results indicate that increasing the concentration of FAS in the solution increases the packing density of the microwave-enhanced silane-based SAMs.

The quality of SAMs formed in various concentrations of FAS in toluene are tested. To eliminate the presence of toluene on the surface as a main reason for the change in the wettability, a silicon oxide substrate is irradiated in pure toluene. The contact angle of this surface is measured to be 23 ± 0.2 degrees, which is much lower than the contact angles measured for the substrates covered with SAMs. This study enables us to eliminate the adhesion of toluene onto the surface as a reason for the increase in the wettability of the substrates. The contact angle values measured for SAMs generated in different concentrations of FAS are shown in Figure 2-2. This graph suggests that the initial increase in the concentration (from 0 mM to 3.5 mM) leads to a rapid

increase in the wettability of the surface. The contact angles of SAMs generated in solutions with higher concentrations of FAS increase slowly. Increasing the concentration of FAS in solution generates SAMs with high packing density of molecules and increases the wettability of the surface.

It is consistently observed that SAMs formed from a 7 mM solution of FAS tend to have reduced wettability compared to those formed in 3.5 or 14 mM solutions. The reaction parameters such as solvent, temperature, and microwave power are kept constant for these reactions. The 1 mM, 3.5 mM, 14 mM and 18 mM solutions of FAS are prepared from a few month old bottle of FAS. The 7 mM solutions are, however, made later from a brand new bottle. Although both bottles are originally purchased from the same company with the same purity, the older bottle has been exposed to air for much longer. The exposure to air may have increased the water content in the silane bottle. The amount of water present in the solution during the formation of SAMs plays an important role in the hydrolysis of silane molecules.[32, 33] It is suspected that the higher concentration of water in the old bottle compared to the new bottle of FAS, may have lead to the formation of more densely packed SAMs on the surface. A new bottle of FAS is used to prepare 7 mM solutions and the low water content in these solutions results in the slower hydrolysis of the silane molecules. This slow hydrolysis leads to the formation of SAMs with lower water contact angle values.

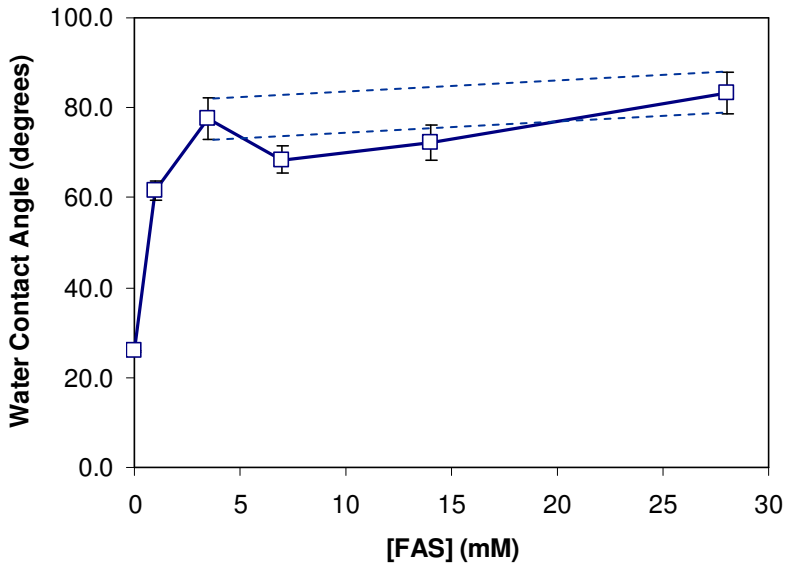

Figure 2-2 The effect of FAS concentration on the packing density of molecules in SAMs is monitored using contact angle measurements. Silicon oxide substrates are immersed in solutions with varying concentration of FAS in toluene and irradiated for 75 seconds at 300 Watts. An increase in the FAS concentration results in an increase in the wettability of the resultant SAMs.

Further increase in the concentration of FAS beyond 7 mM causes a subtle increase in the resultant contact angles. Highly hydrophobic SAMs may be formed by increasing the concentration of FAS in the solution.

Increasing the concentration of the FAS molecules in the solution enabled us to increase the packing density of the molecules in silane-based SAMs. The water contact angle value (~ 80 degree) achieved by irradiation of a substrate in the highest concentration of FAS tested (28 mM) is lower than that achieved using the conventional thermal techniques (96 degrees).[102] Thus, other methods are needed to increase the packing density of the FAS molecules in the resulting SAMs.

2.3.3 Improving the Packing Density of the Physically Adsorbed Monolayers Prior to Irradiation

The presence of densely packed layers of molecules in SAMs is the main requirement for their ability to modify the physical and chemical properties of substrates. To further increase the packing density of the molecules in the microwave-prepared SAMs, the substrates are immersed in a solution of FAS at room temperature prior to irradiation. This immersion provides the necessary time for FAS molecules to physically align themselves onto the surface of the substrate. As explained in Chapter 1, this alignment is an energetically favorable process and occurs spontaneously due to the surface-silane interactions as well as van der Waals interactions between linker chains of the silane molecules.[9] Once the physically adsorbed monolayers are formed, microwave irradiation provides the required energy for the silane molecules to condensation reaction at the surface of the substrate.

Physically adsorbed silane-based SAMs are generated at room temperature and condensed onto a clean substrate in a household microwave oven. The contact angles of the resultant SAMs are studied as a means to evaluate the packing density of the molecules in these monolayers. Silicon oxide coated single crystalline silicon substrates are cleaned in a piranha solution, rinsed with 18.2 MΩ water, and dried under a stream of nitrogen gas. They are subsequently immersed into a solution of 3.5 mM FAS in toluene for 2 hours, followed by 75 seconds of irradiation in the domestic household microwave oven. The 3.5 mM, 14 mM, and, 28 mM solutions of FAS are prepared from an older bottle (four to five months old) of FAS, but a new bottle of FAS is used to form

the 7 mM solutions. Due to the difference in the water content in the old and new bottles, the wettability of the resultant SAMs follows a slightly different trend for those experiments performed with 7 mM solutions of FAS in toluene and this date will be discussed separately.

The contact angle values for the different concentration of FAS with different immersion times are presented in Figure 2-3. These contact angle values are collected from various regions of at least five substrates. The error bars are calculated as twice the standard deviation values to provide 95% accuracy in these data. The increase in the concentration of FAS in toluene results in an increase in the packing density of the silane-based SAMs on the surface. Self-assembled monolayers deposited from 3.5 mM, 14 mM and 28 mM solutions show a rapid increase in their wettability after 5 minutes of immersion at room temperature. This rapid increase in the contact angle highlights the importance of the formation of physically adsorbed SAMs on the surface, prior to their condensation onto the substrate. Immersion of the substrates in FAS solutions beyond 5 minutes results in a further increase in the contact angle of the surface. This increase is, however, much more subtle than that seen in the first part of the graph (0 to 5 minutes). The decrease in the rate at which the contact angles increase may be due to the low diffusion rate of the silane molecules in the solution. The intermolecular forces between silane molecules as well as the interactions between these molecules and the substrate are considered weak, short-range forces. To align the molecules in a monolayer, these molecules are required to be in close proximity to each other. The low

diffusion rate of the molecules in the solution is one reason for the reduced rate of adhesion of the molecules onto the surface. Immersing the substrate into the solution prior to heating provides the required time for the diffusion of molecules in the solution and their alignment onto the surface.

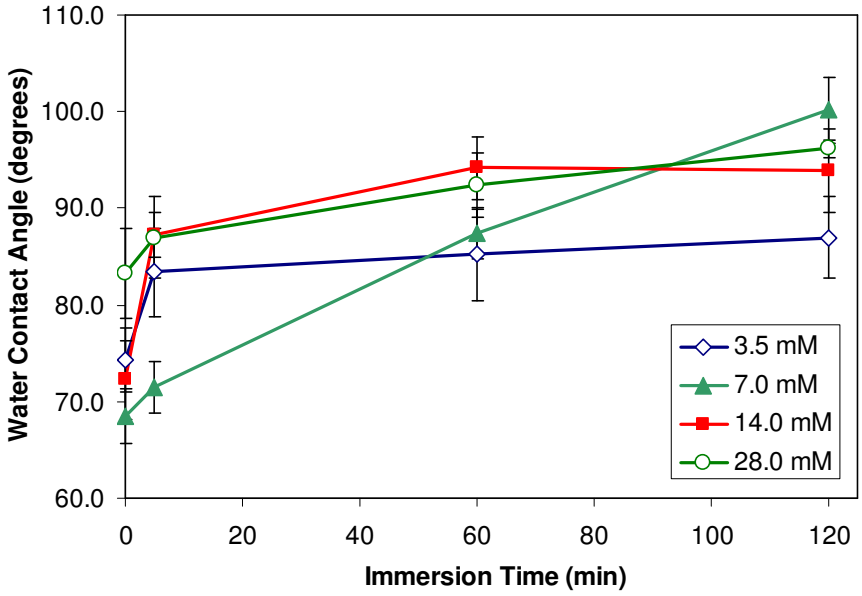

Figure 2-3 The effect of immersion time on the quality of microwave-prepared SAMs, after 75 seconds of heating at 300 Watts in a microwave oven, is evaluated by contact angle measurements. Increasing the immersion time results in the formation of densely pack silane-based SAMs. The 3.5 mM, 14 mM, and 28 mM solutions of FAS are prepared from silanes with a higher water content than those used for the preparation of the 7 mM solutions.

Silane molecules in the solution react with the residual water on the surface or in the solvent to produce silanol bonds. This hydrolysis is the first step in the formation of silane-based SAMs. The hydrolyzed silane molecules subsequently arrange onto the surface and form physically adsorbed monolayers. These monolayers are condensed onto the surface using microwave irradiation. The FAS molecules used to prepare the 7 mM solutions

are from a recently opened bottle of FAS, which has not been repeatedly exposed to the moisture in the air. One possible explanation in the difference observed in these graph is that compared to the old bottle, the water content is much lower in the new bottle of silane. Therefore, SAMs formed from the 7 mM solutions of FAS (from the new bottle) follow a slightly different trends in wettability as a function of immersion time than the other samples discussed previously in this section.

There are two major differences observed for the contact angles of SAMs formed from the older bottle of FAS (3.5 mM, 14 mM, and 28 mM solutions) compared to those made from the newer bottles (7 mM). Firstly, the initial contact angle observed for the monolayers deposited from the 7 mM solution of FAS is ~70 degrees. These values are much lower than the corresponding contact angle values measured for the same immersion times, but different concentration of FAS (3.5 mM, 14 mM and the 28 mM solutions). This difference in the contact angle values is attributed to the water content of the various silane precursors. Some silanes in the older bottle have been hydrolyzed before being diluted in toluene. In the presence of the substrates, these molecules rapidly align to form physically adsorbed monolayers onto the surface. The silane molecules of the newer bottle are not hydrolyzed to the same extent as those from the older bottle and thus require more time to form the silanol groups, prior to their alignment onto the surface. The short immersion time may be sufficient for the alignment of previously hydrolyzed molecules onto the surface, but does not provide the necessary time for hydrolysis of the molecules prior to their

alignment. These results suggest that the rate at which the silane molecules hydrolyze in the solution is slower than the rate of the formation of the physically adsorbed monolayers on the surface.

Another important difference observed in the graphs in Figure 2-3 is the variation in the contact angles as a function of immersion time. The contact angles of SAMs formed from partially hydrolyzed silanes (from the older bottle) plateau after 5 minutes immersion in the silane solution. In contrast, the contact angles for SAMs formed from the 7 mM solution of the FAS (from the newer bottle) increase linearly with an increased immersion time. This trend indicates that the number of silane molecules attached to the surface increases with immersion time for SAMs deposited from a 7 mM solution of FAS. This change in the trend is also attributed to the difference in the water content in each silane bottle. The concentration of hydrolyzed silane molecules is higher in the older bottle than the newer one. These hydrolyzed molecules can react with each other and result in the polymerization of the silane molecules in the bottle. The FAS molecules are chosen because they contain one reactive (Si-Cl) group and the reaction of these molecules with one another prevents their adhesion to and copolymerization on the surface. These oligomers may physically adsorb to the substrate, but are not able to form a covalent linkage to the silicon oxide surface. The increased water content in the older bottle leads to a decrease in the concentration of reactive FAS molecules in the solution. The silane molecules from the newer bottle contain less polymerized molecules and have more reactive molecules available to align onto the surface. The presence of reactive

FAS molecules in the solution results in the formation of densely packed molecules in SAMs and leads to the observed increase in the contact angle of the surface after longer immersion times.

Formation of microwave-prepared FAS SAMs is highly dependent on various environmental factors such as the reaction time, choice of solvent, concentration of silane molecules in the solution, water content in the solution, along with the time spent to generate physically adsorbed SAMs at room temperature (in this thesis referred to as the immersion time). Densely-packed SAMs are deposited after 75 seconds of microwave irradiation in toluene (a low absorbance solvent with a high boiling point). Self-assembled monolayers with high packing density are formed by increasing the concentration of the silane molecules in the solution and the immersion time prior to the condensation of molecules in the microwave oven. By modifying the factors mentioned above, microwave-prepared SAMs are formed with the same packing density and wettability as the conventional SAMs in a third of the time.

2.4 Conclusions on Microwave-Assisted Deposition of SAMs

Silane-based SAMs are deposited using microwave irradiation. The overall formation of densely packed SAMs in a microwave oven takes nearly a third of the time of the conventional method. Silane-based SAMs with low packing density may be formed in only 75 seconds (with no immersion time), which is roughly 300 times faster than that required in the conventional method. The condensation time for all microwave reactions are 75 seconds, which is 150 times less than that required in the conventional method. The quality of

microwave-prepared SAMs is highly dependant on the water content and the concentration of FAS in the solution. The solvent used for these studies also plays an important role in the packing density of the molecules in the silane-based SAMs. It is shown that immersion of the substrate in the FAS solution for a period of time prior to irradiation in the microwave enables the molecule to align densely and form high quality SAMs. By optimizing these factors, microwave-assisted deposition of SAMs has lead to contact angles similar to that of the conventional thermal technique in roughly a third of the time.

Similar to SAMs formed in the convection oven, microwave-prepared SAMs contain various types of defects. It is important to investigate the presence and density of defects in these SAMs to evaluate the molecular-scale quality of these monolayers. In the next chapter, investigations into the identification of the location and density of defects in the conventional and microwave-prepared SAMs are reported.

CHAPTER 3: DEFECTS IN SILANE-BASED SAMS

3.1 Introduction to Dominant Types of Defects and Correction Techniques

There are two dominant types of defects present in both conventional and microwave-prepared SAMs (Figure 3-1A). The first type of defects are known as pinhole defects, which consist of the areas of the substrate that are not covered with silane molecules during the silane deposition step, either due to intrinsic or extrinsic sources (Figure 3-1i). The second type of defect is the presence of physically adsorbed molecules on the surface. These defects are caused by van der Waals interactions between the fluoroalkyl chains of the FAS molecules or the adhesion of solvent impurities (Figure 3-1ii). Lowering the density of defects is the first step in improving the quality of SAMs.

Two techniques are developed to decrease the density of defects in silane-based SAMs. As-deposited SAMs are formed on cleaned and dried silicon oxide coated single crystalline silicon substrates. Removing the physically adsorbed defects from the surface and refilling the pinholes reduce the density of defects in the silane-based SAMs. To correct for these defects, an extraction technique is used to remove the physically adsorbed molecules from the surface (Figure 3-1B). In this process, the substrate covered with SAMs is placed in a Soxhlet extractor and repeatedly washed with toluene for a minimum of 3 hours. This extraction process continuously removes physically adsorbed silane

molecules or impurities from the surface and ultimately may expose more bare regions of the substrate. The density of pinhole defects is subsequently decreased by refilling the holes with more silane molecules (Figure 3-1C). One may use the same silane molecules as the original SAMs or different silane derivatives (e.g., IR-active silanes) to label defects when refilling these pinholes. Various techniques are developed to correct for these defects and to monitor their density using several microscopy and spectroscopy techniques.

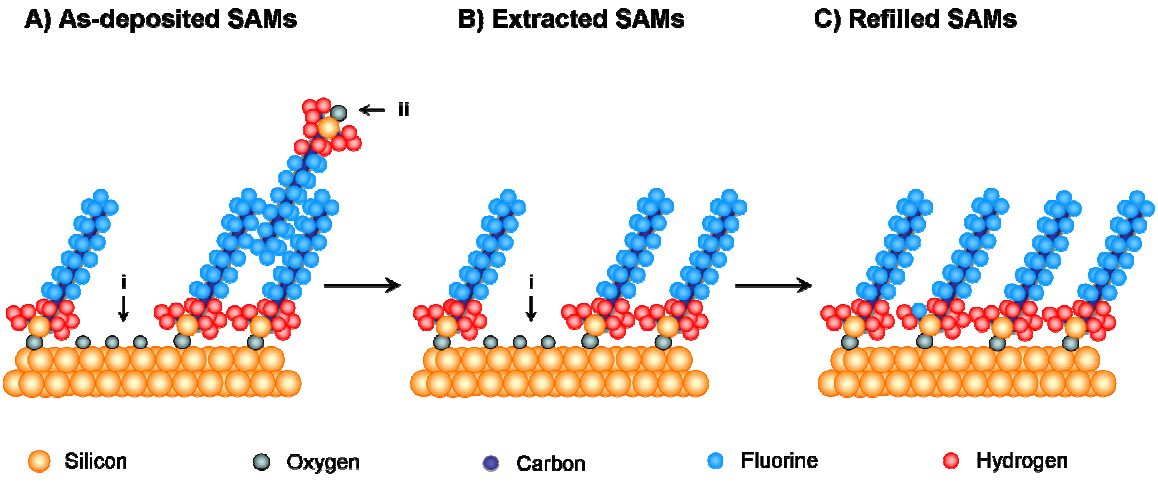

Figure 3-1 This schematic represents two types of defects in SAMs. (i) The pinhole defects and (ii) physically adsorbed molecules present on the surface after different correction steps. (A) The as-deposited silane-based SAMs are shown as well as (B) the extracted SAMs, where self-assembled monolayers are repeatedly washed with solvents to remove physically adsorbed molecules from the surface. (C) The refilling method is used to decrease the density of the pinhole defects in monolayers.

In this chapter, the focus is on identifying the presence of the two dominant sources of defects in silane-based SAMs. In addition, two different approaches to depositing silane-based SAMs are briefly explained. The methods used to identify the location and density of defects in these monolayers using chemical amplification of defects, coupled with various spectroscopy and

microscopy techniques are discussed. Various procedures used to correct for the defects in silane-based SAMs are also reported.

3.1.1 Silane-Based Self-Assembled Monolayers

The solution-phase deposition of silane-based SAMs occurs in two steps, as shown in Figure 1-2. In the first step, the silane molecules align to form a physically adsorbed monolayer on the surface. This assembly is due to the surface-silane interactions as well as the van der Waals interactions between the linker chains of molecules in the monolayer and may be affected by the surface roughness. In the second step, the physically adsorbed monolayers are heated and the silane molecules condense onto the substrate, forming covalently bound self-assembled monolayers on the surface. The energy for this condensation step is conventionally generated using a convection oven. This technique requires 6 hours to generate silane-based SAMs on the surface.[102] As explained in chapter two, a technique is developed in which microwave irradiation provides the required energy for the condensation of silane molecules onto the silicon oxide substrate. This technique reduces the condensation period to 75 seconds, which is ~ 150 faster than the conventional technique. The decrease in the time required for the deposition of SAMs directly correlates to the energy required for the formation of these monolayers. The quality and packing density of both conventional and microwave-prepared SAMs are monitored and compared using various microscopy and spectroscopy techniques.

3.1.2 Conventional Synthesis of Silane-Based SAMs

The conventional thermal technique is commonly used to form silane-based self-assembled monolayers on silicon oxide substrates.[14, 35] This technique is a convenient and reproducible approach to patterning and modifying various properties of surfaces such as friction and wettability. In this technique, the formation of physically adsorbed self-assembled monolayers occurs at room temperature and is followed by the condensation of silane molecules to the surface in a convection oven at 100 °C for 3 hours. The silane-based SAMs formed using this technique are reproducible and require a low (1 mM) concentration of FAS. These SAMs are only a few nanometers thick, but can protect surfaces against chemical etchants, such as hydrofluoric acid.[104] On the other hand, the deposition of these monolayers in a convection oven is a highly time and energy consuming process. It is, therefore, important to develop new techniques to form these monolayers in a shorter time than the conventional method. This technique should reduce the cost and increase time efficiency of the condensation process without sacrificing the quality of the resultant SAMs.

3.1.3 Microwave-Prepared Deposition of SAMs

In the microwave approach to the deposition of silane-based SAMs, the time required for the formation of physically adsorbed self-assembled monolayers is reduced to less than two hours (compared to 3 hours in the conventional technique). The condensation time is reduced to ~75 seconds (compared to 3 hours in the conventional thermal technique). The microwave approach to deposition of these monolayers also requires ~750 times less energy

than the conventional method. In this technique, the energy required for the condensation of silane molecules to the substrate is produced by heating the substrate in a domestic household microwave oven. Microwave irradiation heats up both the silicon substrate and the polar molecules in the solution. The heat generated is sufficient for the condensation of the silane molecules on the substrate and the formation of covalently bound monolayers on the surface. The microwave approach reduces the overall time required for the formation of self-assembled monolayers and is considered a green approach to generate heat for chemical reactions.[95] Similar to the conventional method, microwave irradiation is also considered a high throughput method, in which reel-to-reel processing would allow for an industrially applicable system.[38]

There are many advantages to a microwave-prepared deposition of self-assembled monolayers, but there are also minor disadvantages to be considered. One disadvantage of this microwave approach is the high silane concentration (3.5 to 28 mM) required during the self-assembly process compared to that for the conventional technique (1 mM). This increase in concentration compensates for the short reaction time during the formation of physically adsorbed monolayers on the surface and is the first step in the process of forming well ordered silane-based SAMs. The increase in the silane concentration adds a negligible amount to the total cost of the formation of these SAMs. For example, the additional cost in the formation of microwave-prepared SAMs due to the increased silane concentration to the conventional method is less than $2 per three-inch diameter circular substrate. This cost is easily

compensated for by the decrease in the time and energy required for the deposition process. All other material costs (solvents, wafers, and other chemicals) are equal for both microwave-prepared and the conventional approach to the deposition of SAMs. Another disadvantage to microwave synthesis is the generation of hazardous solvent decomposition products, which prevents researchers from using chlorinated and nitrogenous solvents. The overall advantages of microwave-prepared deposition of SAMs make this technique highly valuable to materials scientists, regardless of its minor disadvantages.

All microwave reactions reported in this chapter are carried out in a domestic household microwave oven. This microwave oven is an affordable and readily available substitute to expensive microwave reactors. It is important to note that household microwave ovens do not provide precise control over the temperature of the reaction vessel. They also do not provide a uniform distribution of microwaves in the heating chamber. This non-uniform heating may cause variation in the temperature of different regions of the reaction vessel, and decrease the reproducibility of this technique. Silane-based SAMs have been condensed onto the silicon oxide surface using a domestic household microwave oven, but one may be able to increase the reproducibility and quality of SAMs by using a microwave reactor for these experiments.

In this chapter, the quality of microwave-prepared SAMs formed in a household microwave oven are compared to those formed using the conventional thermal technique. The number of molecular-scale defects in these

monolayers are evaluated as a measure of the quality of the silane-based SAMs formed using both techniques. In addition, the density of defects in both types of SAMs is studied using contact angle measurements. The correction techniques used to improve the packing density of molecules in these monolayers will also be discussed.

3.1.4 Characterization of Defects in SAMs

There are various types of defects present in silane-based self-assembled monolayers. Identifying the types and density of these defects is the first step in correcting for them. Various methods are used to characterize the FAS-based SAMs and monitor the quality of these monolayers after extracting the physically adsorbed defects and refilling the pinhole defects.

Water contact angle measurements are used as a quick measure of the quality (wettability) of FAS-based SAMs. The fluoroalkyl chains on the silane molecules convert the hydrophilic silicon oxide substrate into a hydrophobic surface. This change in the wettability is easily monitored using water contact angle measurements. The wetting hysteresis obtained from the advancing and receding contact angles indicates variations in the wettability across various regions of the surface. It does not, however, provide any molecular level information about the monolayer. This analysis is, therefore, valuable for macro-scale measurements.

Ellipsometry is used to measure the thickness of the monolayers on a surface. The presence of pinhole defects results in a lower packing density of

the molecules in SAMs. The decrease in the packing density of the molecules in SAMs results in a reduction in the overall thickness of the monolayers. The thicknesses of SAMs were studied after each extraction step to monitor the density of pinhole defects in the silane-based self-assembled monolayers.

Another method used to identify the presence of defects is chemical amplification of defects coupled with FTIR measurements. This technique identifies the presence of organic molecules on the surface. The defects are chemically amplified by reacting the substrates covered with FAS-based SAMs with IR-active silane molecules such as chloro-dimethyl-(2-pentafluorophenyl-ethyl)-silane (FPS). The IR-active FPS molecules bind to silicon substrates on pinhole sites as well as any physically adsorbed FAS molecules on the surface. The high intensity IR peaks for the FPS molecules are more easily detectable than those of FAS molecules, especially when the FPS is physically adsorbed onto SAMs, away from the surface. The FTIR spectrum can identify the presence of FPS molecules in the monolayer, but it does not provide any information about the location of defects in SAMs. In addition, due to the low concentration of silane molecules on the surface, it is difficult to observe all the expected peaks for the FAS and FPS molecules in SAMs. Other techniques are required to identify the exact location and density of defects.

The pinhole defects in SAMs are too small to be detected using conventional spectroscopy and microscopy techniques. Most of the surface analysis methods such as spectroscopy and microscopy techniques available to a chemist lack the ability to provide molecular-scale spatial resolution. Some

techniques average the information over a large area of the substrate. In order to identify the location and density of defects, it is important to develop new techniques to amplify these molecular-scale defects.[104]

Electroless metal deposition (EMD) is the technique of choice to highlight the location of defects. It is a convenient and accessible approach to amplify these molecular-scale (or larger) defects. During electroless silver deposition, silver particles form in the absence of SAMs on a silicon oxide surface and highlight the location of pinhole defects. Electroless silver deposition is carried out by immersing a substrate covered with SAMs into an aqueous solution containing silver nitrate and buffered hydrofluoric acid. The hydrofluoric acid in the solution removes the native oxide on the substrate and exposes the underlying silicon. The silane-based SAMs protect the substrate from HF etching, preventing silver from depositing on the densely packed regions of SAMs. In the presence of exposed silicon — at the site of the pinhole defects — silver ions reduce and grow into silver particles. The overall electroless silver deposition reaction is as follows:

$$4Ag^{+} + Si_{(s)} + 6HF \rightarrow 4Ag_{(s)} + H_2SiF_6 + 4H^{+} \qquad \textbf{Equation 3-1}$$

The exposed silicon is oxidized to silicon oxide, which further reacts with the remaining hydrofluoric acid to generate a silicon fluoride complex.

(Silicon oxidation) $Si + 2H_2O \rightarrow SiO_2 + 4H^+ + 4e^-$ **Equation 3-2**

(Silicon dissolution) $SiO_2 + 6HF \rightarrow H_2SiF_6 + 2H_2O$ **Equation 3-3**

$E^{o}_{anodic} = 1.24$ V

Previous studies have shown that electroless deposition of silver on silicon substrate can occur in the absence of HF. This process, however, only produces a monolayer of silver on the substrate.[105] The main function of hydrofluoric acid is to remove the oxide layer and expose the underlying silicon substrate. Silicon is the reducing agent in this redox reaction. Silver ions are reduced to form silver seed, which further grow into silver nanoparticles on the site of defects.

(Silver reduction) $Ag^+ + e^- \rightarrow Ag$ **Equation 3-4**

$E^{o}_{cathodic} = -0.7996$ V

The substrates covered with silver particles are subsequently imaged by atomic force microscopy (AFM), scanning electron microscopy (SEM), and X-ray photoelectron spectroscopy (XPS). These techniques reveal the density of silver nanoparticles (and defects) in silane-based SAMs.

The presence of defects in silane-based SAMs has been identified using water contact angle measurements and ellipsometry. The reaction of IR-active molecules with the defects present in SAMs is monitored using FTIR spectroscopy. The changes in the intensity of IR peaks are noted before and after the Soxhlet extraction of physically adsorbed molecules on SAMs.

Electroless metal deposition is coupled to AFM, SEM and XPS analysis to identify the location and density of defects in the silane-based SAMs. It is shown that these defect correction techniques (extraction and refilling of the defects) can effectively reduce the number of pinhole defects and physically adsorbed molecules on SAMs using the analysis techniques mentioned above.

3.2 Experimental

3.2.1 Materials

Single-side polished (100) silicon wafers (SiliconSense, Inc.) were used as the substrate of choice for the deposition of silane-based self-assembled monolayers. These substrates were cleaned using a 7:2 mixture of sulfuric acid (Anachemia Canada Inc.) and 50% (v/v) hydrogen peroxide (VWR) to remove any organic molecules from the surface. A solution of FAS (90%, Alfa Aesar) or FPS (95%, Gelest Inc.) in toluene (Reagent Grad, Caledon Laboratories Ltd.) was prepared. The cleaned substrates were immersed in this solution.

The defects in SAMs were highlighted using electroless silver deposition technique. The silver solution consisted of silver nitrate (Aldrich) and ammonium fluoride buffered hydrofluoric acid (20:1 v/v, Transene Company, Inc.). For the microwave-base SAMs, a Sharp Carousel II kitchen microwave oven (pulsed at 300 Watt) was used to irradiate the substrate in the solution. A digital AST Optima contact angle system with a horizontal light beam was employed to study the wettability of SAMs. A Jobin-Yvon UVISEL NIR phase modulated ellipsometer was used to measure the thickness of the silane-based self-

assembled monolayers. The FTIR spectra were acquired with a Nicolet Nexus-IR 560 with a liquid nitrogen cooled mercury-cadmium-telluride detector. Atomic force microscopy images were collected on a MFP3D AFM (Asylum Research) in AC mode by silicon cantilevers (Asylum Research, and VistaProbes). The amount of silver deposited on SAMs was quantized by a Kratos Ultra X-ray photoelectron spectrometer. The substrates were also studied by FEI Dualbeam Field-Emission scanning electron microscope. The TEM analysis of silver particles was accomplished using a FEI TECNAI G2 transmission electron microscope.

3.2.2 Cleaning the Substrate

Please refer to section 2.2.2 for detailed information on cleaning the substrate.

3.2.3 Deposition of Conventional SAMs

Conventional SAMs were prepared by immersing clean silicon oxide substrates into a solution of FAS (20 mL) in various toluene in an evaporating dish covered with a watch glass. This step provided the required time for the generation of the physically adsorbed monolayers on the SiO_2 surface. These SAMs were covalently linked to the substrate through the condensation step in the convection oven.

Physically adsorbed silane monolayers were formed on clean silicon substrates by immersing the clean and dry substrate into a 1 mM solution of FAS (20 mL) in toluene for 3 hours at room temperature. Once the immersion time

completed, the substrates were rinsed with roughly 200 mL of toluene and dried with nitrogen gas. The energy for the condensation of silane molecules to the surface was provided by heating the rinsed, dried substrate in a convection oven at 100 °C for 3 hours. This procedure was modified from previously reported work by various groups.[9,24,28] The substrate was studied using contact angle measurements, microscopy, and spectroscopy techniques coupled with chemical amplification of defects.

3.2.4 Extraction and Refilling of Defects in Silane-Based SAMs

Please refer to section 2.2.4 for detailed information on extraction and refilling of the silane-based SAMs.

3.2.5 Contact Angle Measurements

Please refer to section 2.2.5 for detailed information on contact angle measurements.

3.2.6 Spectroscopic Ellipsometry Analysis

The extracted SAMs (E1, E2, and E3) were analyzed using a Jobin-Yvon UVISEL NIR variable angle spectroscopic ellipsometer with a 75 Watts xenon lamp light source. Multiple spots (1 mm^2) were studied at 450 nm and at a 70° angle of incident. A three layer model (Si/SiO_2/SAMs) with a Cauchy transparent modeling was constructed with DeltaPsi2 software and were used to calculate the thickness of SAMs for each spot. The average thickness value for each substrate was calculated and reported.

3.2.7 Chemical Amplification and FTIR Measurements

As-deposited SAMs were immersed into a 1 mM solution of FPS in toluene for 3 hours to physically adsorb IR-active molecules to the mis-oriented FAS molecules on the surface. The substrates were rinsed with toluene and dried under a stream of nitrogen gas, prior to condensation of FPS molecules to FAS molecules in a convection oven at 100 ℃ for 3 hours. Absorption FTIR spectra were collected from 700 cm^{-1} to 4000 cm^{-1} on a Nicolet Nexus-IR 560 with a liquid nitrogen cooled mercury-cadmium-telluride detector. One thousand spectra were collected and averaged for each sample. The background spectrum was acquired from a bare silicon substrate.

3.2.8 Electroless Silver Deposition and AFM, SEM, and XPS Analysis

Silane-treated substrates were immersed into a 20 mL aqueous silver deposition solution prepared from various concentrations of silver nitrate, and hydrofluoric acid. Disposable plastic cups were used as reaction vessels and the substrates were clamped using plastic clamps for the duration of the reaction. The deposition time varied for different experiments. The substrates were always rinsed with 18.2 MΩ water and dried under a stream of nitrogen before imaging with a MFP3D atomic force microscope (Asylum Research). The images were acquired in AC mode with the scan speed of 0.50 MHz using silicon cantilevers (Asylum Research, and VistaProbes). The analysis was done using the Igor Pro program provided with the AFM instrument.

The same substrates were also imaged using a FEI Dualbeam Field-Emission scanning electron microscope with Focused Ion Beam. The SEM and

EDS analysis were performed at an accelerating voltage of 10 kV on 2 μm^2 area for 100 seconds. A FEI TECNAI G2 transmission electron microscope with an accelerating voltage of 200 kV was used to collect TEM images and perform EDS analysis on silver nanoparticles.

The amount of silver deposited on SAMs after each silane deposition, extraction, as well as the SiO_2 substrate was measured using a Kratos Ultra X-ray photoelectron spectrometer. The analysis area of each sample was 700 µm x 300 µm. A survey scan with the passing energy (energy of the initial electron beam) of 160 eV was collected along with a high resolution Ag (3d) with the passing energy of 40 eV and dwell time of 100 milliseconds for each substrate.

3.3 Results and Discussion on the Analysis of Defects

Packing density of silane molecules in SAMs plays an important role in their ability to protect silicon substrates or modify their chemical and physical properties. Pinhole defects and physically adsorbed molecules are two dominant types of defects in silane-based SAMs. During the silane deposition step, only some of the silicon oxide surface is covered with SAMs while some areas of the surface remain exposed (pinholes) and display the properties of the bare silicon oxide surface. Another source of defects is the presence of physically adsorbed silane molecules or solvent impurities on the surface. These molecules adhere to the substrate and SAMs through weak van der Waals interactions. These defects are chemically amplified and further identified by FTIR spectroscopy, as well as AFM and SEM imaging, and XPS analysis.

These defects are corrected by removing physically adsorbed impurities from the surface using a Soxhlet extraction procedure. The packing density of silane molecules in SAMs is increased to reduce the density of pinholes in these monolayers. The improvement in SAMs is monitored using contact angle and ellipsometry measurements, as well as various imaging and analysis techniques following chemical amplifications.

3.3.1 Contact Angle Measurements on Silane-Based SAMs

The density of defects in both conventional silane-based SAMs and microwave-prepared SAMs are evaluated after each silane deposition and extraction step using contact angle measurements. Conventional SAMs are assembled at room temperature and condensed in a convection oven at 100 ℃ for three hours. These monolayers are extracted for three hours using a Soxhlet extractor with toluene as the solvent. They are subsequently refilled with new silane molecules. The extraction and refilling steps are repeated and the wettability of these SAMs is monitored after each step using contact angle measurements.

The results of extraction and refilling of defects are shown in the exaggerated schematics in Figure 3-2. These defects are exaggerated to clearly indicate the goals of each extraction and refilling step. The silane deposition (S) and extraction (E) steps are repeated three times for each substrate and the wettability of SAMs is measured after each step. The wettability is a measure of the packing density of the molecules in SAMs.

In this study, FAS-based SAMs are generated on a clean silicon oxide coated single crystalline silicon substrate using the conventional method mentioned above. This substrate is referred to as “S1” (for Silane deposition #1). The S1 substrate is covered with the hydrophobic FAS molecules and displays a

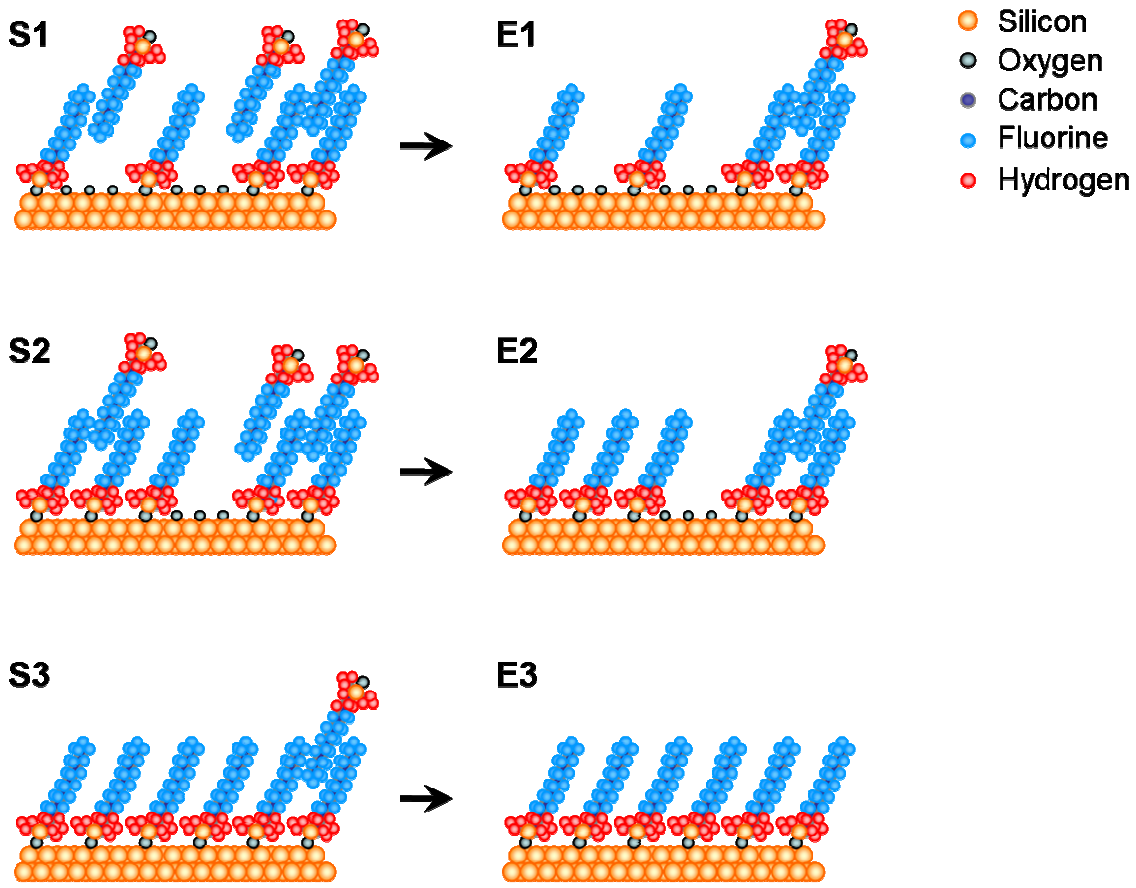

Figure 3-2 This schematic representation shows each silane deposition (S) and extraction (E) step. The number defects in silane-based SAMs decreases with repeated extraction and refilling steps. These images are of exaggerated samples to demonstrate the effect of extraction and refilling of defects.

hydrophobic surface. This wettability is expected due to the hydrophobic terminal functional groups of the FAS molecules. The contact angle values for SAMs after each correction step are shown in Figure 3-3. These values are the average of the contact angle measurements collected from various regions of at

least five samples. The error bars are calculated as twice the standard deviation values to ensure 95% accuracy. As-deposited SAMs are subsequently extracted with toluene in a Soxhlet extractor. This substrate is referred to as “E1” (for Extraction #1). As seen in Figure 3-3, the water contact angle on this surface decreases after extraction. This decrease in the contact angle is due to the removal of the physically adsorbed molecules from the surface, exposing the underlying hydrophilic silicon oxide substrate and resulting in a less hydrophobic surface.

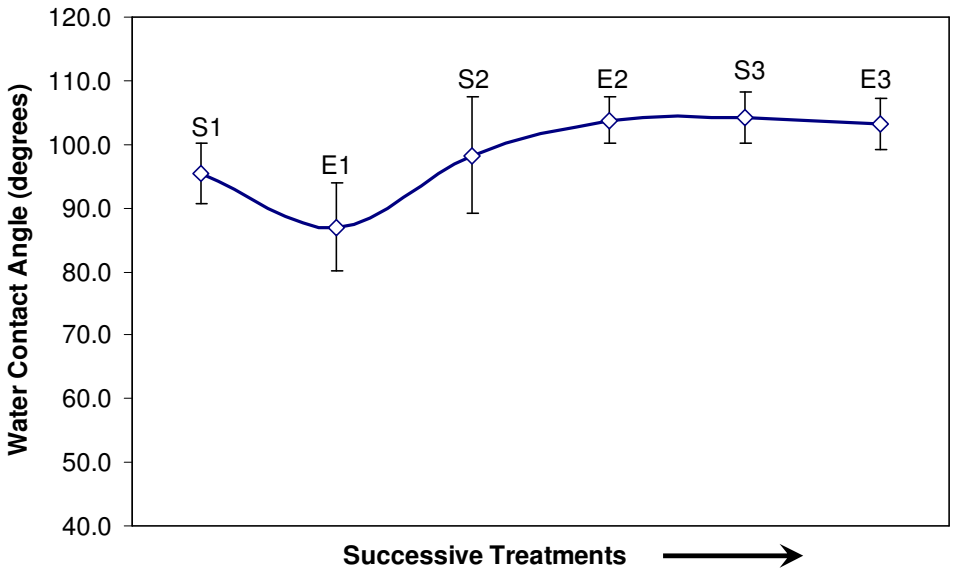

Figure 3-3 Water contact angle measurements after each silane deposition (S) and extraction (E) step indicate an overall improvement in the wettability of SAMs. The silane molecules are deposited using the conventional approach during each deposition step. Note: the line is used as a guide for the eye to observe the trend.

The number of pinhole defects in silane-based SAMs is reduced by immersing the substrate in a silane deposition solution. The exposed regions of the substrate are refilled with new silane molecules and this refilled substrate is

referred to as “S2”. This refilling increases the contact angle of the surface, as pinhole defects are filled with hydrophobic FAS molecules. The refilled substrate still contains physically adsorbed FAS molecules on the surface. These molecules have a hydrophilic Si-OH group. Extracting these physically adsorbed FAS molecules results in an increase in the wettability of the surface (E2) as shown in Figure 3-3. Further refilling and extraction steps (S3 and E3) do not significantly increase the water contact angle of the surface. This lack of sensitivity to further a decrease in the density of defect is due to an inability to identify molecular-scale structural changes on the surface with contact angle measurements.

Successive silane deposition and extraction steps improve the packing density and, ultimately, the quality of SAMs deposited by the conventional method. Contact angle measurements enable us to monitor the initial changes in the density of defects in silane-based SAMs. The quality of SAMs deposited in a convection oven and those deposited in a household microwave oven may be effectively compared by monitoring the wettability of the microwave-prepared SAMs after each silane deposition and extraction step.

As reported in chapter two, immersing the substrates in the FAS solution prior to irradiation leads to an increase in the wettability of the resultant SAMs. In this study, microwave-prepared SAMs are generated by immersing a silicon substrate in a 7 mM solution of FAS in toluene for 5 minutes, followed by condensation in a pulsed 300 Watts household microwave oven for 75 seconds. These substrates are subsequently extracted with toluene in a Soxhlet extractor

for 3 hours. The water contact angles are collected after each silane deposition and extraction step. Figure 3-4 demonstrates these values along with those collected for conventional SAMs for the purpose of comparison. These values are the average of multiple measurements taken from various regions of at least three samples. The error bars are twice the standard deviation values to provide 95% accuracy of the data.

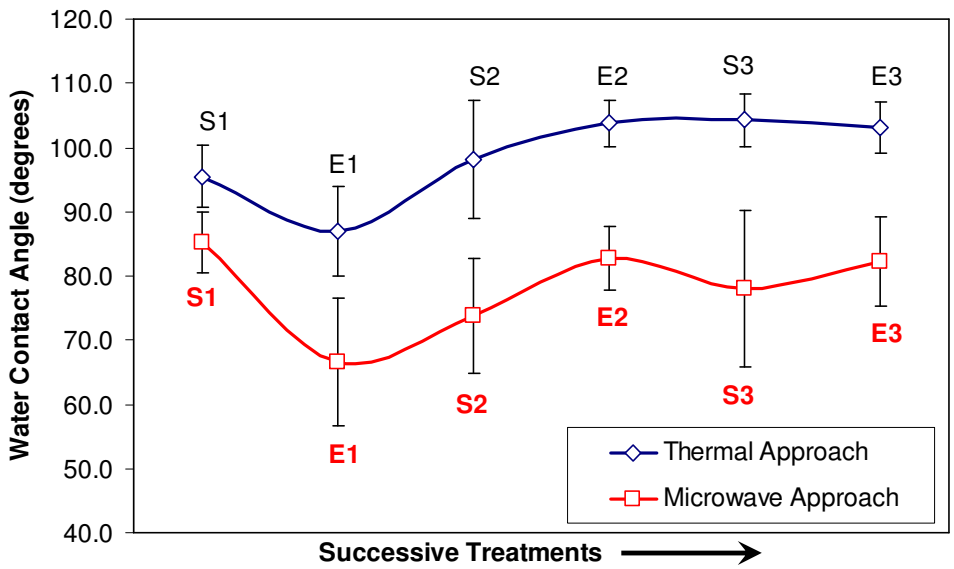

Figure 3-4 Water contact angles are collected after each silane deposition and extraction step for SAMs formed using both the microwave-prepared and conventional SAMs. Note: these lines are used as guides for the eye to observe the trends.

As shown in Figure 3-4, microwave-prepared SAMs follow the same overall trend as conventional SAMs. As-deposited microwave-prepared SAMs (S1) are hydrophobic, but have a lower water contact angle than the as-deposited conventional SAMs. This difference in the contact angles indicates that there are more defects present in FAS-based SAMs formed in a microwave oven than in the conventionally synthesized SAMs. Extraction of the physically

adsorbed molecules from the surface exposes the underlying silicon oxide surface and decreases the contact angle value of the substrate (E2). This trend is also seen in conventional SAMs. The pinhole defects are refilled with new silane molecules (S2) using the microwave approach mentioned above and leads to an increase in the contact angle as expected. As was observed for conventional SAMs, repeating the refilling (S3) and extraction (E3) steps does not further increase the contact angle value of microwave-prepared SAMs. This lack of sensitivity to molecular-scale variations is a major limitation in using contact angle measurements to characterize the quality of molecular packing in self-assembled monolayers.

Contact angle measurements easily indicate the presence of large (micron-scale) defects in the silane-based SAMs, but they are not able to provide any information on the presence of molecular-scale defects in these monolayers. Hence, further characterization techniques are needed to identify the presence and density of molecular-scale defects in the E2, S3, and E3 substrates. Another important factor to pay attention to is that the wettability of the surfaces is not increased beyond its original S1 value by repeating the refilling and extraction. This result is contrary to what was observed for the conventional SAMs and may be due to variations in the microwave intensity through the heating chamber of the microwave oven.

The microwave-prepared SAMs in this study are all generated in a domestic household microwave oven. The intensity of microwave irradiation varies across different regions of the reaction vessel. In addition, the reaction

time is very short. All these factors may cause the formation of microwave-prepared SAMs with lower packing densities than those formed using the conventional technique. Regardless of these factors, the microwave-prepared SAMs used for these studies form after 5 minutes of immersion in a FAS solution followed by 75 seconds of irradiation in the microwave oven. The overall process to deposit silane-based SAMs in the microwave requires less than 7 minutes. Compared to the 6 hours required for the formation of SAMs in the conventional method, this microwave approach reduces the reaction time by over 50 times. Carrying out these reactions in a microwave reactor and further optimization of the solvent system should result in SAMs with a higher packing density and lower density of defects than is achieved with a household microwave oven.

The wettability of SAMs deposited using the microwave technique is lower than those formed using the conventional method. To further investigate the density and types of defects in silane-based SAMs and the effectiveness of these correction techniques, SAMs formed using the conventional method are studied in more detail with various spectroscopy and microscopy techniques. These investigations are discussed in detail in the following sections.

3.3.2 Spectroscopic Ellipsometry Measurements

Spectroscopic ellipsometry is often used to measure the thickness of self-assembled monolayers. The molecules in densely packed self-assembled monolayers are attached to the surface at an angle, Θ, to the surface normal. This angle increases as the density of the molecules in SAMs decreases (Figure 3-5). Correcting for pinhole defects in silane-based self-assembled monolayers

results in an increase in the thickness of the SAMs. This variation in the thickness of the monolayer is easily monitored with spectroscopic ellipsometry.

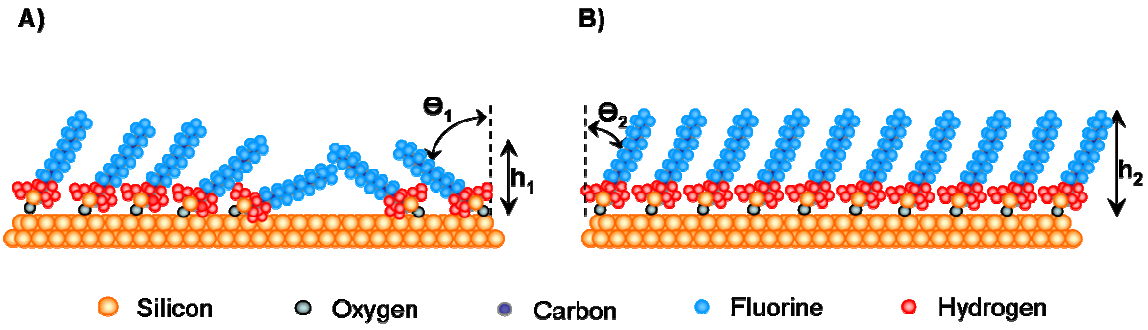

Figure 3-5 In this schematic representation, SAMs with (A) a low packing density of molecules are compared to (B) those with high packing density. The film thickness (h) increases and the adhesion angle (Θ) decreases as the molecules pack more densely in these monolayers.

The packing density of the silane-based SAMs is evaluated using a spectroscopic ellipsometer. Silane-based SAMs are deposited using the conventional technique mentioned earlier in this chapter. The defects are subsequently corrected using the extraction and refilling steps. Thicknesses of the SAMs are evaluated with a spectroscopic ellipsometer operating at a wavelength of 450 nm and a 70° angle of incidence. The tan Ψ and Δ values are measured for each sample by comparing the phase and amplitude of the incident and reflected light. Using a three layer (Si/SiO_2/SAMs) model and Cauchy fitting routine,[106, 107] the thicknesses of SAMs are estimated. This procedure and simple calculations are used to identify the thicknesses of SAMs on a silicon oxide coated single crystalline silicon substrate.

The thickness of the extracted SAMs is measured as they have little to no physically adsorbed molecules influencing the overall thickness of the

monolayers. The reported values are the average of at least three different spots on the substrate (Figure 3-6). Refilling the pinhole defects in silane-based SAMs increases the packing density of the molecules in the monolayer. After each silane deposition step, the physically adsorbed molecules are removed through Soxhlet extraction. These extracted substrates are analyzed to measure the thickness of the silane-based SAMs on the surface. The increase in the packing density of the molecules in the silane-based SAMs (due to the correction of defects) increases the thickness and changes the refractive index SAMs. The

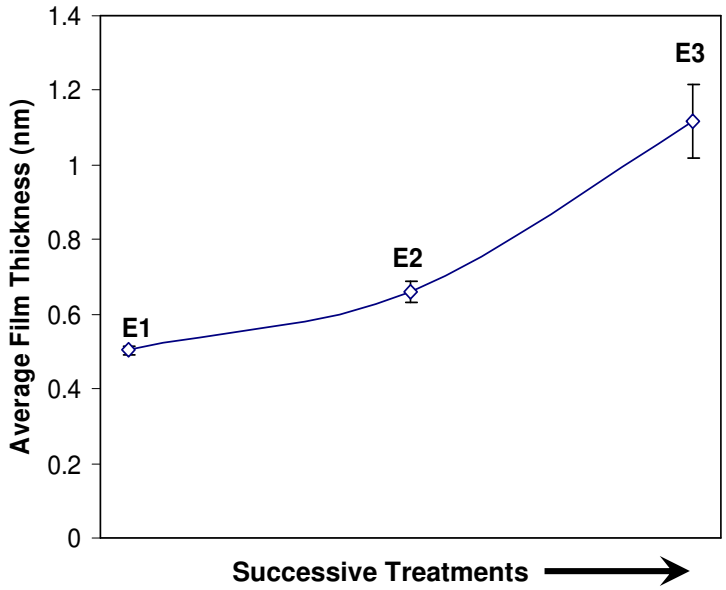

Figure 3-6 The average thickness of E1, E2, and E3 SAMs are measured for at least three points on each substrate using a spectroscopic ellipsometer. The thickness of the monolayers increases as the number defects decreases in silane-based SAMs.

reported height of the methoxy derivative of FAS molecules is 1.34 nm, which is higher than that measured for SAMs on the E3 substrates.[108] The continuous

elimination of the pinhole defects with each refilling of SAMs is easily monitored with spectroscopic ellipsometry.

The ellipsometry data indicates that the refilling of the defects in the silane-based SAMs is a valuable method in increasing the packing density of the molecules in the silane-based SAMs. This technique effectively identifies the changes in the packing density of the molecules in SAMs. A limitation of this technique is the inability to highlight the exact location of defects in the silane-based self-assembled monolayers.

3.3.3 Chemical Amplification of Defects and FTIR Measurements

Based on the previous contact angle measurement studies, conventional SAMs show better packing of molecules and a lower density of defects than microwave-prepared SAMs. The type and density of defects in the silane-based SAMs formed are studied using the conventional thermal technique. The improvement in the quality of these monolayers is monitored by chemically amplifying defects with IR-active silane molecules and using FTIR spectroscopy.

Conventionally formed FAS-based SAMs (E1) are deposited using the thermal technique mentioned previously. The defects in E1 substrates are subsequently amplified. This amplification is achieved by immersing the substrate into a solution of IR-active FPS molecules in toluene for 3 hours. These substrates are heated in a convection oven at 100 ℃ for 3 hours. The pinhole defects in the as-deposited SAMs are filled by chemical or physical adhesion of FPS molecules to the bare regions on the substrate. In addition, the

FPS molecules condense on exposed silanol groups of the physically adsorbed FAS molecules. Figure 3-7 contains a schematic representation of this amplification. The theoretical and experimental IR frequencies for the FPS peaks are summarized in

Table 3-1. The FTIR spectra for the S1 as well as the amplified SAMs are shown in Figure 3-8 (A and B).

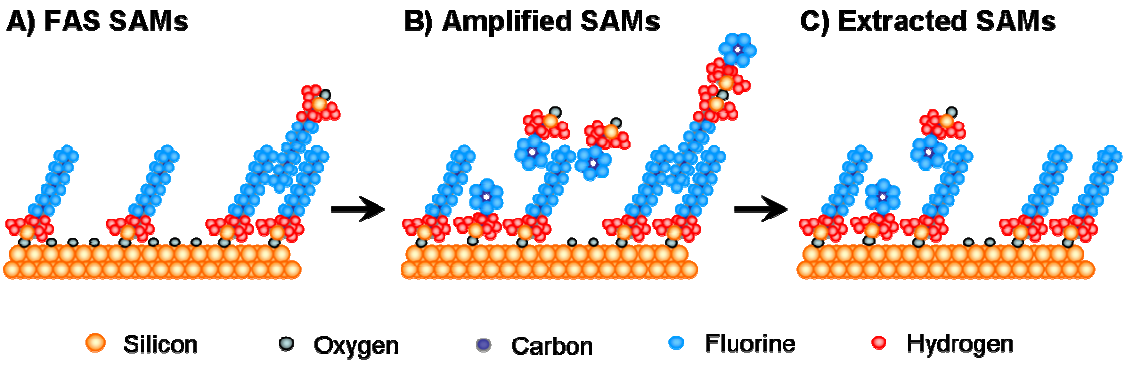

Figure 3-7 Schematic representations of (A) FAS-based SAMs, (B) FPS-amplified SAMs, and (C) the extracted SAMs show FPS molecules attaching to the exposed silanol groups on the substrate or the physically adsorbed molecules on the surface. They may also physically adsorb to SAMs. Extraction removes the majority of the physically adsorbed molecules from the surface.

The bond vibrations of FAS molecules on the surface are difficult to detect due to dampening of the signal by the neighbouring rigid substrate. The high intensity bonding vibrations of FPS molecules are detected more easily than those of FAS molecules. Spectrum B in Figure 3-8 suggests that FPS molecules are adhered (either physically or chemically) to the FAS-based SAMs. The spectra for wave numbers below 1000 cm^{-1} are not resolved due to a low signal-to-noise ratio of the spectrometer, but the presence of IR peaks above 1000 cm^{-1}

is a clear indication of the physical or chemical attachment of FPS to the FAS-covered substrate. Even though, the IR chamber is purged for about 1 hour with

Table 3-1 IR vibrations of FPS molecules.[19, 24, 109]

IR mode	Theoretical peaks (cm^{-1})	Observed peaks (cm^{-1})
Si-OH Stretch	3730	3732
CH_2 Asymmetric Stretch	2918	2912
CH_2 Symmetric Stretch	2850	Not observed
Si-CH_2 Stretch	1600	1611
Si-CH_2 Scissoring	1466	1457
Si-CH_2 Rocking	1261	1261
CF_2 Symmetric Stretch	971	Not observed
CF_2 Asymmetric Stretch	732	Not observed
C-Si Stretch	805, 688	Not observed
CF_2 Rocking	643	Not observed

dry air before and during the experiments, there is no control on the concentration of CO2 gas present in the IR chamber. These limitations are a few disadvantages of using IR spectroscopy to study defects in self-assembled monolayers. This investigation indicates that FPS molecules are adhered to the surface during the amplification step and that the majority of physically adsorbed FPS molecules are removed by Soxhlet extraction.

The physically adsorbed molecules are rinsed off the amplified substrate with toluene in a Soxhlet extractor for three hours. After the surface is extracted,

the intensity of the IR peaks due to FPS decreases (Figure 3-8C). This decrease in the intensity suggests that most of the physically adsorbed FPS molecules are removed from the surface. The presence of the residual peaks indicates that the FPS molecules covalently linked on the surface are not removed by extraction. It may also suggest that Soxhlet extraction is unable to remove all the physically adsorbed molecules from the surface.

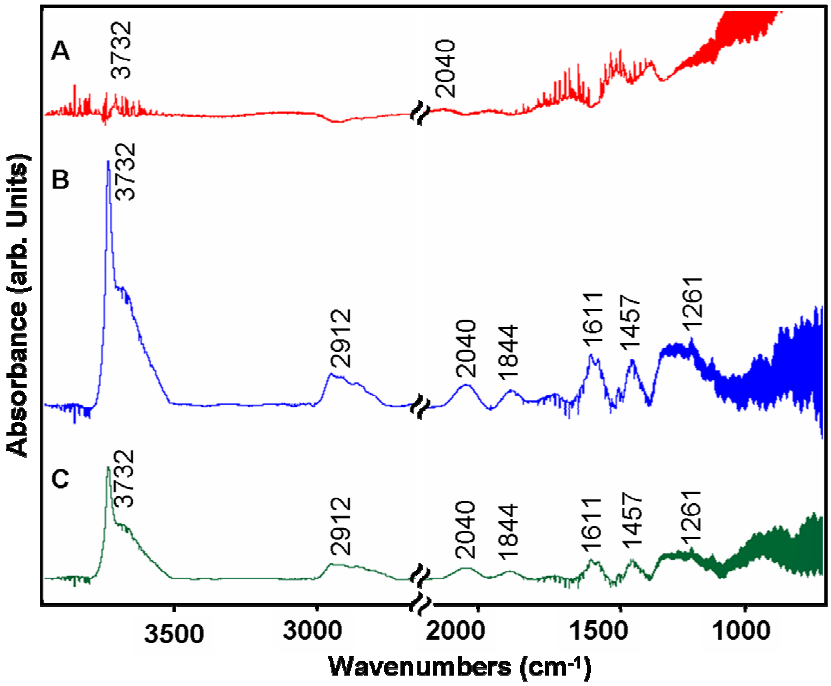

Figure 3-8 FTIR spectra of (A) untreated FAS-based SAMs is compared to those after (B) chemical amplification of defects in SAMs with IR-active FPS molecules. This chemical amplification enables us to monitor the presence of defects before and (C) after extraction of the FPS-treated FAS-based SAMs. The intensity of the IR peaks decreases after the extraction of physically adsorbed molecules from the surface.

The FTIR spectroscopy results indicate that there are two main sources of defects in silane-based SAMs. The first type of defect is the presence of physically adsorbed molecules on the surface. The second type is caused by the low packing density of the silane molecules in SAMs, exposing bare regions of

the substrate. The FTIR spectra acquired after the extraction of physically adsorbed molecules indicates that most FPS molecules physically adsorbed to SAMs or FPS molecules covalently linked to the physically adsorbed FAS molecules are removed from the surface. This data does, however, not provide any information about the location of defects in silane-based SAMs. Thus, there is a need for complimentary analytical techniques to identify the location and packing density of defects in the silane-based SAMs.

3.3.4 Detection of Defects by AFM and SEM Imaging and XPS Analysis

Defects in self-assembled monolayers consist of nano- or microscale pinholes and molecules physically adsorbed on the surface. These defects are simply too small to be directly detected using any imaging technique such as scanning electron microscopy (SEM) or atomic force microscopy (AFM). The defects are amplified and their location and density is identified using various spectroscopy and microscopy techniques.

Electroless metal deposition (EMD) amplifies the defects in the silane-based SAMs. In order to electrolessly deposit silver particles onto the defects, the substrates covered with FAS-based SAMs are immersed into a silver deposition solution. This solution is prepared by combining silver nitrate (1 mM) and buffered hydrofluoric acid (1% v/v) in water. The substrate covered with SAMs is immersed into this solution for 5 minutes at room temperature. Silver nanoparticles are deposited on the exposed defects and the location and density of defects in FAS-based SAMs are identified by SEM and AFM imaging techniques. The density of these defects (amplified by silver particles) is

compared by estimating the number of the particles in the AFM image after each extraction and refilling step. The estimated data enables us to evaluate the effect of these correction techniques on the silane-based SAMs. The relative amount of silver deposited on SAMs after each correction step is quantified using XPS measurements.

The conventional technique is used to deposit SAMs onto silicon wafers and investigate them using the microscopy and spectroscopy techniques. Our contact angle and ellipsometry measurements as well as the FTIR results indicate that repeated steps of extraction and silane deposition decrease the number of defects present in the self-assembled monolayers. The correction of defects has two main effects on the silver deposition. Firstly, the densely packed SAMs will prevent the formation of silver particles on the surface. Secondly, SAMs with a low density of defects prevent the transfer of electrons from the surface to the silver solution, resulting in the formation of disperse low-density silver particle films on the surface.

A scanning electron microscope is used to image the silver particles deposited on the FAS-based SAMs after each silane deposition and extraction step. The images for S1 to E3 substrates are shown in Figure 3-9 where silver particles appear as the white spots on the dark surface. As-deposited FAS-based SAMs show silver particle deposition on almost the entire surface. There is a very small region of the surface with no silver particles present. In this region, densely packed SAMs prevent the silver ions and hydrofluoric acid from approaching the surface. No silver particles are formed on this region of the

surface. The rest of the S1 substrate is fully covered with silver particles, indicating that there are a large number of defects present in these monolayers.

The S1 substrate is placed in a Soxhlet extractor to remove the physically adsorbed molecules. Silver deposition on this extracted (E1) substrate show larger protected regions, where SAMs have prevented the formation of silver ions (Figure 3-9 E1). These results suggest that silver particles form on the physically adsorbed silane molecules. Hence, by extracting the physically adsorbed

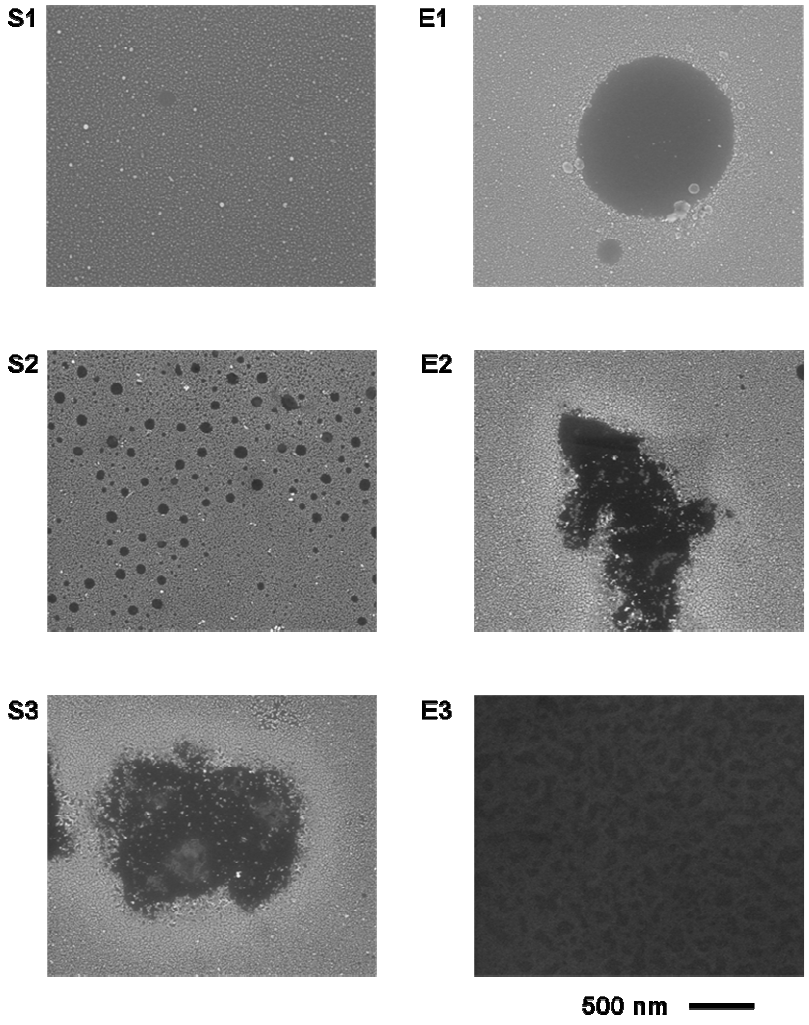

Figure 3-9 SEM images of electroless silver deposition on S1 to E3 substrates (in a silver nitrate (1 mM) and buffered hydrofluoric acid (1% v/v) solution for 5 minutes) indicate that the density of silver particles (white spots) decreases on refilled and extracted substrates.

molecules from the surface, the number of silver particles deposited on a silane-based SAMs is reduced.

The defects in SAMs are further corrected by subsequent refilling and extracting steps and, as seen in Figure 3-9, the S2 and E2 substrates show large areas with no silver particles. The electroless silver deposition on the S3 and E3 substrates results in the formation of an even lower density of silver particles. These results suggest that the packing density of silane-based SAMs increases by repeating the silane deposition and extraction steps. These densely packed SAMs prevent electron transfer from the substrate to the silver solution, resulting in the formation of fewer and smaller silver particles than seen in previous stages of correction (S1 to E2). Reducing the defects in SAMs increases their ability to protect the substrate from silver deposition.

Atomic force microscopy is used to obtain images with a higher resolution than the SEM images shown in Figure 3-9. Atomic force microscopy has an angstrom-scale vertical resolution, but its spatial resolution is limited to a few nanometers. This relatively low spatial resolution prevents researchers from identifying the molecular-scale defects in self-assembled monolayers. Hence, amplification these defects is required prior to AFM imaging. In these studies, the electroless silver deposition is carried out using the procedure mentioned

previously. Figure 3-10 shows the AFM images of silver deposition after different stages of silane deposition and extraction (S1 to E3).

The AFM images collected after EMD on SAMs suggest that as-deposited SAMs (S1) are mostly covered with silver particles. The small regions with no silver particles are indications that densely packed FAS-based SAMs in these areas prevent the silver ions and hydrofluoric acid from approaching the silicon

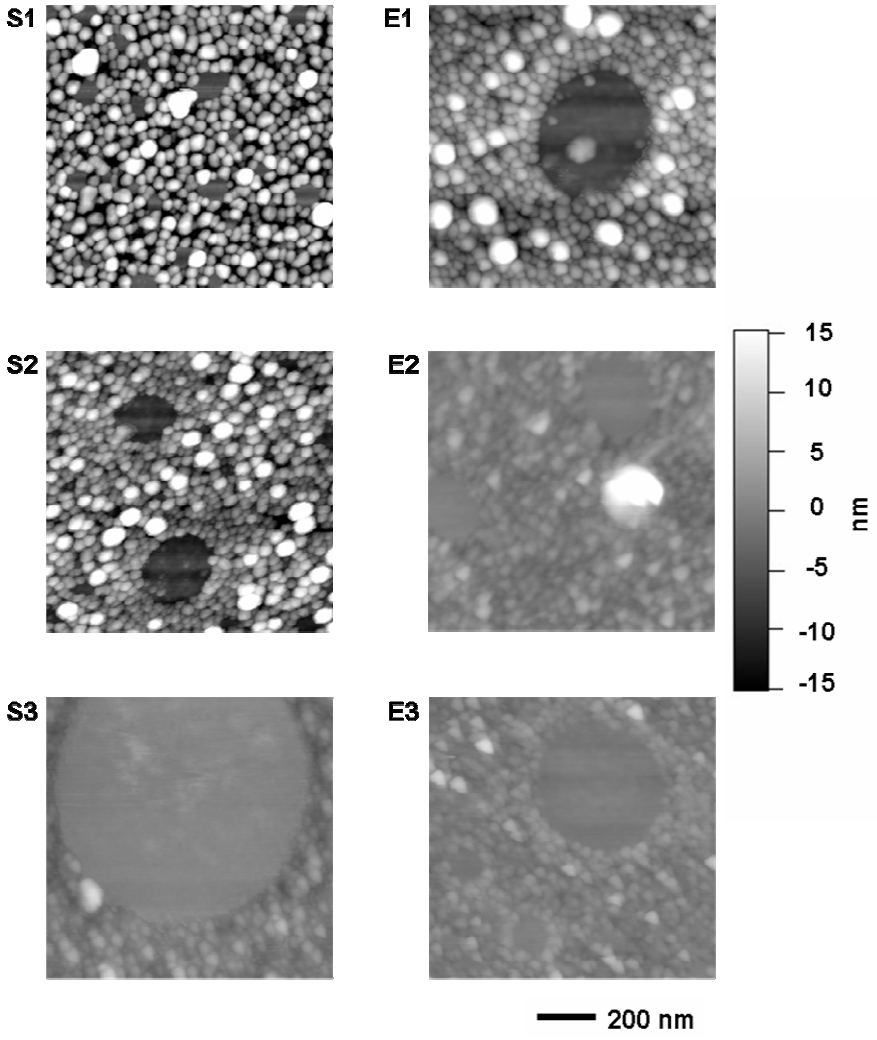

Figure 3-10 AFM images of SAMs are collected after electroless silver deposition by immersion of S1 to E3 substrates in to a silver nitrate (1 mM) and buffered hydrofluoric acid (1% v/v) solution for 5 minutes. Extraction and refilling of the defects increase the size and density of regions protected by SAMs.

oxide substrate. The E1 substrate reveals a much larger protected area than the S1 substrate. The average size of the silver particles on the E1 substrate is smaller than the particles on the S1 substrates. This data suggests that the physically adsorbed silane molecules can cause the formation of silver particles on the surface. After extracting these molecules, fewer silver particles are deposited on the E1 substrate. Extraction is a valuable technique to decrease the number of defects in silane-based SAMs.

In addition to the physically adsorbed silane molecules, pinhole defects also allow the formation of silver particles on the surface. The extraction step removes physically adsorbed molecules from the SAMs and exposes the underlying silicon oxide surface. The densely packed silver particles form on this exposed surface. Compared to the S1 substrate, the particles formed on the E1 substrates are more densely packed. Similar to what was concluded from the contact angle studies, these results indicate that the extraction of physically adsorbed molecules from the surface exposes pinhole defects in SAMs.

Each silane deposition and extraction step reduces the number of defects. This decrease in the number of defects is clearly shown from the size and the density of the silver particles formed on the corrected surfaces. The AFM images of silver deposition on the S3 and E3 substrates show large regions with no silver particles present. These regions of densely packed SAMs prevent the silver ions and hydrofluoric acid from approaching the surface and forming silver particles. In addition, the particles formed on the S3 and E3 substrates are much smaller in size than those formed on the S1 to E2 substrates. This decrease in the particle

size is due to the ability of SAMs to prevent electron transfer from the silicon substrate to the silver ions in the solution, and will be discussed in detail later in this section. The reduced transfer of electrons also decreases the number of silver ions reduced in the solution. The overall density of defects and the size of the silver particles formed on the S3 and E3 substrates are similar. This data indicates that repeated extraction and refilling of SAMs increases the packing density of molecules in silane-based SAMs. These relatively dense monolayers contain fewer defects than the as-deposited SAMs and can more effectively modify the properties of silicon oxide substrates and protect this substrate from etchants such as hydrofluoric acid.

The SEM and AFM images indicate that the as-deposited SAMs are unable to protect the surface from silver ion and the hydrofluoric acid solution and result in the deposition silver particles over the entire surface. Silver deposition on the extracted substrate reveals regions of the substrate that are not covered with silver particles. Refilling the pinhole defects increases the packing density of molecules in the silane-based SAMs and protects the substrate from the hydrofluoric acid and silver ion solution. This data indicates that extracting and refilling the defects in silane-based SAMs are important steps to correct defects in SAMs.

The number of defects may be quantified by identifying the exact amount of silver deposited on each substrate using an energy dispersive X-ray spectrometer and a scanning electron microscope. To confirm that this technique has the ability to detect silver particles on the surface, a control sample

is generated and scanned. This sample is prepared by immersing a clean silicon oxide coated single crystalline silicon substrate in an aqueous 5 mM solution of silver nitrite with 1% (v/v) buffered hydrofluoric acid. A few micrometer-thick layer of silver deposits over the entire surface after 16 hours of silver deposition. Figure 3-11 shows the SEM image and the corresponding energy dispersive X-ray spectrum for this sample. The network of silver particles on the surface are clearly observed in this SEM image and the silver peaks are easily detected by EDS. Energy dispersive X-ray spectroscopy is, however, unable to detect the presence of silver in the silver-treated S1 to E3 substrates. This lack of sensitivity is due to the lower concentration of silver particles on the surface of S1 to E3 substrates compared to the control sample. The EDS spectrum collected from a 2 μm^2 area of the control sample with 100 seconds acquisition time shows a strong silver signal, but this technique cannot be used as a quantitative method to compare the amount of silver deposition after each extraction and refilling step in silane based SAMs.

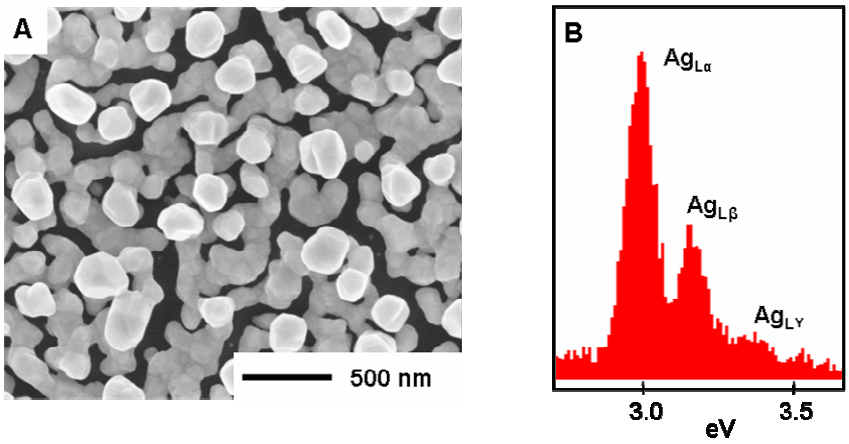

Figure 3-11 Scanning electron microscopy image of electroless silver deposition (5 mM $AgNO_3$, 1% (v/v) HF, 16 h deposition) on a (A) silicon oxide substrate and (B) the corresponding EDS spectrum (2 μm^2 area and 100 seconds acquisition time) indicate that silver particles form on the surface of silicon oxide in the absence of silane-based SAMs.

The amount of silver deposited on SAMs after each silane deposition and extraction step is quantified by X-ray photoelectron spectroscopy (XPS). The deposition of SAMs, following by the extraction and refilling of defects, as well as the electroless silver deposition steps are carried out using the techniques mentioned previously in this chapter. A control sample is prepared by immersing a piranha cleaned and N_2 gas dried silicon oxide covered single crystalline silicon substrate in a silver deposition solution (1 mM $AgNO_3$ and 1% (v/v) HF) for 5 minutes. This substrate is subsequently rinsed with 18.2 MΩ water and dried with N_2 gas prior to analysis by XPS. The silver-treated S1, E1, S2, E2, S3, E3 and control substrate are analyzed using XPS (Figure 3-12). Carbon 1S electrons are used to calibrate the graphs for each sample. Survey scans (with passing energy of 160 eV) and high resolution Ag(3d) scans are collected for each sample. The survey scans are presented in Appendix 2. Silver doublets are identified at 374.2 eV ($3d_{3/2}$) and 368.2 eV ($3d_{5/2}$) and are in precise agreement with the spectrum for silver.[74] All the spectroscopic measuring parameters are kept constant for the samples to provide a quantitative measurement for the presence of silver on each surface. The shift in the binding energy of the E2 samples may indicate the formation of silver oxide.[72] Considering that silver particles on all these substrates are formed under the same conditions, this shift may be due to instrumental errors.

X-ray photoelectron spectroscopy is a precise technique and the area under the XPS peaks is often used to quantify the amount of specific atoms present on a surface.[74] The peak area for each spectrum in Figure 3-12 is

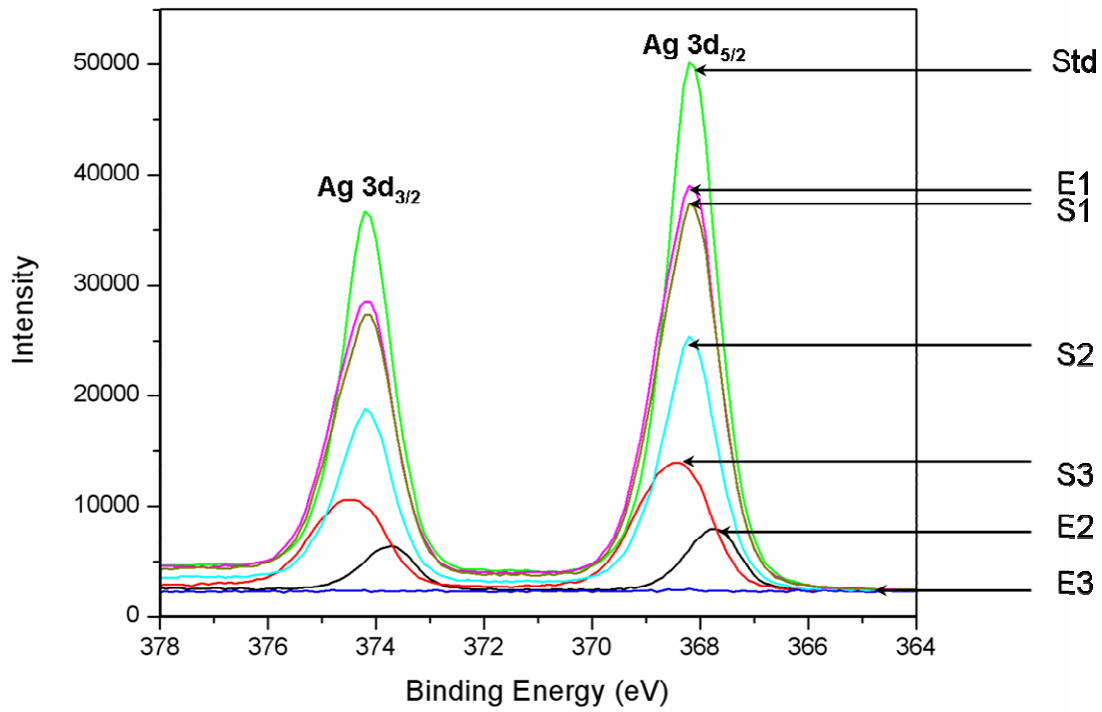

Figure 3-12 X-ray photoelectron spectra of silver (3d) peak after performing EMD (1 mM $AgNO_3$ and 1% (v/v) HF) on S1, E1, S2, E2, S3, E3 and bare SiO_2 (Std) substrates suggest that correcting for defects reduces the amount of silver deposited on the substrates protected by SAMs.

calculated and the amount of silver deposited on SAMs after each correction step is quantified (Figure 3-13). This data indicates that amount silver deposited on a bare silicon oxide substrate (standard) is greater than the silver deposited on the substrates covered with SAMs. The density of silver particles (proportional to the number of defects in SAMs) is lower in S1 substrates than the E1 samples. This

can be due to the exposure of a high number of pinhole defects when the physically adsorbed molecules are extracted from the surface. Further refilling of the defects in S2 substrates result in a decrease in the concentration of silver in comparison to S1 and E1 substrates. The extraction of physically adsorbed SAMs from the S2 substrates results in a dramatic decrease in the silver particle concentration on the surface. This decrease in the concentration suggests that the physically adsorbed molecules are an important source of defects in SAMs and removing these defects improves the quality of the resultant self-assembled monolayers.

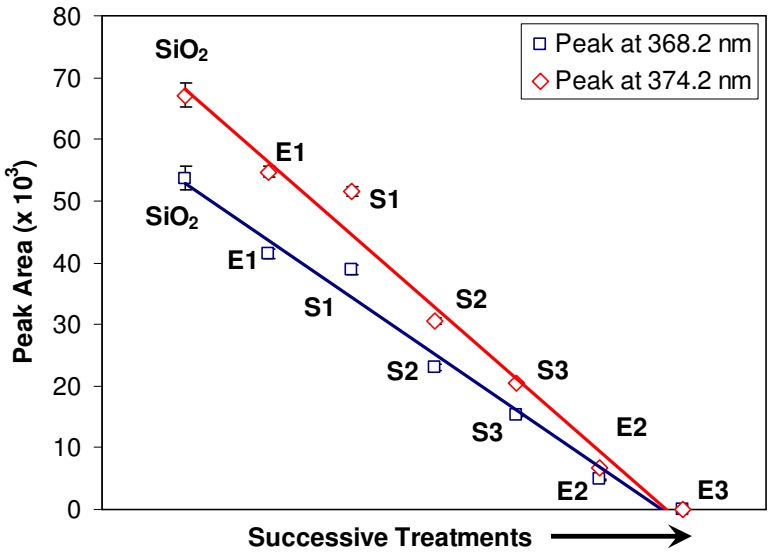

Figure 3-13 The quantity of the silver on different surfaces is monitored by calculating the area under the XPS peaks for EMD treated (1 mM $AgNO_3$, 1% (v/v) HF, 5 minutes of deposition) SiO_2 and corrected SAMs. Note: the lines are used as guides for the eye to observe the trends.

Further silane deposition on these extracted SAMs forms new physically adsorbed silane molecules onto the surface. These molecules are then covered with silver particles, which ultimately results in an increase in the silver peak

intensity in Figure 3-12 S3. Extracting these molecules from the surface decreases the amount of silver deposited onto SAMs, as expected. The explanation for the shift in the peak position of the E2 and S3 spectra (to slightly higher and lower energy, respectively) is unclear. The XPS results are a further indication that these correction steps substantially improve the ability of SAMs to protect a substrate from etchants (such as hydrofluoric acid) and adhesion of molecules or growth of particles (such as silver nanoparticles) on the surface.

Electroless deposition is an autocatalytic process.[52] In such processes, increasing the number of electrons transferred from the substrate to the solution increases the size of the metal particles on the surface. Large pinhole defects provide a large surface area from which the electrons can be transferred through silver particles to the silver ions in the solution. Decreasing the size of the pinholes through extraction and refilling steps should result in a decrease in the size of the particles formed during the electroless silver deposition. The effect of extraction and refilling is further monitored by measuring the average particle size formed on the sites of defects. The error values are calculated as twice the value of standard deviation. The AFM images shown in Figure 3-10 are used for these measurements. The result of this particle size analysis study is shown in Figure 3-14.

The particles formed on the as-deposited SAMs (S1) tend to have the largest size among those shown in Figure 3-14. This formation of large particles on the S1 substrates is expected since these SAMs have a high density of defects present in them. The size of these particles is highly variable (see the

error bars in Figure 3-14) due to the difference in the size of the defects present in the monolayers. Electroless metal deposition on extracted SAMs (E1, E2, and E3) produces smaller particles than those deposited before extraction (S1, S2, and S3). This decrease in the particle size suggests that the average size of defects is reduced and there are fewer physically adsorbed silane molecules on SAMs. The overall variation in the size of particles at each step also decreases as the corrections continue. This decrease in the variability is due to the decrease in the size and number of defects present in the monolayers. Reducing the number of defects and generating a high packing density of molecules in silane-based self-assembled monolayers enables SAMs to efficiently protect a surface.

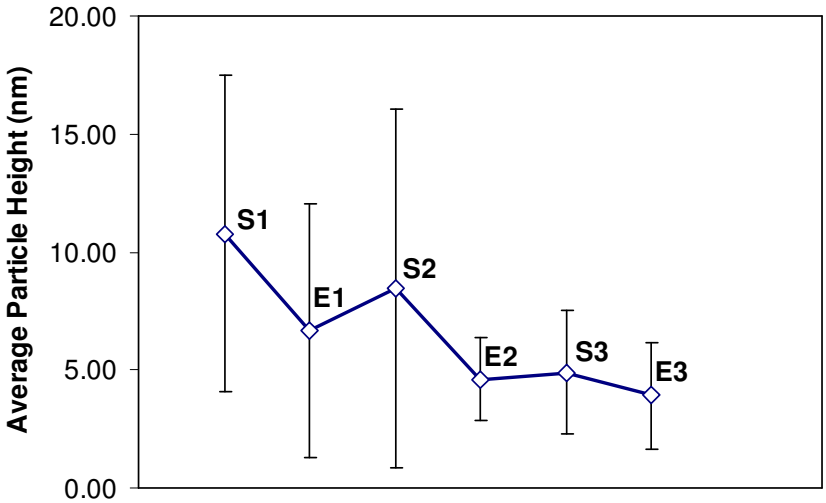

Figure 3-14 The average size of the particles formed by EMD on S1 to E3 SAMs indicates that the corrected SAMs prevent the formation of large particles on the sites of the defects. The error bars are calculated as twice the standard deviation values. Note: the line is used as a guide for the eye to observe the trend.

In the previous experiments, the formation of silver particles due to the presence of physically adsorbed silane molecules on silane-based self-assembled monolayers was observed. In order to confirm that silver particles form on the physically adsorbed silane molecules, 7 μL of FAS is added to 20 mL of a silver salt solution (1 mM in 1% (v/v) hydrofluoric acid). The resulting white precipitate is collected, rinsed it with 18.2 MΩ water and dried it under a stream of nitrogen gas prior to imaging by transmission electron microscopy (TEM). The composition of the powder is also analyzed with energy dispersive X-ray spectroscopy (Figure 3-15). The TEM image and EDS analysis of this powder indicate that silver particles are formed due to the presence of the silane molecules in the silver nitrate and hydrofluoric acid solution. Hence, these molecules could cause the formation of silver particles in the presence of hydrofluoric acid and silver ions when physically adsorbed on SAMs. Similar results are also obtained in the absence of buffered hydrofluoric acid. Physically adsorbed molecules are considered one of the main sources of defects, which can be removed through a simple extraction step.

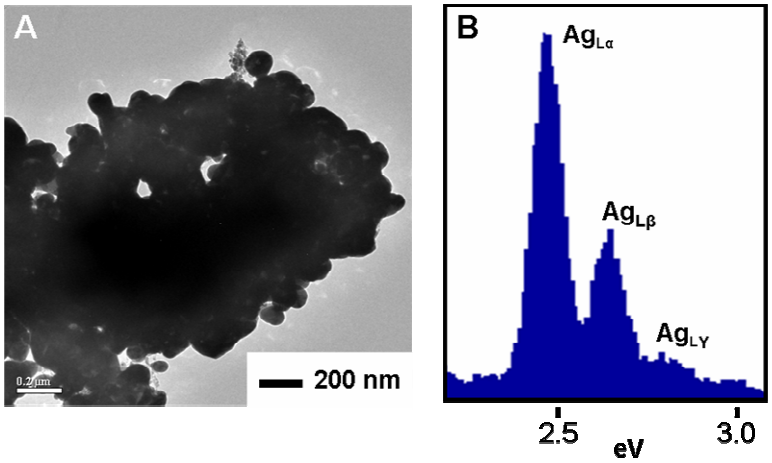

Figure 3-15 Reaction of FAS molecules with silver ions in the presence of hydrofluoric acid results in the formation of a white powder. This powder is imaged using (A) transmission electron microscopy and analyzed by (B) energy dispersive X-ray spectroscopy. This data suggests that silver particles may form in the presence of silane molecules, but in the absence of a silicon oxide substrate.

Extracting the physically adsorbed molecules from the silane-based SAMs and refilling the pinholes with new silane molecules, enables us to form densely packed silane-based self-assembled monolayers on silicon oxide substrates. The chemical amplification of defects using EMD techniques enlarges the size of the defects such that they are detectable using various spectroscopy and microscopy techniques. The SEM and AFM images along with XPS analysis confirm that the density of silver particles on these surfaces decreases after each correction step. In addition, the particle size analysis indicates that the average size of the particles decreases and the particle size distribution narrows after repeated silane-deposition and extraction steps. Lastly, the TEM and EDS results indicate that silver particles can be formed in the presence of the physically adsorbed silane molecules.

The imaging techniques mentioned above are useful due to the ability of electroless silver deposition to highlight the location of defects in the self-assembled monolayers in both the presence and absence of light. The process for the electroless metal deposition is, however, not fully understood. To gain a better understanding of this process, the effect of concentrations of both the silver salt and the buffered hydrofluoric acid is on the size of the silver particles formed on SAMs are monitored.

For this study, the E3 substrates, which have the least number of defects compared to their predecessors (S1, E1, S2, E2, S3), are immersed in the silver ion solution with varying concentrations of either the silver salt or the buffered hydrofluoric acid in the solution for various deposition periods. The substrates covered with silver are subsequently imaged using atomic force microscopy. These AFM images are presented in Appendix 2, but the particle analysis results are summarized in Figure 3-16 and Figure 3-17.

Atomic force microscopy images are used to calculate the quantity and average size of the deposited silver particles. This data is then correlated to the silver deposition time and solute concentrations to gain a better understanding of the electroless metal deposition process. The AFM images are used to calculate the sizes of the particles and to generate a histogram of the particle sizes. The data presented in Figure 3-16 and Figure 3-17 are obtained using the mean value calculated from these histograms. An overall increase in the size of the particles formed upon increasing the silver ion concentration is observed (Figure 3-16). This size increase is due to the increase in the quantity of silver ions present near the reduction site. The reduced silver, on the substrate, serves as a catalyst site to further accelerate the reduction of silver ions to form particles. It takes a high concentration of silver ions in the solution to let these ions diffuse through the solvent to the sites of the defects and reduce to form silver particles. Thus, an increase in the concentration of silver results in the formation of larger silver particles on the surface.

Another important factor influencing the size of the silver particles is the time the substrate spends in the silver ion and buffered HF solution. It takes time for the silver ions to diffuse to and reduce at the sites of defect. A longer deposition time (5 minutes vs. 1 minute or 0.5 minute) results in the formation of larger particles. Electroless deposition is an autocatalytic process and the reduction of ions continues for as long as ions are present in the solution and electrons can be transferred from the silicon substrate to the silver ions through the silver particles. The particles continue to grow with time and the size of these particles to increase as the concentration of metal salt in the solution increases.

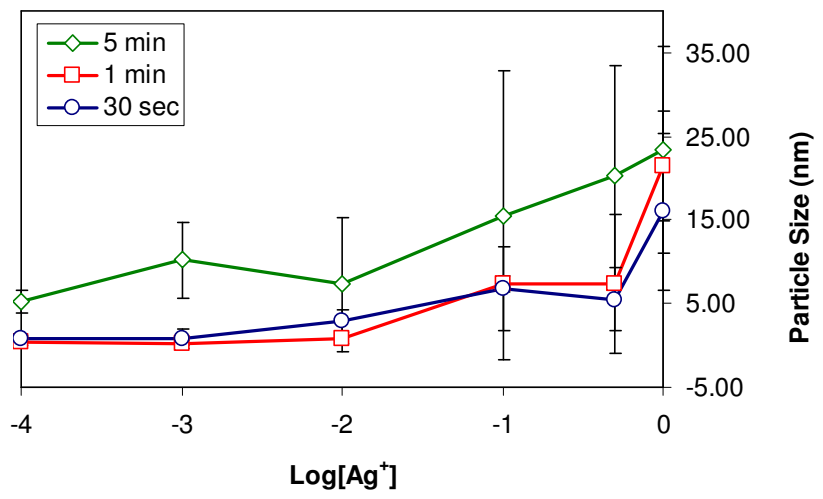

Figure 3-16 Increasing the silver salt concentration and the deposition time lead to an increase in the size of the silver particles formed on the E3 SAMs. The silver salt concentration is calculated in millimolar. The concentration of the buffered hydrofluoric is kept constant (1% v/v) for all the data points shown in this graph. Note: the lines are used as guides for the eye to observe the trends.

The concentration of silver ion is not the only variable in the electroless deposition process. The reducing agent in this experiment is the silicon

substrate. The amount of silicon present in the reaction is dependent on the rate at which hydrofluoric acid removes the silicon oxide and exposes the underlying silicon atoms. The effect of the concentration of buffered hydrofluoric acid on the size of the deposited silver particles is examined.

The E3 substrates are used for these studies as they contain a low density of defects. These substrates are immersed into a 1 mM aqueous solution of silver nitrate. The concentration of buffered hydrofluoric acid varies (0.01%, 0.1% and 1% by volume) for these experiments. The effect of the acid concentration is studied for various deposition times (30 seconds, 1 minute and 5 minutes). The atomic force microscopy images of each sample are collected and are presented in Appendix 2. The average size of the particles on each substrate is calculated and graphed as a function of the concentration of buffered hydrofluoric acid (Figure 3-17).

The results indicate that increasing the concentration of buffered hydrofluoric acid from 0.01% (v/v) to 0.1% (v/v) causes a significant increase in the size of the particles. This increase in the particle size is due increase in the rate at which the silicon oxide is removed from the underlying silicon substrate. This substrate acts as a reducing agent in the electroless deposition reaction and by increasing the number of silicon atoms present for the reaction, the number of electrons available in the solution is increased.[47-48] The abundance of electrons in the solution accelerates the growth of the silver particles on the defects in SAMs.

In addition to etching the silicon oxide, hydrofluoric acid can slowly etch the silicon substrate.[110] Exposure to a high concentration of hydrofluoric acid may result in under-etching the substrate and lead to increased roughness on the surface. The AFM images indicate that average size of the silver particles slightly decreases as the concentration of the buffered HF is increased from 0.1% (v/v) to 1% (v/v). This decrease may be due to the increased surface roughness. The difference between an increase in the surface roughness and particle size is no longer discernable using atomic force microscopy. Other techniques such as Kelvin probe force microscopy (KFM) may be used to obtain such information. This technique maps the work function of a surface and can easily distinguish the semiconducting substrate from the silver particles. The topographical map is often collected concurrently to the work function measurements. Topographical and work function maps may be overlaid to identify the size variations due to the surface roughness versus those due to the presence of the silver particles on the surface. Atomic force microscopy imaging alone does not provide sufficient information to differentiate between the surface roughness and the particles on the surface.

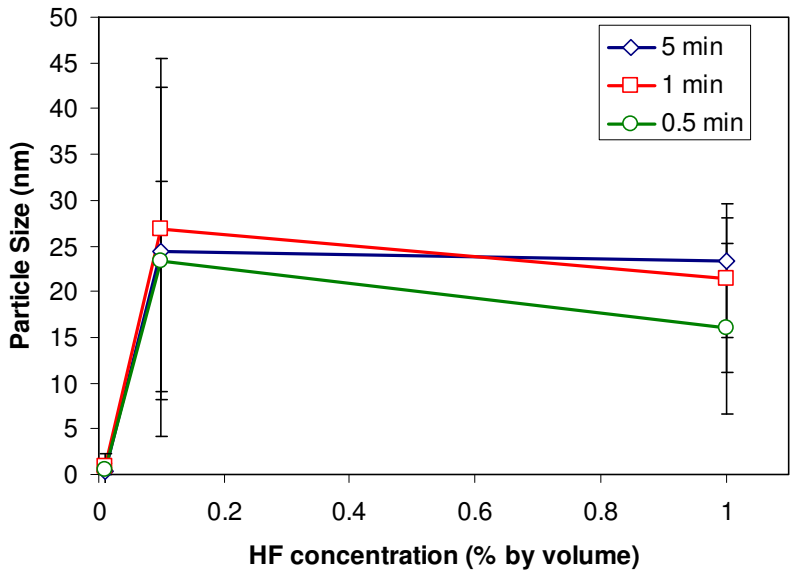

Figure 3-17 The size of particles formed by immersing the E3 SAMs into a 1 mM solution of silver nitrate reduces upon decreasing the concentration of the buffered hydrofluoric acid and the reaction time. Note: the lines are used as guides for the eye to observe the trends.

The change in the concentration of buffered hydrofluoric acid in the deposition solution plays a more significant role in determining the size of the particles than the silver-deposition time (Figure 3-17). This data indicates that the rate

of diffusion of the fluoride ions in the solution is lower than the rate at which buffered hydrofluoric acid etches the substrate. The low diffusion rate of fluoride ions enables us to amplify the defects in silane-based self-assembled monolayers by increasing the silver ion concentration and deposition time, without causing significant under-etching of the substrate by hydrofluoric acid.

Electroless deposition and other chemical amplifications are used to highlight the location of molecular-scale defects in silane-based SAMs. The

process of electroless deposition as an amplification technique to highlight defects in silane-based SAMs is not fully understood. Yet, it has enabled us to identify the location and density of defects in SAMs. This technique is coupled to various imaging and analysis methods to quantify the number of defects in silane-based SAMs after each extraction and refilling step. These results indicate that extraction and refilling of the defects are valuable tools to improve the quality of silane-based SAMs.

3.4 Conclusions on Identification and Correction of Defects

Molecular-scale and larger defects are present in self-assembled monolayers. The first step in the correction of these defects is identifying their location and density in SAMs, but these defects are too small to be located using conventional analytical techniques. Various techniques have been developed to study and compare the density of two main types of defects in SAMs deposited by both conventional and microwave-prepared routes. The quality of SAMs is improved by extracting the physically adsorbed molecules and refilling the exposed regions of the substrate with more silane molecules.

Conventional studies, such as contact angle measurements, provide valuable information about the presence of self-assembled monolayers on a substrate and can be used to monitor the improvement in the quality of the silane-based SAMs. After a certain point in the improvement, these measurements are not sensitive to molecular-scale defects. There is a need to develop new analytical techniques to monitor and identify the density and location of defects in SAMs.

Chemical amplification is coupled to FTIR spectroscopy, AFM and SEM imaging, as well as XPS analysis to further investigate these defects. Some industries rely on self-assembled monolayers for etch resists, low friction coatings, and biosensors amongst other applications.[6, 7] Defects in SAMs may act as sites for adhesion of unwanted bio-molecules or cause the failure of SAMs as etch resists. They may result in quick fatigue of SAMs as friction layers. The presence of molecular-scale (and larger) defects may be the source of unexpected inaccuracy in the application of SAMs in these and other fields of science and engineering.

The microwave approach to the deposition of silane-based SAMs saves a tremendous amount of time and energy in formation of these monolayers. These SAMs contain a higher density of defects than those formed using the conventional approach. Microwave deposition of SAMs may only be used for applications where the density of defects in the monolayers does not diminish the overall outcome of the application. These correction techniques can lower the amount of defects present in silane-based SAMs. Using a microwave reactor should improve the quality and increase the reproducibility in microwave-prepared SAMs. Various techniques have been developed to monitor defects in silane-based self-assembled monolayers and have been able to monitor the influence of the experimental parameters on the quality of SAMs. This feedback loop is essential for successive iterations and further improvement of the packing density of molecules in these monolayers.

CHAPTER 4: OVERALL CONCLUSIONS AND FUTURE DIRECTIONS

4.1 Conclusions

Silane-based self-assembled monolayers are commonly used in materials and biological sciences as a convenient tool to modify the physical and chemical properties of surfaces.[9] These monolayers are considered to be a highly ordered arrangements of molecules on a surface. In this thesis, it has been shown that regardless of the route taken to generate silane-based self-assemble monolayers, there are various intrinsic and extrinsic defects present in these SAMs.

Two techniques are employed to form silane-based SAMs, both of which benefit from immersion of substrates in the silane solution prior to the condensation period. The condensation step in the formation of SAMs is sped up by a factor of 300 using microwave irradiation as the source of energy. Microwave-prepared deposition of SAMs is quick and can generate monolayers with similar wettability as SAMs deposited using a more conventional technique. Our studies indicate that SAMs deposited in a microwave oven contain more molecular-scale defects than the conventionally deposited SAMs. Some applications of SAMs do not require a high packing density of molecules in the monolayers (e.g., those used for altering the wettability of a substrate). For such applications, thousands of silicon oxide substrates can be coated with silane-

based SAMs using the microwave approach in the same amount of time that would take to generate SAMs on half a dozen substrates using the more conventional approach. This time saving technique also reduces the number of technicians required, and ultimately could translate into major financial savings in the formation of these monolayers.

The number of defects in SAMs may play an important role in other applications of these monolayers. Two types of defects are identified and methods are developed to reduce their density in silane-based SAMs. This decrease in the density of defects is monitored using various spectroscopy and microscopy techniques. Densely packed monolayers are required to protect surfaces against etchants and the adhesion of unwanted biomolecules. Decreasing the number of defects improves the quality of silane-based SAMs on silicon oxide substrates. Our results show that the repeated extraction and refilling of defects in silane-based SAMs decreases the number of the defects in these self-assembled monolayers. This result is important in microelectronic and microfabrication processes.

4.2 Future Work

4.2.1 Investigating the Effect of Water Content on the Formation of SAMs

Many studies indicate the importance of surface bound water to the formation of silane-based SAMs in solution.[32] It is known that the silane molecules hydrolyze in the presence of water.[33] This hydrolysis is required for the formation of silane-based SAMs on the silicon oxide surface. There are,

however, no investigations to identify the effect of the water content in the silane solution on the formation of these monolayers. It is important to identify and monitor the influence of the water on the quality of silane-based SAMs.

As explained in Chapter 2, different wettability was observed in SAMs formed from different bottles of silane molecules. The initial purity of both batches of silanes were identical, however, one bottle has been exposed to air for a few months longer than the other bottle. Exposure to the moisture in the air may increase the water content in these silane bottles. This increased water content can result in the hydrolysis and possible polymerization of the silane molecules prior to their dissolution in a solvent. It is important to understand the effect of the water content in the silane-solution to obtain a detailed understanding of the self-assembly process. Microwave condensation of silanes is a valuable technique to use for this study. It increases the rate of the reaction and reduces the exposure of the silane solution to air during the deposition process.

To study the effect of water content in the silane solution on the packing density of SAMs, a stock silane solution should be prepared. Different volumes of water should be added to different aliquots of this silane solution. Cleaned and dried silicon substrates should be used in similar procedure as explained in Section 3.2.3 to identify the effect of the water content on the quality of SAMs. In addition, extra steps maybe taken to control the surface bound water. Identifying the influence of water is important in understanding the self-assembly process and improving the quality of silane-based SAMs.

4.2.2 Study of the Influence of Nitric Acid on the Electroless Metal Deposition Process

Electroless metal deposition is commonly used to generate metal films on silicon substrates.[47] As discussed in Chapter 3, this technique has been used to deposit silver nanoparticles on the defects in silane-based SAMs. For this process, an aqueous solution of silver nitrate and hydrofluoric acid is used. Nitric acid is a side product of this reaction. It is known that the presence of nitric acid increases the rate at which hydrofluoric acid etches the silicon oxide coated silicon substrates.[111, 112] It is important to identify the extent at which the low concentration of nitric acid formed during EMD influences the etching of the substrate. For this study, other silver salts (e.g., silver acetate) can be used to deposit silver particles on the surface. The AFM images of the substrates should be collected and used to estimate the average size of the silver particles formed. The size of the new particles could be compared to those reported in Chapter 3 to identify the influence of the nitric acid formation during electroless silver deposition.

4.2.3 Nuclear Magnetic Resonance (NMR) of Silane-Based SAMs

It is important to quantify the density of defects in silane-based SAMs after each correction and silane deposition step. Nuclear magnetic resonance (NMR) spectroscopy is a useful tool to study molecular dynamics in molecules[113] and may allow us to quantify the amount of FAS molecules present in SAMs on silicon oxide surfaces. This technique enables us to detect interactions such as chemical shielding, nuclear spin coupling, dipole-dipole coupling and quadrupole

coupling in solid state molecules and SAMs on nanoparticles[114] or solid substrates.[115, 116] Solid-state NMR spectroscopy would provide information about the packing density of FAS molecules on silicon substrates before and after extraction.

Solid-state ^{19}F NMR or ^{29}Si NMR were not available during this research. Thus, the samples are modified such that a solution-phase ^{19}F NMR technique can be used for the preliminary study. The FAS molecules have fourteen fluorine atoms that are roughly in the same chemical environment. These atoms should provide an easily detectible signal in the ^{19}F NMR spectrum. To prepare the sample, a 50-μm thick silicon substrate is coated with FAS molecules by immersing the substrate into a 1 mM solution of FAS in toluene for three hours. The substrates are subsequently rinsed with toluene and dried with nitrogen gas prior to the condensation of the silane molecules to the substrate in a convection oven at 100 ºC for three hours . The thin substrates are used to increase the fluorine to silicon ratio for these samples. In order to pack the substrate into a NMR tube, the substrate is ground with a mortar and pestle to a fine powder. (Note: Grinding the sample may remove portions of SAMs.) Deuterated chloroform is added to imitate a solution-phase for NMR spectroscopy. A specific amount of fluorobenzene is added to each sample as an internal standard. The preliminary spectra were obtained, but due to various technical reasons, the necessary spectra for quantitative analysis of SAMs both before and after extraction were not obtained. These studies need to be repeated to obtain results providing some quantitative information about the number of FAS

molecules removed from the surface during each extraction step or added to SAMs after each refilling process.

4.2.4 Attenuated Total Reflectance (ATR) IR Spectroscopy of Molecules in SAMs

In Chapter 3, the investigation into the type of defects present in silane-based SAMs using absorbance FTIR spectroscopy is discussed. The FAS-based SAMs on the substrate are difficult to detect using this technique due to the low concentration of molecules on the surface. The attenuated total reflectance (ATR) IR spectroscopy is sufficiently sensitive to detect small changes in the composition of SAMs. This technique could be used to study the adhesion of IR-active silanes to pinhole defects and physically adsorbed silane molecules on the surface.

The ATR crystals can be coated with SAMs of interest and studied using ATR-IR spectroscopy. The IR beam enters the crystal and reflects internally 10-20 times before exiting the crystal and entering the spectrometer (Figure 4-1).[117] This internal reflection increases the intensity of the IR beam entering the

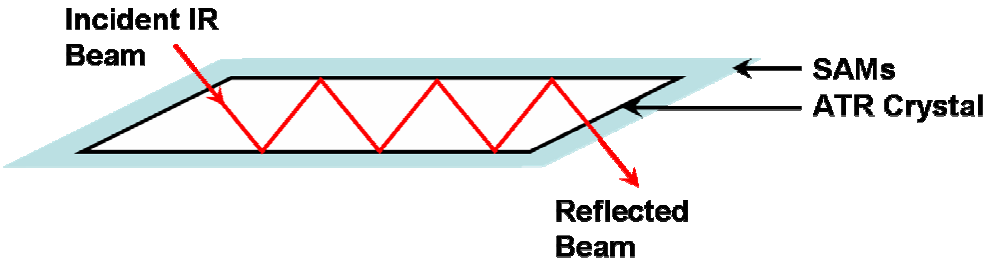

Figure 4-1 An ATR crystal is often covered with SAMs to improve the signal-to-noise ratio of an IR signal to easily detect the molecules present in the monolayers.

spectrometer and results in a higher signal-to-noise ratio than the regular transmittance FTIR. This technique is used to study formation of silane monolayers on a silicon substrate.[63, 118]

Attenuated total reflectance (ATR) spectroscopy is often used to obtain transmittance spectra for highly absorbent materials.[119] The changes in the composition of SAMs before and after silane deposition and extraction could be monitored using this technique. ATR-IR spectroscopy is a highly sensitive technique and could be used to identify the presence of various molecules in self-assembled monolayers. This technique is easily accessible and due to its high signal-to-noise ratio provides highly accurate spectra.

4.2.5 Kelvin Probe Force Microscopy (KFM) of Defects in SAMs

Kelvin probe force microscopy (KFM) is used to map the changes in the work function (Φ) of different parts of an electrically or ionically conducting substrate.[120] This technique is often coupled with atomic force microscopy (AFM) to simultaneously obtain maps of the topography and work function of a surface. In Chapter 3, the amplification of defects using electroless silver deposition is discussed. Atomic force microscopy imaging is used to identify the location of defects in silane-based SAMs. As previously discussed, the small silver particles cannot be differentiated from the roughness of the surface following HF exposure by AFM imaging. Kelvin probe force microscopy coupled to AFM imaging can provide an overlaid map of the work function and topography of the surface. This map may be used to differentiate between the silver particles formed and the roughness of the surface due to chemical

mechanical polishing or HF etching. Substrates with thick (thermally grown) silicon oxide layers (200 – 500 nm) may be used to increase the surface roughness due to hydrofluoric acid etching of the surface. The AFM images collected from this surface combined with KFM maps can be used to clearly distinguish silver particles from surface roughness.

The spatial resolution of KFM is dependent on the diameter of the tip used (usually >10 nm) and consequently, it cannot provide information about molecular-scale defects in SAMs. This technique can provide valuable information when the defects are sufficiently amplified with metal particles and can be used to provide a better understanding of the EMD process.

4.2.6 Correction of Defects by Refilling Pinholes with Different Molecules

Pinholes defects are commonly found in self-assembled monolayers. They range in size from a nanometer to a few micrometers. Various types of molecules can be used to fill in these pinholes. Both FAS and FPS molecules are used as the refilling silane molecules in the studies reported in this thesis. Molecules with different physical and chemical properties can be used to fill in these gaps. For example, bulky silane molecules may be used to fill in large pinholes in SAMs followed by a smaller silane to fill the remaining gaps. Once the large molecules bind to the surface, most of the gaps are filled. It may only take a few smaller molecules to fill the remaining gaps and form densely packed monolayers.

One may also choose to form mixed SAMs of phenyl silane and fluorophenyl silane (such as FPS). The quadrupole-quadrupole interactions between FPS and phenyl silane molecules increase the intermolecular forces in monolayers (Figure 4-2).[121] These interactions provide extra incentive for molecules to form densely packed physically adsorbed SAMs on the surface. These SAMs can be condensed onto the surface using the conventional thermal technique or microwave irradiation. The increased intermolecular forces can result in the formation of densely packed silane-based SAMs.

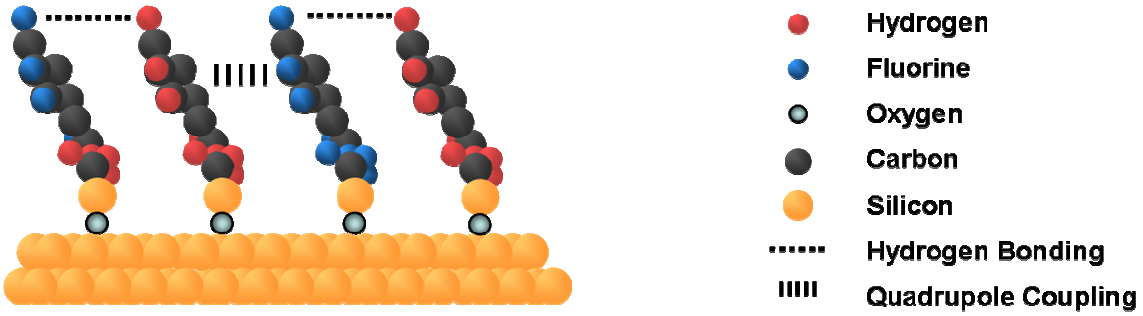

Figure 4-2 Fluorophenyl silane-based SAMs are refilled with phenyl silanes to increase the intermolecular forces within the self-assembled monolayers. Note: The methyl groups of FPS molecules have been removed to enhance the clarity of the image.

Pinhole defects in silane-based SAMs may also form due to the presence of defects in the silicon substrates. For instance, metal impurities are often found on these substrates. These metals are remained from the polishing step in the manufacturing of these substrates and are considered sources of extrinsic defects. They prevent silane molecules from accessing the silicon substrate. A different approach may be taken to fill in these types of pinhole defects. Acids such as oleic acid can bind to the metal molecules on the surface. The functional

groups of these molecules can be modified to provide properties similar to the functional group of the molecules forming the original SAMs. In oleic acid, the exposed alkyl chains would interact with the fluoroalkyl chains of the silane molecules in SAMs and modify the wettability of the pinholes. Many molecules can be used to fill the pinholes and reduce the number of defects in silane-based SAMs.

In this thesis, a method for rapid deposition of silane-based SAMs is reported. Various methods are developed to improve the quality of these monolayers. These SAMs are important in modifying surfaces and further improvement in the quality and efficiency of formation of these monolayers will increase their applicability in various aspects of science and engineering.

APPENDIX 2: ADDITIONAL DATA

Electroless metal deposition is used to amplify defects in silane-based self-assembled monolayers. The defects in SAMs are too small to be detected by AFM imaging, but the amplified defects are large enough to be easily detected and viewed using this microscopy technique. During the EMD process, silver ions reduce in the presence of exposed silicon substrate. Figure A.1A shows an AFM image of a bare silicon oxide substrate. Once this substrate is immersed into a solution of silver salt (1 mM) and buffered hydrofluoric acid (1% v/v) silver nanoparticles deposit all over the substrate (Figure A.1B). In this study, the surface of the silicon oxide is not covered with self-assembled monolayers and therefore, the silicon substrate is fully exposed to the electroless deposition solution. As expected, nanometer size particles grow on the entire surface and completely alter its topography.

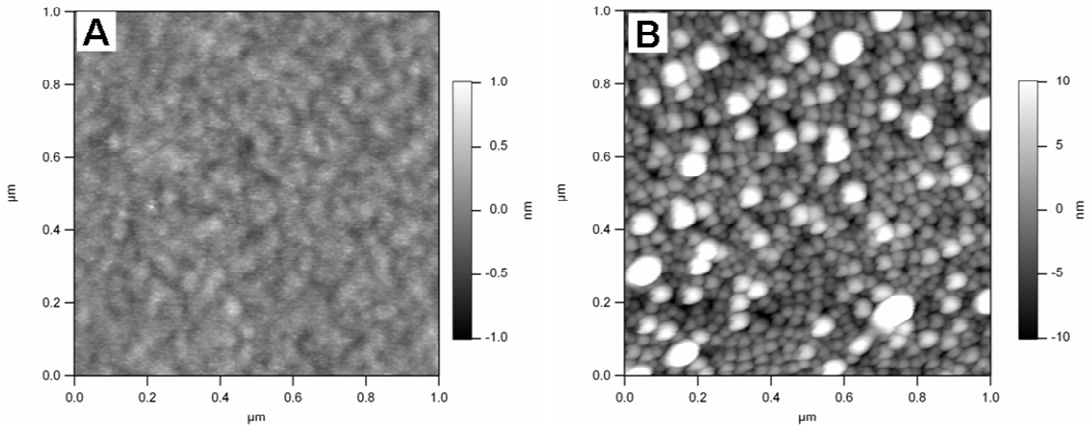

Figure A.1 The AFM image of silicon substrate before the electroless deposition of silver (A) shows much smoother topography than (B) after the immersion of the substrate into 1 mM silver nitrate and 1% (v/v) buffered HF for 5 minutes.

In Chapter 4, a summary of the results on the affect of silver ion concentration, buffered hydrofluoric acid concentration, and the reaction time on the average size of the particles formed on E3 substrates are reported. These results show the change in the average size of the particles in relation to the concentration of the silver ions and buffered hydrofluoric acid in the solution. For both sets of data, the EMD process is carried out on E3 substrates as they contain the low number of defects. In this section, the original AFM images are provided, from which the data is collected to generate Figure 3-16 and Figure 3-17. The following sets of images are provided for reader's reference.

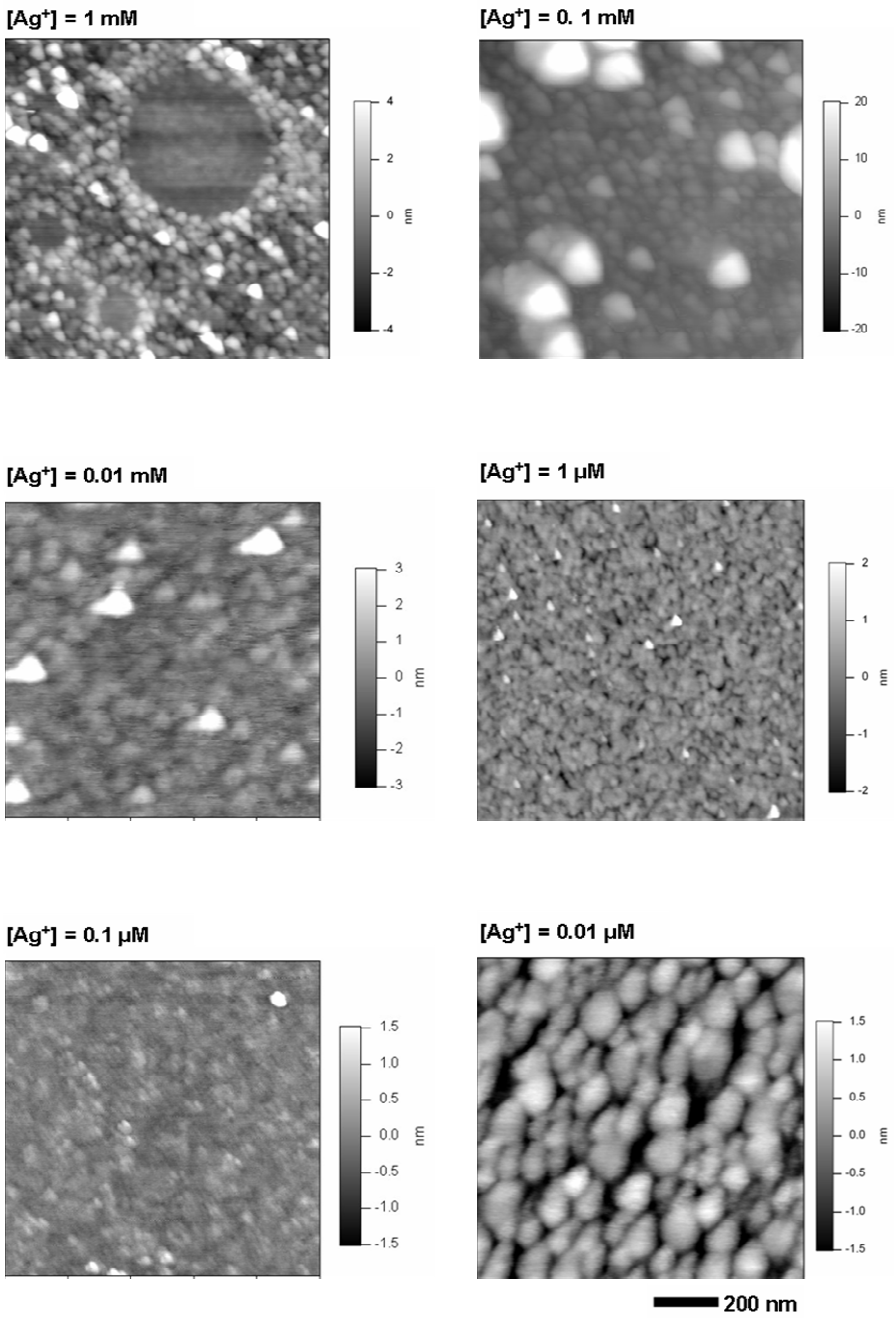

Figure A.2 AFM images of EMD on E3 substrates indicate that the number of silver particles decreases upon reducing the concentration of silver salt in the solution. The concentration of the buffered HF (1% v/v) and the deposition time (5 min) for these samples are kept constant.

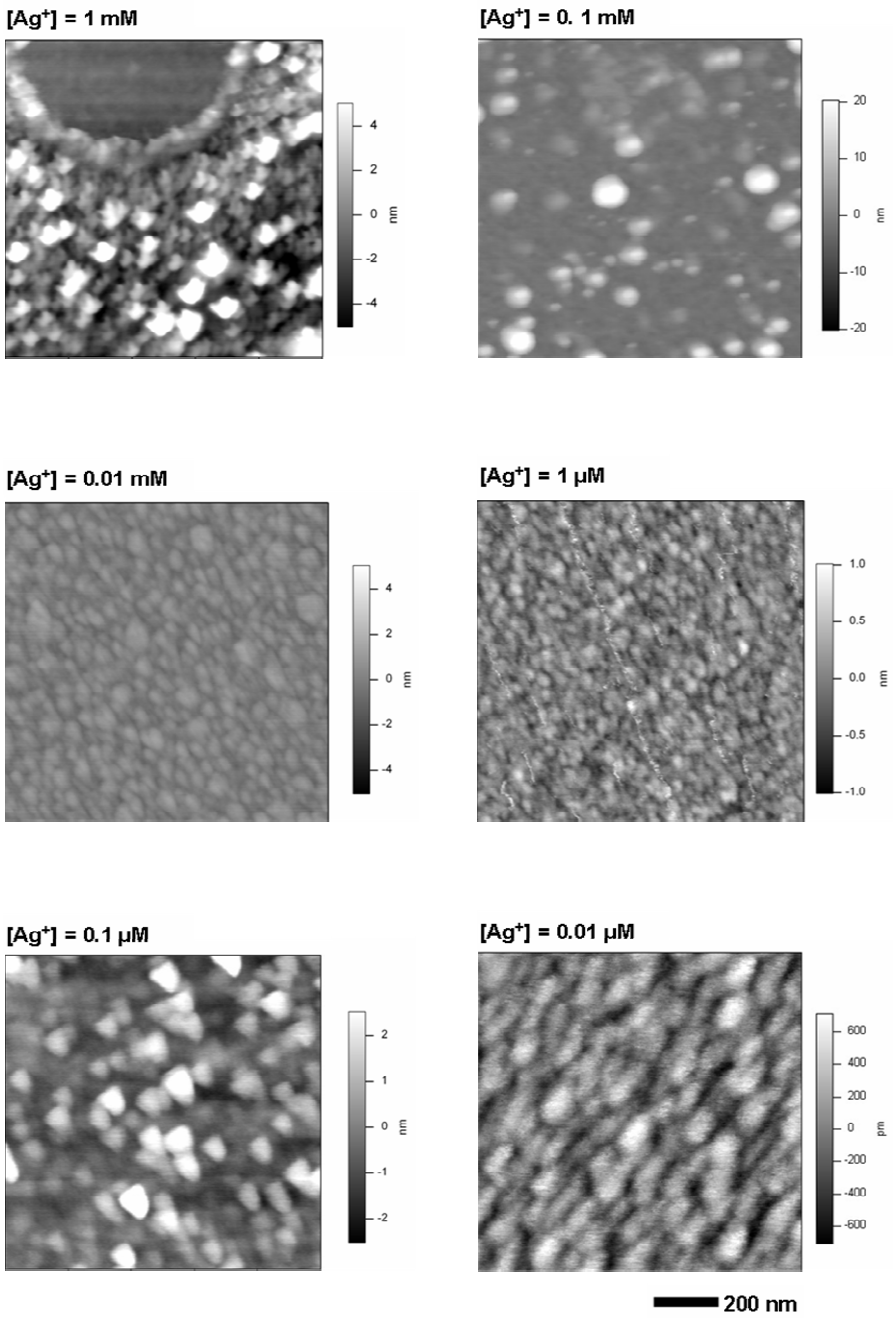

Figure A.3 AFM images of EMD on E3 substrates indicate that the number of silver particles decreases upon reducing the concentration of silver salt in the solution. The concentration of the buffered HF (1% v/v) and the deposition time (1 min) for these samples are kept constant.

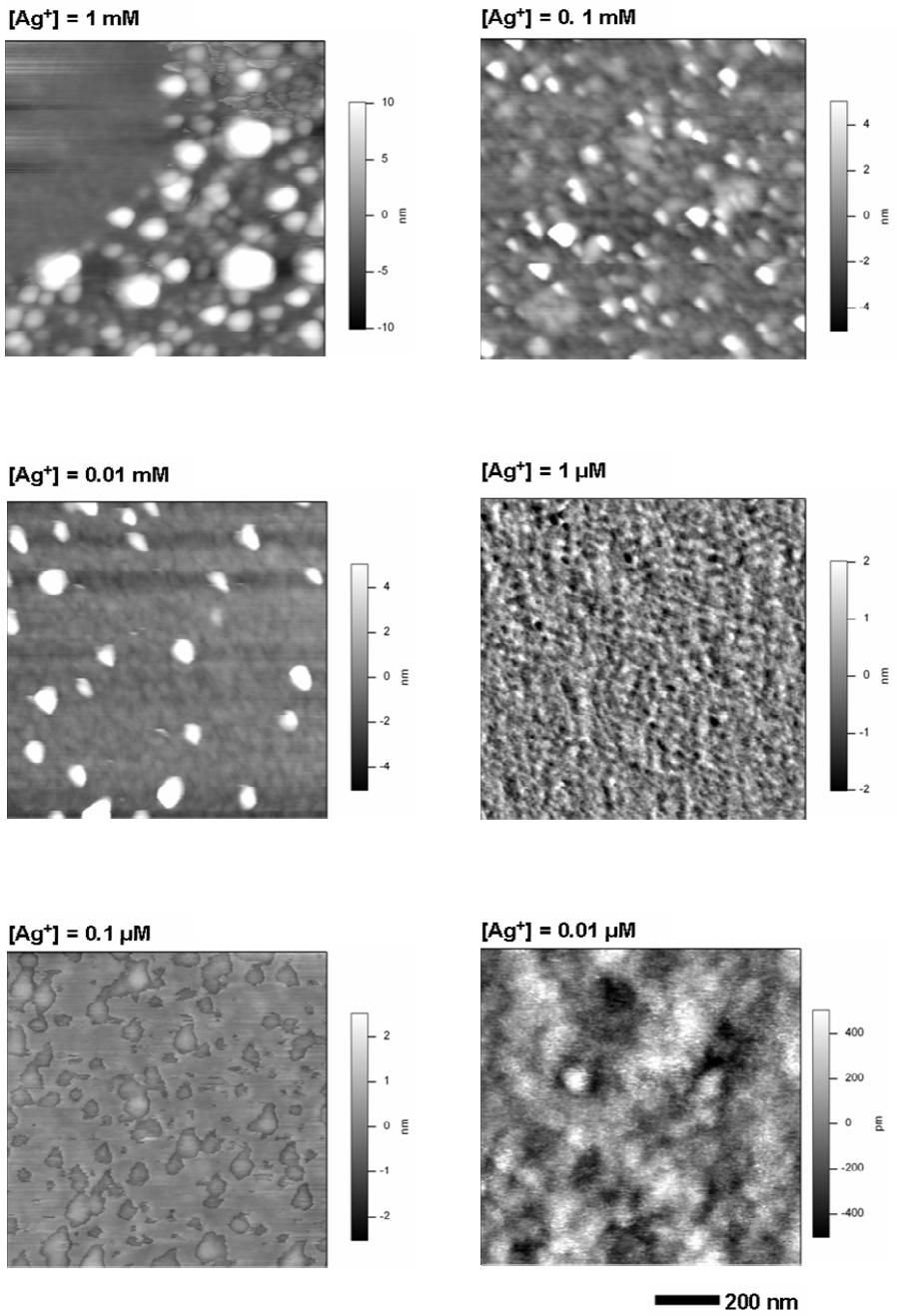

Figure A.4 AFM images of EMD on E3 substrates indicate that the number of silver particles decreases upon reducing the concentration of silver salt in the solution. The concentration of the buffered HF (1% v/v) and the deposition time (30 sec) for these samples are kept constant.

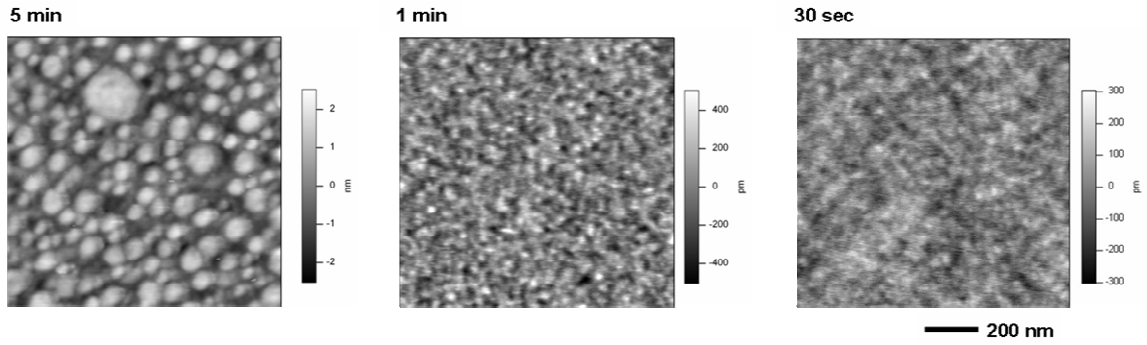

Figure A.5 AFM images of E3 substrates immersed in a 1% (v/v) HF solution for varying period of time indicate that the surface roughness due to HF decreases as the deposition time is decreased.

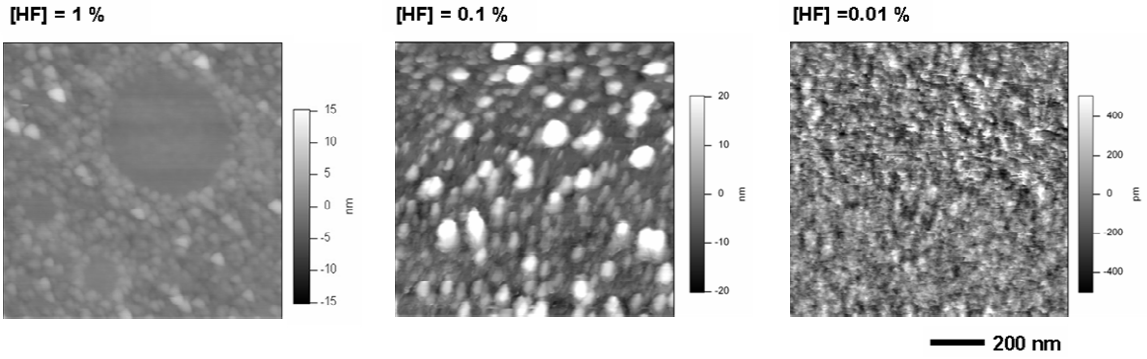

Figure A.6 AFM images of EMD on E3 substrates indicate that the number of silver particles decreases upon decreasing the concentration of buffered HF in the solution. The concentration of the silver nitrate (1 mM) and the deposition time (5 min) for these samples are kept constant.

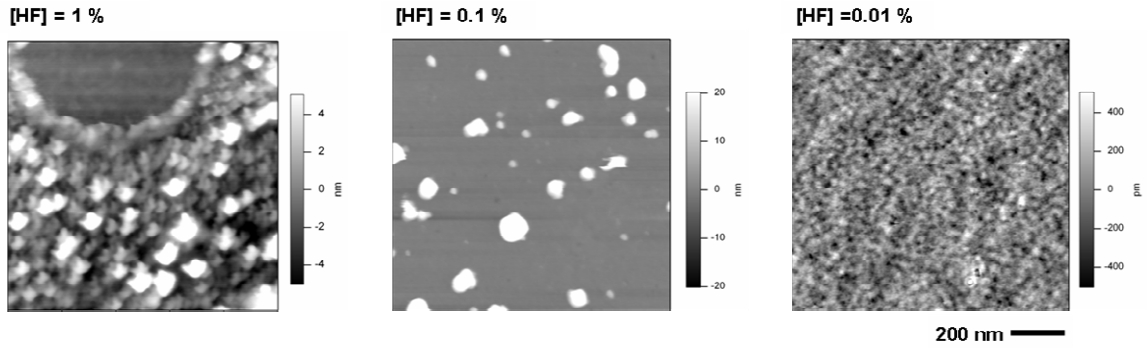

Figure A.7 AFM images of EMD on E3 substrates indicate that the number of silver particles decreases upon decreasing the concentration of buffered HF in the solution. The concentration of the silver nitrate (1 mM) and the deposition time (1 min) for these samples are kept constant.

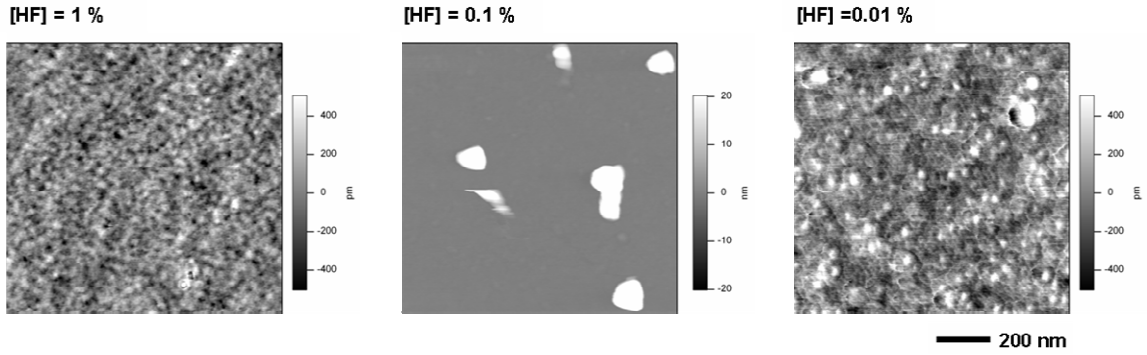

Figure A.8 AFM images of EMD on E3 substrates indicate that the number of silver particles decreases upon decreasing the concentration of buffered HF in the solution. The concentration of the silver nitrate (1 mM) and the deposition time (30 sec) for these samples are kept constant.

In chapter three, the XPS data was presented for EMD treated (1 mM $AgNO_3$, 1% HF, 5 minutes immersion time) SAMs (S1, E1, S2, E2, S3, E3 and standard SiO_2 surfaces). The survey scan collected for these substrates are shown in Figure A.9.

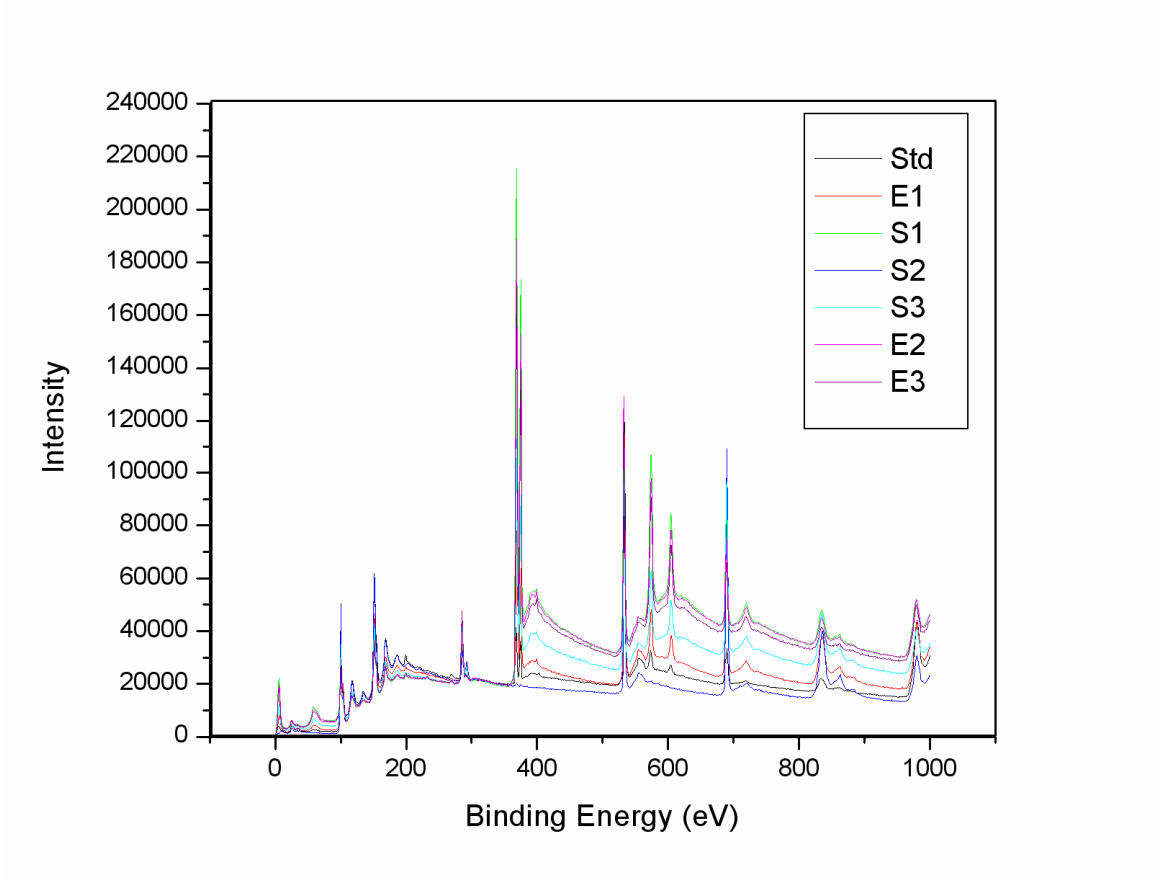

Figure A.9 The XPS survey scans are shown for the substrates (S1, E1, S2, E2, S3, E3, and standard SiO_2) after the silver treatment.

APPENDIX 3: REFERENCES

(1) Bigelow, W. C.; Pickett, D. L.; Zisman, W. A. *J. Colloid Sci.* **1946**, *1*, 513-538.

(2) Bohringer, K. F. *J Micromech. Microeng.* **2003**, *13*, S1-S10.

(3) Losic, D.; Shapter, J. G.; Gooding, J. J. *J.Solid State Electrochem.* **2005**, *9*, 512-519.

(4) Yan, L.; Huck, W. T. S.; Whitesides, G. M. *J. Macromol. Sci., Polym. Rev.* **2004**, *C44*, 175-206.

(5) Wilbur, J. L.; Kumar, A.; Biebuyck, H. A.; Kim, E.; Whitesides, G. M. *Nanotechnology* **1996**, *7*, 452-457.

(6) Bhushan, B. *Springer Handbook of Nanotechnology (2nd Edition)* **2007**, , 1379-1415.

(7) Zhuang, Y. X.; Hansen, O.; Knieling, T.; Wang, C.; Rombach, P.; Lang, W.; Benecke, W.; Kehlenbeck, M.; Koblitz, J. *J. Micromech. Microeng.* **2006**, *16*, 2259-2264.

(8) Shaporenko, A.; Cyganik, P.; Buck, M.; Ulman, A.; Zharnikov, M. *Langmuir* **2005**, *21*, 8204-8213.

(9) Ulman, A. *Chem. Rev.* **1996**, *96*, 1533-1554.

(10) Chaudhury, M. K.; Whitesides, G. M. *Science* **1992**, *255*, 1230-1232.

(11) Ulman, A. *An introduction to ultrathin organic films : from Langmuir-Blodgett to self-assembly;* Academic Press Inc: San Diego, CA, 1991; .

(12) Love, J. C.; Estroff, L. A.; Kriebel, J. K.; Nuzzo, R. G.; Whitesides, G. M. *Chem. Rev.* **2005**, *105*, 1103-1170.

(13) Poirier, G. *Chem. Rev.* **1997**, *97*, 1117-1128.

(14) Fadeev, A. Y.; McCarthy, T. J. *Langmuir* **1999**, *15*, 3759-3766.

(15) Gates, B. D.; Xu, Q.; Stewart, M.; Ryan, D.; Willson, C. G.; Whitesides, G. M. *Chem. Rev.* **2005**, *105*, 1171-1196.

(16) Patel, N.; Davies, M. C.; Hartshorne, M.; Heaton, R. J.; Roberts, C. J.; Tendler, S. J. B.; Williams, P. M. *Langmuir* **1997**, *13*, 6485-6490.

(17) Ulman, A.; Eilers, J. E.; Tillman, N. *Langmuir* **1989**, *5*, 1147-1152.

(18) Cicero, R. L.; Linford, M. R.; Chidsey, C. E. D. *Langmuir* **2000**, *16*, 5688-5695.

(19) Tripp, C. P.; Hair, M. L. *Langmuir* **1995**, *11*, 149-155.

(20) Tripp, C. P.; Hair, M. L. *Langmuir* **1992**, *8*, 1120-1126.

(21) Lenk, T. J.; Hallmark, V. M.; Hoffmann, C. L.; Rabolt, J. F.; Castner, D. G.; Erdelen, C.; Ringsdorf, H. *Langmuir* **1994**, *10*, 4610-4617.

(22) Vericat, C.; Vela, M. E.; Salvarezza, R. C. *Phys. Chem.Chem. Phys.* **2005**, *7*, 3258-3268.

(23) Gun, J.; Iscovici, R.; Sagiv, J. *J. Colloid Interface Sci.* **1984**, *101*, 201-213.

(24) Tillman, N.; Ulman, A.; Schildkraut, J. S.; Penner, T. L. *J. Am. Chem. Soc.* **1988**, *110*, 6136-6144.

(25) Carson, G. A.; Granick, S. *J. Mater. Res.* **1990**, *5*, 1745-1751.

(26) Kessel, C. R.; Granick, S. *Langmuir* **1991**, *7*, 532-538.

(27) Gun, J.; Sagiv, J. *J. Colloid Interface Sci.* **1986**, *112*, 457-472.

(28) Sagiv, J. *J. Am. Chem. Soc.* **1980**, *102*, 92-98.

(29) Flink, S.; van Veggel, F. C. J. M.; Reinhoudt, D. N. *Adv. Mater.* **2000**, *12*, 1315-1328.

(30) Reynaert, J.; Cheyns, D.; Janssen, D.; Muller, R.; Arkhipov, V. I.; Genoe, J.; Borghs, G.; Heremans, P. *J. Appl. Phys.* **2005**, *97*, 114501/1-114501/5.

(31) Sirringhaus, H.; Kawase, T.; Friend, R. H.; Shimoda, T.; Inbasekaran, M.; Wu, W.; Woo, E. P. *Science* **2000**, *290*, 2123-2126.

(32) Schwartz, D. K.; Steinberg, S.; Israelachvili, J.; Zasadzinski, J. A. N. *Phys. Rev. Lett.* **1992**, *69*, 3354-3357.

(33) Silberzan, P.; Leger, L.; Ausserre, D.; Benattar, J. J. *Langmuir* **1991**, *7*, 1647-1651.

(34) Banga, R.; Yarwood, J.; Morgan, A. M.; Evans, B.; Kells, J. *Langmuir* **1995**, *11*, 4393-4399.

(35) Fadeev, A. Y.; McCarthy, T. J. *Langmuir* **2000**, *16*, 7268-7274.

(36) Barriga, J.; Coto, B.; Fernandez, B. *Tribol. Int.* **2007**/**6**, *40*, 960-966.

(37) Gedye, R.; Smith, F.; Westaway, K.; Ali, H.; Baldisera, L.; Laberge, L.; Rousell, J. *Tetrahedron Lett.* **1986**, *27*, 279-282.

(38) Kappe, C. O. *Angew. Chem., Int. Ed. Engl.* **2004**, *43*, 6250.

(39) Kingston, H. M.; Haswell, S. J., Eds.; *Microwave-enhanced chemistry. Fundementals, sample preparation and applications;* American Chemical Society: Washington DC, 1997.

(40) Mastrovito, C.; Lekse, J. W.; Aitken, J. A. *J. Solid State Chem.* **2007**, *180*, 3262-3270.

(41) Bardts, M.; Gonsior, N.; Ritter, H. *Macromol. Chem. Phys.* **2008**, *209*, 25-31.

(42) Kappe, C. O.; Stadler, A. *Microwave in Organic and Medicinal Chemnistry;* Wiley-VCH: Weinheim, 2005.

(43) Gerbec, J. A.; Magana, D.; Washington, A.; Strouse, G. F. *J. Am. Chem. Soc.* **2005**, *127*, 15791-15800.

(44) Hayes, B. L. *Microwave Synthesis: Chemistry at the Speed of Light;* CEM Publishing: Matthews, NC, 2002.

(45) Zhao, X.; Wilbur, J. L.; Whitesides, G. M. *Langmuir* **1996**, *12*, 3257-3264.

(46) Sur, U. K.; Lakshminarayanan, V. *J. Electroanal. Chem.* **2004**, *565*, 343-350.

(47) Porter, L. A.; Choi, H. C.; Schmeltzer, J. M.; Ribbe, A. E.; Elliott, L. C. C.; Buriak, J. M. *Nano Lett.* **2002**, *2*, 1369-1372.

(48) Porter, L. A.; Choi, H. C.; Ribbe, A. E.; Buriak, J. M. *Nano Lett.* **2002**, *2*, 1067-1071.

(49) Twardowski, M.; Nuzzo, R. G. *Langmuir* **2002**, *18*, 5529-5538.

(50) Zhang, Z. G. *Electrochemistry of silicon and its oxide;* Kluwer Academic/Plenum Publishers: New York, 2001.

(51) Lide, D. R.; Baysinger, G.; Berger, L. I.; Goldberg, R. N.; Kehiaian, H. V.; Kuchitsu, K.; Rosenblatt, G.; Roth, D. L.; Zwillinger, D. CRC Handbook of Chemistry and Physics. *CRC Handbook of Chemistry and Physics* (accessed 06/13, 2008).

(52) Okinaka, Y.; Osaka, T. *Adv. Electrochem. Sci. Eng.* **1994**, *3*, 55-116.

(53) Okinaka, Y.; Hoshino, M. *Gold Bulletin (London)* **1998**, *31*, 3-13.

(54) Kallury, K. M. R.; Thompson, M.; Tripp, C. P.; Hair, M. L. *Langmuir* **1992**, *8*, 947-954.

(55) Chibowski, E. *Adv. Colloid Interface Sci.* **2007**, *133*, 51-59.

(56) Erbil, H. Y.; McHale, G.; Newton, M. I. *Langmuir* **2002**, *18*, 2636-2641.

(57) Tavana, H.; Neumann, A. W. *Adv. Colloid Interface Sci.* **2007**, *132*, 1-32.

(58) Yeh, K. Y.; Chen, L. J.; Chang, J. Y. *Langmuir* **2008**, *24*, 245-251.

(59) Yang, Y.; Bittner, A. M.; Baldelli, S.; Kern, K. *Thin Solid Films* **2008**, *516*, 3948-3956.

(60) Parikh, A. N.; Allara, D. L.; Azouz, I. B.; Rondelez, F. *J. Phys. Chem.* **1994**, *98*, 7577-7590.

(61) Hoffmann, C.; Tovar, G. E. M. *J. Colloid Interface Sci.* **2006**, *295*, 427-435.

(62) Ochiai, S.; McClelland, J. F.; Kobayashi, K.; Takaoka, K. *Appl. Spectrosc.* **1994**, *48*, 1287-1289.

(63) Cheng, S. S.; Scherson, D. A.; Sukenik, C. N. *J. Am. Chem. Soc.* **1992**, *114*, 5436-5437.

(64) Barbot, C.; Bouloussa, O.; Szymczak, W.; Plaschke, M.; Buckau, G.; Durand, J.; Pieri, J.; Kim, J. I.; Goudard, F. *Colloids and Surfaces A: Physicochemical and Engineering Aspects* , *In Press, Corrected Proof*.

(65) Rucki, A.; Cerva, H. *ECS Trans.* **2007**, *10*, 97-108.

(66) Wells, O. C.; Joy, D. C. *Surf. Interface Anal.* **2006**, *38*, 1738-1742.

(67) Davis, S. *Colloid Sci.* **2005**, 266-282.

(68) Amemiya, S.; Guo, J.; Xiong, H.; Gross, D. A. *Anal. Bioanal. Chem.* **2006**, *386*, 458-471.

(69) Kiani, A.; Alpuche-Aviles, M. A.; Eggers, P. K.; Jones, M.; Gooding, J. J.; Paddon-Row, M. N.; Bard, A. J. *Langmuir* **2008**, *24*, 2841-2849.

(70) Brown, G. E.; Henrich, V. E.; Casey, W. H.; Clark, D. L.; Eggleston, C.; Felmy, A.; Goodman, D. W.; Gratzel, M.; Maciel, G.; McCarthy, M. I.; Nealson, K. H.; Sverjensky, D. A.; Toney, M. F.; Zachara, J. M. *Chem. Rev.* **1999**, *99*, 77-174.

(71) Fernandez-Garcia, M.; Martinez-Arias, A.; Hanson, J. C.; Rodriguez, J. A. *Chem. Rev.* **2004**, *104*, 4063-4104.

(72) Umarji, G.; Ketkar, S.; Hawaldar, R.; Gosavi, S.; Patil, K.; Mulik, U.; Amalnerkar, D. *Microelec. Int.* **2008**, *25*, 46-57.

(73) Walton, J.; Fairley, N. *Surf. Interface Anal.* **2008**, *40*, 478-481.

(74) Tseng, C.; Chen, C. *Nanotechnology* **2008**, *19*, 035606/1-035606/8.

(75) Kaminskyj, S. G. W.; Dahms, T. E. S. *Micron* **2008**, *39*, 349-361.

(76) Cheran, L.; Sadeghi, S.; Thompson, M. *Analyst (Cambridge, United Kingdom)* **2005**, *130*, 1569-1576.

(77) Szunerits, S.; Pust, S. E.; Wittstock, G. *Anal. Bioanal. Chem.* **2007**, *389*, 1103-1120.

(78) Ulman, A. *Thin Solid Films* **1996**, *273*, 48-53.

(79) Chaudhury, M. K.; Whitesides, G. M. *Science (Washington, DC, United States)* **1992**, *256*, 1539-1541.

(80) Milling, A. J., Ed.; *Surface characterization methods : principles, techniques, and applications;* Marcel Dekker: New York, 1999; Vol. 87, pp 412.

(81) Adamson, A. W.; Gast, A. P. *Physical chemistry of surfaces;* Wiley: New York, 1997; pp 784.

(82) Hare, E. F.; Shafrin, E. G.; Zisman, W. A. *J. Phys. Chem.* **1954**, *58*, 236-239.

(83) Yeh, K.; Chen, L.; Chang, J. *Langmuir* **2008**, *24*, 245-251.

(84) Gruska, B.; Rosele, A. *UV-Vis-IR Ellipsometry;* Bubert, H., Jenne, H., Eds.; *Surface and thin film analysis: principles, instrumentation, applications*; Wiley-VCH: Weinheim, 2002; pp 265-267.

(85) Johnston, S. F. *Fourier transform infrared : a constantly evolving technology;* E. Horwood: New York, 1991; pp 340.

(86) Smith, B. C. *Fundamentals of Fourier transform infrared spectroscopy;* CRC Press: Boca Raton, 1996; pp 202.

(87) Vij, D. R., Ed.; *Handbook of applied solid state spectroscopy;* Marcel Dekker: New York, 2006; pp 741.

(88) Silverstein, R. M.; Webster, F. X. *Spectrometric Identification of Organic Compounds, 6th Edition.* Section Title: Organic Analytical Chemistry; 1997; pp 76-78.

(89) Davis, S. *Colloid Sci.* **2005**, , 266-282.

(90) Wells, O. C.; Joy, D. C. *Surf. Interface Anal.* **2006**, *38*, 1738-1742.

(91) O'Connor, D. J.; Sexton, B. A.; Smart, R. S. C. *Electron microscope techniques for surface characterization;* Surface analysis methods in materials science ; Springer: New York, 2003; pp 98.

(92) Goldstein, J.; Newbury, D.; Lyman, C.; Echlin, P.; Lifshin, E.; Sawyer, L.; Michael, J. *Scanning electron microscopy and x-ray microanalysis*; Kluwer Academic/Plenum Publishers: New York, 2002; pp 1-5.

(93) Sun, L.; Crooks, R. M. *Langmuir* **1993**, *9*, 1951-1954.

(94) Tsuji, M.; Hashimoto, M.; Nishizawa, Y.; Kubokawa, M.; Tsuji, T. *Chem. Eur. J.* **2005**, *11*, 440-452.

(95) Dahl, J. A.; Maddux, B. L. S.; Hutchison, J. E. *Chem. Rev.* **2007**, *107*, 2228-2269.

(96) Yu, J. C.; Hu, X.; Li, Q.; Zhang, L. *Chem. Comm.* **2005**, , 2704-2706.

(97) Qu, Y.; Carter, J. D.; Sutherland, A.; Guo, T. *Chem. Phys. Lett.* **2006**, *432*, 195-199.

(98) Huang, H.; Zhang, S.; Qi, L.; Yu, X.; Chen, Y. *Surf. Coat. Technol* **2006**, *200*, 4389-4396.

(99) Hoogenboom, R.; Schubert, U. S. *Macromol. Rapid Commun.* **2007**, *28*, 368-386.

(100) Dorwald, F. Z. *Organic Synthesis on Solid Phase;* Wiley-VCH: Weinheim, 2002.

(101) Wolfenden, R.; Snider, M.; Ridgway, C.; Miller, B. *J. Am. Chem. Soc.* **1999**, *121*, 7419-7420.

(102) Jalali, H.; Gates, B. D. *Mater. Res. Soc. Symp. Proc.* **2007**, *1021E*, No pp. given, Paper #: 1021-HH05-17.

(103) Harris, D. C. *Statistics and Spreadsheets;* Quantitative chemical analysis; W.H. Freeman: New York, 1999; pp 69-76.

(104) Zhao, X.; Wilbur, J. L.; Whitesides, G. M. *Langmuir* **1996**, *12*, 3257-3264.

(105) Ye, W.; Chang, Y.; Ma, C.; Jia, B.; Cao, G.; Wang, C. *Appl. Surf. Sci.* **2007**, *253*, 3419-3424.

(106) Jerman, M.; Qiao, Z.; Mergel, D. *Appl. Opt.* **2005**, *44*, 3006-3012.

(107) Lee, K. J.; Kang, T. D.; Lee, H. S.; Lee, H.; Cho, M. J.; Lee, S. H.; Choi, D. H. *J. Appl. Phys.* **2005**, *97*, 083543/1-083543/5.

(108) Sugimura, H.; Hayashi, K.; Saito, N.; Nakagiri, N.; Takai, O. *Appl. Surf. Sci.* **2002**, *188*, 403-410.

(109) Tripp, C. P.; Veregin, R. P. N.; Hair, M. L. *Langmuir* **1993**, *9*, 3518-3522.

(110) Williams, K. R.; Gupta, K.; Wasilik, M. *J. Microelectromech. Syst.* **2003**, *12*, 761-778.

(111) Xue, G.; Dong, *J. Anal. Chem.* **1991**, *63*, 2393-2397.

(112) Kulkarni, M. S.; Erk, H. F. *J. Electrochem. Soc.* **2000**, *147*, 3977.

(113) Duer, M. J. *Annu. Rep. NMR Spectros.* **2006**, *59*, 41-116.

(114) Bower, P. V.; Louie, E. A.; Long, J. R.; Stayton, P. S.; Drobny, G. P. *Langmuir* **2005**, *21*, 3002-3007.

(115) Hasan, M.; Bethell, D.; Brust, M. *J. Am. Chem. Soc.* **2002**, *124*, 1132-1133.

(116) Osman, M. A.; Ernst, M.; Meier, B. H.; Suter, U. W. *J. Phys. Chem. B* **2002**, *106*, 653-662.

(117) Vallant, T.; Kattner, J.; Brunner, H.; Mayer, U.; Hoffmann, H. *Langmuir* **1999**, *15*, 5339-5346.

(118) Maoz, R.; Sagiv, J. *J. Colloid Interface Sci.* **1984**, *100*, 465-496.

(119) Johnston, S. F. *Attenuated total reflectance;* Fourier transform infrared : a constantly evolving technology; E. Horwood: New York, 1991; pp 303-304.

(120) Albrecht, P. M.; Baddorf, A. P.; Alvarez, D.; Bachelot, R.; Anderson, M. L.; Anlage, S. M.; Ban, D.; Boag, A. *Scanning Probe Microscopy: Electrical and Electromechanical Phenomena at the Nanoscale Volume II;* Kalinin, S., Gruverman, A., Eds.; Springer: .

(121) Hernandez-Trujillo, J.; Costas, M.; Vela, A. *J. Chem. Soc., Faraday Trans.* **1993**, *89*, 2441-2443.